www.reanimatology.com
ISSN 2411-7110 (online)

GENERAL REANIMATOLOGY

ОБЩАЯ РЕАНИМАТОЛОГИЯ

SCIENTIFIC-AND-PRACTICAL JOURNAL

научно-практический журнал

Volume 19 **Том 19**

№ 6

Moscow
Москва
2023

Коллектив ФНКЦ РР — Лауреат Премии Правительства Российской Федерации в области науки и техники 2023 г.!

Председатель Правительства России М. В. Мишустин вручил директору Федерального научно-клинического центра реаниматологии и реабилитологии Министерства науки и высшего образования Российской Федерации (ФНКЦ РР) члену-корреспонденту РАН А. В. Гречко Премию Правительства Российской Федерации в области науки и техники.

Это событие является уникальным для Российской медицинской науки, так как впервые в истории страны Государственная Премия вручена за комплексную работу в области реабилитации!

Коллектив ФНКЦ РР удостоен высокой награды за большой вклад в развитие российской медицины. За короткое время в центре была проделана уникальная работа:

- Разработан и реализован чёткий маршрутный алгоритм ранней нейрореабилитации пациентов, нуждающихся в протезировании жизненно важных функций.
- Впервые были валидированы межведомственные и разноуровневые методы эвакуации, спасения и восстановления пациентов в критическом состоянии. Впервые для данной категории пострадавших был обобщен и систематизирован опыт специализированных организаций Минобрнауки России, Минздрава России, Минобороны России, ФМБА и регионов страны.
- Разработаны и внедрены технологии этапного спасения и восстановления пациентов с мозговыми катастрофами на примере 10000 клинических случаев.
- Достигнута экономическая эффективность внедрённых организационно-клинических алгоритмов.

Лауреаты Премии:

Руководитель работы:

— *А. В. Гречко*, доктор медицинских наук, профессор, член-корреспондент РАН, директор ФНКЦ РР.

Коллектив:

— *А. Н. Кузовлев*, доктор медицинских наук, доцент, заместитель директора-руководитель НИИ общей реаниматологии им. В. А. Неговского ФНКЦ РР;

— *М. В. Петрова*, доктор медицинских наук, профессор, заместитель директора по научно-клинической деятельности ФНКЦ РР;

— *С. Н. Пузин*, доктор медицинских наук, профессор, академик РАН, заместитель директора по науке ФНКЦ РР;

— *Г. Е. Иванова*, доктор медицинских наук, профессор, главный внештатный реабилитолог Минздрава России, главный редактор журнала «Физическая и реабилитационная медицина, медицинская реабилитация» ФНКЦ РР;

— *А. А. Яковлев*, кандидат медицинских наук, заместитель директора-руководитель НИИ реабилитологии им. проф. Пряникова И. В. ФНКЦ РР;

— *Д. Ф. Алиев*, кандидат экономических наук, Первый проректор РГСУ;

— *Е. Е. Ачкасов*, доктор медицинских наук, профессор, заведующий кафедрой Первого Московского государственного университета им. И. М. Сеченова;

— *А. А. Белкин*, доктор медицинских наук, профессор, директор Клиники Института Мозга (г. Екатеринбург), главный внештатный специалист по медицинской реабилитации в Уральском федеральном округе;

— *Т. Ю. Сафонова*, кандидат медицинских наук, главный врач Клиники Института Мозга (г. Екатеринбург).

Поздравляем коллектив ФНКЦ РР
с заслуженной наградой и желаем новых свершений!

ISSN 1813-9779 (print) ISSN 2411-7110 (online)

GENERAL REANIMATOLOGY

OBSHCHAYA REANIMATOLOGIYA

Scientific-and-Practical Peer-Reviewed Journal
Since 2005

• Covers issues of critical care medicine
• Manuscripts in Russian and English are published free-of-charge
• Included in SCOPUS (since 2015), RINTs, RSCI, DOAJ, and other databases, as well as in the Official list of editions recommended for publication of dissertations (PhD, DSci) by the Russian Higher Attestation Commission

Registration certificate of the Journal «Obshchaya reanimatologiya» (General Reanimatology): ПИ № ФС77-18690, November 2, 2004, Federal Service for Supervision of Compliance with Legislation in the Sphere of Mass Communications and Protection of Cultural Heritage
Publication Frequency: 6 numbers per year.
Founder:

ОБЩАЯ РЕАНИМАТОЛОГИЯ

OBŜAÂ REANIMATOLOGIÂ

научно-практический рецензируемый журнал
Выходит с 2005 г.

• охватывает вопросы медицины критических состояний
• публикует рукописи на русском и английском языках бесплатно
• включен в базы данных SCOPUS (с 2015 г.), РИНЦ, RSCI, DOAJ и др. базы данных; Перечень изданий, рекомендованных ВАК для публикации результатов диссертационных работ

Свидетельство о регистрации: ПИ № ФС77-18690 от 02 ноября 2004 г. Печатное издание журнал «Общая реаниматология» зарегистрирован Федеральной службой по надзору за соблюдением законодательства в сфере массовых коммуникаций и охране культурного наследия.
Периодичность: 6 раз в год
Учредитель:

Publisher:
Federal Research and Clinical Center of Intensive Care Medicine and Rehabilitology, Moscow, Russia
Издатель:
Федеральный научно-клинический центр реаниматологии и реабилитологии (ФНКЦ РР), Москва, Россия

Supported by Russian Federation of Anesthesiologists and Reanimatologists
При поддержке Общероссийской общественной организации «Федерация анестезиологов и реаниматологов»

Artwork: Natalia V. Golubeva
Page-proof: Sergey V. Shishkov
Printing House:
Printed at LLC «Advanced Solutions». 19, Leninsky prospekt, build. 1, Moscow, 119071. www.aov.ru
Contacts:
25 Petrovka Str., Bldg. 2, 107031 Moscow, Russia.
Tel. +7-495-694-17-73.
E-mail: **journal_or@mail.ru;**
Web: **www.reanimatology.com**

Subscription:
Index 46338, refer to catalog of «Книга-Сервис»
Signed for printing: 29.12.2023

Оригинал-макет: Н. В. Голубева
Верстка: С. В. Шишков
Типография: отпечатано в ООО «Адвансед солюшнз». 119071, г. Москва, Ленинский пр-т, д. 19, стр. 1. www.aov.ru
Контакты с редакцией:
Россия, 107031, г. Москва, ул. Петровка, д. 25, стр. 2.
Тел.: +7-495-694-17-73.
E-mail: **journal_or@mail.ru;**
сайт: **www.reanimatology.com**

Подписка и распространение: индекс издания по каталогу «Книга-Сервис» — 46338.
Цена свободная
Подписано в печать: 29.12.2023

CONTENTS **СОДЕРЖАНИЕ**

https://doi.org/10.15360/1813-9779-2023-6-4-12

Sepsis-Associated Metabolites and Their Biotransformation by Intestinal Microbiota

Ekaterina A. Chernevskaya[1]*, Mariya L. Getsina[1], Rostislav A. Cherpakov[1,2], Ekaterina A. Sorokina[1], Aslan K. Shabanov[1,2], Victor V. Moroz[1], Natalia V. Beloborodova[1]

[1] V. A. Negovsky Research Institute of General Reanimatology, Federal Research and Clinical Center of Intensive Care Medicine and Rehabilitology, 25 Petrovka Str., Bldg. 2, 107031 Moscow, Russia
[2] N. V. Sklifosovsky Research Institute of Emergency Medicine, Moscow City Health Department, 3 Bolshaya Sukharevskaya Square, Bldg. 1, 129090 Moscow, Russia

For citation: *Ekaterina A. Chernevskaya, Mariya L. Getsina, Rostislav A. Cherpakov, Ekaterina A. Sorokina, Aslan K. Shabanov, Victor V. Moroz, Natlya V. Beloborodova.* Sepsis-Associated Metabolites and Their Biotransformation by Intestinal Microbiota. *Obshchaya Reanimatologiya = General Reanimatology.* 2023; 19 (6): 4–12. https://doi.org/10.15360/1813-9779-2023-6-4-12 [In Russ. and Engl.]

***Correspondence to:** Ekaterina A. Chernevskaya, chea05@inbox.ru; echernevskaya@fnkcrr.ru

Summary

High serum levels of microbial metabolites of aromatic amino acids (AMM) stands as a prognostically unfavorable factor, indicating the progression of multiple organ dysfunction and an increased risk of death in patients with sepsis and septic shock. This study is based on a hypothesis that excess of sepsis-associated AMM in patients with sepsis is caused by metabolic alterations (dysfunction) in the intestinal microbiota.

The aim of this study was to compare the potential of normobiota and pathobiota to bio-transform sepsis-associated metabolites of aromatic amino acids tyrosine and phenylalanine, such as phenyllactic acid (PLA) and 4-hydroxyphenyllactic acid (4-HPLA).

Materials and methods. Samples of intestinal contents of patients with septic shock (N=10, pathobiota) and healthy volunteers (N=9, normobiota) were placed in test tubes with the omnipurpose thioglycol medium. The clinical model of excessive inflow of sepsis-associated AMM into the intestine (for example, from blood or sites of inflammation) was reproduced in the *in vitro* experiment by adding PLA or 4-HPLA in clinically significant concentrations (25 μM) into each test tube with pathobiota and normobiota. After incubation in a thermostat (37°, 24 hours), AMM concentrations were measured in the samples with pathobiota and normobiota using GC-MS analysis.

Results. Concentration of AMM decreased within 24 hours in the tubes with normobiota after PLA or 4-HPLA were added. In the tubes with pathobiota, no decrease in AMM concentrations was documented after loading with PLA or 4-HPLA. Concentrations of PLA (P=0.002) and 4-HPLA (P<0.001) were statistically significantly higher in pathobiota samples compared to normobiota.

Conclusion. The *in vitro* experiment demonstrates that after excessive load with sepsis-associated metabolites (PLA, 4-HPLA), the microbiota of healthy people is capable to bio-transform such metabolites to the end products of microbial metabolism, while pathobiota of septic patients exhibits altered biotransformational potential. This data demonstrate that microbiota dysfunction may contribute to the pathogenesis of sepsis.

Keywords: sepsis; pathobiota; aromatic microbial metabolites; phenyllactic acid; 4-hydroxyphenyllactic acid; phenylpropionic acid; microbiota; biomarkers; aromatic amino acid metabolites

Conflict of interest. The authors declare no conflict of interest.

Read the full-text English version at www.reanimatology.com

Introduction

Sepsis remains a continuing challenge of the 21st century, and intensive research into new pathogenetic therapies to reduce its incidence and mortality is ongoing [1–4]. Contemporary studies revealing the impact of the gut microbiota to critical illness and sepsis development attract special attention [5–7]. In patients with sepsis, severe disturbances in the taxonomic composition of the intestinal microbiota, increased permeability of the intestinal wall, changes in immunoreactivity, and the development of antibiotic resistance in microorganisms are observed, all of which lead to metabolomic perturbations [8, 9]. For example, significant accumulation of metabolites of aromatic amino acids phenylalanine and tyrosine in blood serum has been found in patients with sepsis of various etiologies, such as severe pneumonia, abdominal diseases, postoperative complications of cardiac surgery, etc. [6, 10]. High serum levels of microbial metabolites of aromatic amino acids (Aromatic Microbial Metabolites, AMM [6, 10, 11]) such as phenyllactic acid (PLA), 4-hydroxyphenyllactic acid (4-HPLA), and 4-hydroxyphenylacetic acid (4-HPAA) have been shown to most frequently correlate with disease severity and mortality. This has led to the introduction of the term «sepsis-associated metabolites» for these metabolites [11]. Previous studies have shown that several aromatic metabolites are predominantly of microbial origin [12–14]. Biotransformation of aro-

matic amino acids takes place in the gut, normally hundreds of bacterial species of healthy microbiota feed on metabolic intermediates, and as a result, in a healthy organism, small amounts of the end products of microbial metabolism, mainly phenylpropionic acid (PPA) and phenylacetic acid (PAA), enter the systemic circulation [15]. In sepsis, microbial metabolism of aromatic amino acids occurs both in the gastrointestinal tract and at sites of inflammation. Therefore, the intermediates of metabolism enter the bloodstream in excess, leading to an increase in the levels of circulating sepsis-associated metabolites, PLA, 4-HPLA, and 4-HPAA.

Metabolomic monitoring of patients with sepsis has shown that even after surgical treatment of purulent foci, the high levels of PLA and 4-HPLA often do not decrease, but even increase, which is associated with progression to multiorgan failure and an unfavorable prognosis. We have proposed that this may be due to metabolic dysfunction of the microbiota. When the pool of normal anaerobic bacteria is depleted in a septic patient, aromatic amino acids and their intermediates are not fully biotransformed into end products, contributing to the accumulation of sepsis-associated microbial metabolites in the body.

Our study was based on the idea that an important function of a healthy microbiota consists in utilizing potentially toxic products by biodegrading them to metabolic end products under the conditions of a normal microbial community functioning in the gut of a healthy individual («normobiota»). The working hypothesis of the study was that the microbiota of a septic patient is unable to eliminate the excess of sepsis-associated metabolites that originate from the blood and/or are produced in the intestinal lumen and do not undergo biotransformation. This hypothesis was tested in an in vitro model experiment by culturing the intestinal microbiota with the addition of sepsis-associated metabolites to simulate their excessive entry into the intestine from the blood or from inflammatory foci, with subsequent measurement of metabolites.

Thus, the aim of this study was to compare the ability of normobiota and pathobiotato biotransform sepsis-associated metabolites of the aromatic amino acids tyrosine and phenylalanine using PLA and 4-HPLA as examples.

Materials and Methods

The biomaterial for the model experiment included

- Blood serum from healthy donors (*N*=48) and patients with sepsis (*N*=10);
- Intestinal contents from healthy volunteers (*N*=9) and patients with septic shock (*N*=10).

Sepsis patients. The study included 10 patients (9 men and 1 woman) admitted to the Sklifosovsky Research Institute for Emergency Medicine in December 2022.

Inclusion criteria were:

- age older than 18 and younger than 80 years;
- sepsis;
- septic shock.

Exclusion criterion was terminal condition with life expectancy less than 24 hours.

Patients were admitted with the diagnosis of combined trauma (*N*=6), closed traumatic brain injury (*N*=1), non-traumatic subarachnoid and parenchymal intraventricular hemorrhage (*N*=1), and acute abdominal disease (*N*=2). The mean age of the patients was 43 (34–60) years. Pulmonary sepsis predominated in 60% of the patients included in the study, with abdominal and mixed (cerebral/pulmonary) sepsis accounting for 20% each. All patients received mechanical ventilation, intensive therapy including combinations of antibiotics, inotropic support and others. Serum samples were collected from all patients to determine biomarkers of sepsis. For the in vitro experiment, samples of intestinal contents were collected once from all patients.

Healthy donors. Blood serum samples from healthy donors (*N*=48) were obtained from the Federal State Budgetary Institution N.N. Burdenko Main Military Clinical Hospital (Moscow, Russia). The age of the donors was 39 (33–45) years, 35 were men and 13 were women. Healthy donors had no general clinical signs of acute inflammation and no chronic liver or kidney disease.

Determination of serum biomarkers of inflammation and sepsis. Serum biomarkers of inflammation and sepsis, including protein S100, IL-6, NT-proBNP, and PCT, were measured using the Cobas e411 electrochemiluminescence analyzer (Roche, Basel, Switzerland). Elecsys S100/NT-proBNP/IL-6/PCT (Roche Diagnostics) reagent kits were used for the measurement.

Evaluation of microbiota composition in samples using the Colonoflor-16 (Biocenosis) test system. Qualitative and quantitative composition of obligate and opportunistic microorganisms of the microbiota was evaluated by real-time PCR with fluorescence detection using the Colonoflor-16 (Biocenosis) test system (AlfaLab, Russia). The system allowed to detect 23 parameters, including 21 groups/species of microorganisms and total bacterial count.

Description of the *in vitro* experimental model. Samples of healthy gut microbiota or microbiota from sepsis patients were placed in nutrient medium with the addition of one of the sepsis-associated PLA or 4-HPLA metabolites. After 24 hours of incubation in a thermostat, the qualitative and quantitative composition of AMM was measured and evaluated.

Culturing of intestinal samples in thioglycol medium with PLA or 4-HPLA addition. Universal

thioglycol medium (TGM) was used to create *in vitro* growth conditions for facultative anaerobic and anaerobic bacteria. The experimental scheme for each intestinal content sample is shown in Fig. 1. AMM composition was investigated in healthy volunteers (*N*=9) and sepsis patients (*N*=10) before and after incubation of intestinal contents in TGM supplemented with sepsis-associated microbial metabolites at clinically relevant concentrations (25 µM PLA or 4-HPLA) for 24 hours at 37°C. After incubation, the tubes were vortexed, centrifuged at 1000 rpm for 10 minutes, and the supernatant was frozen at –20°C. The concentration of metabolites in the intestinal contents of healthy volunteers and sepsis patients before and after incubation in TGM was measured by GC-MS.

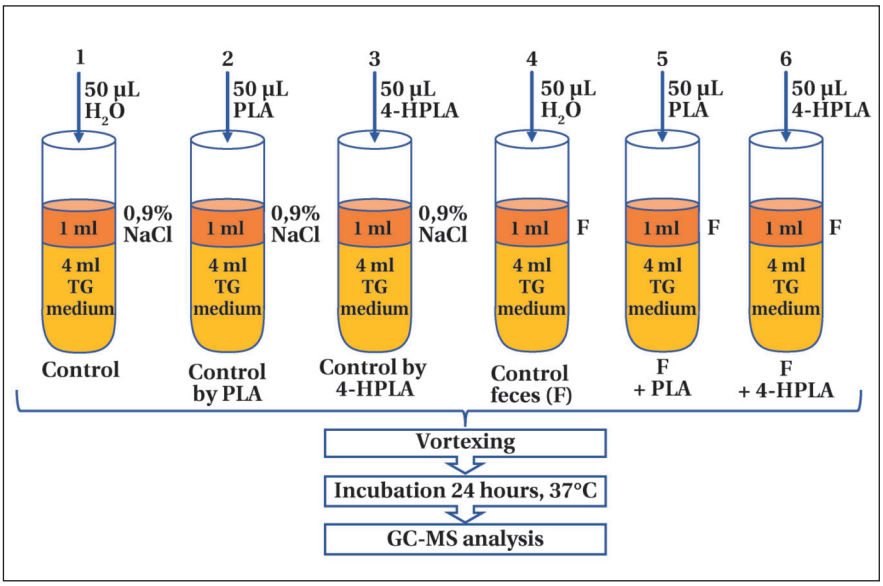

Fig. 1. Scheme of the experiment.
Note. A series of 6 tubes was formed for each sample of intestinal contents (IC), for a total of 19 rows. In each row, four control tubes were assigned: 1) to record the baseline TGM without added reagents, 2) and 3) to record the addition of sepsis-associated metabolites of PLA or 4-HPLA after incubation without IC, 4) to record the baseline values of metabolites in IC without added reagents. Two additional tubes (5 and 6) contained IC and added corresponding sepsis-associated metabolites of PLA or 4-HPLA. After incubation, microbiota metabolites in the TGM were measured by GC-MS analysis.

Analysis of metabolites in intestinal contents and serum using GC-MS. A GC-2010 Plus gas chromatograph and a GCMS-QP2020 mass spectrometer (both from Shimadzu, Japan) were used for metabolite analysis. The test sample was extracted twice with diethyl ether, then evaporated to dryness and derivatized with N,O-bis(trimethylsilyl)trifluoroacetamide. The resulting solution was diluted with n-hexane, and 2 µL of the final solution was injected. For quantitative data analysis, relative signals were calculated as the ratio of the TMS peak area of the target compound derivatives to the peak area of the surrogate internal standard. The concentrations calculated from the calibration graphs were used to present the results. To calculate the relative acid content in percent, the following formula was used:

$$\text{Relative content,\%} = 100\times\left(\frac{\text{relative signal of an acid}}{\Sigma\,\text{relative signals of all measured acids}}\right)$$

Statistical analysis. Statistical analysis of the data was performed using Microsoft Excel 2010 and IBM SPSS Statistic 27. Descriptive statistics were presented as median *(Me)* and interquartile range (IR, 25–75%). The *T*-Wilcoxon test was used for comparison between groups of paired samples. The Mann-Whitney test was used for between-group comparisons of independent samples. The differences between groups were considered significant at two-sided $P<0.05$, where p is the probability of a first-order error when testing the null hypothesis.

Results

Biomarkers and metabolites. We assessed the severity of the disease in the patients at the time of enrollment using several scales. The values were 30 (23–38) points for the APACHE II and 11 (9–15) points for the SOFA. Markers of inflammation and bacterial activity, such as IL-6 and procalcitonin, the heart failure marker NT-proBNP, the brain damage marker S100 (Table 1), and AMM (Table 2), increased multifold.

The sum of concentrations of three metabolites associated with sepsis, namely PLA, 4-HPLA, and 4-HPAA, was found to be more than six times higher in sepsis patients compared to healthy individuals. Such microbial metabolites as phenylpropionic acid, 4-hydroxyphenylpropionic acid, and hydroxybenzoic acid were not detected above the lower limit of quantification, except in one case where the serum concentration of 4-hydroxyphenylpropionic acid was 15.8 µM.

Regarding the microbial metabolites of aromatic amino acids found in the intestinal contents, there was a notable difference between healthy volunteers (*N*=9) and sepsis patients (*N*=10), as shown in Fig. 2. The main metabolites observed in healthy volunteers were PLA and PAA, accounting for 16–86% of the total determined metabolites. In contrast, the proportion of sepsis-associated aromatic metabolites in healthy controls did not exceed 5%. However, in patients with sepsis, the proportion of sepsis-associated phenolic metabo-

Table 1. Biomarkers in patients with sepsis (*N*=10).

Biomarker	Normal value	Result
IL-6, pg/L	<7	235 (126–3320)
Procalcitonin, ng/mL	<0.25	24 (10–49)
NT-proBNP, pg/mL	<125	1404 (728–31368)
S100, pg/mL	<0.1	0.47 (0.26–1.42)
Neutrophil to lymphocyte ratio (NLR)	<4	16 (7–47)

Table 2. Microbial metabolites of aromatic amino acids in serum of healthy donors and sepsis patients, μM.

Metabolites	Concentration, μM		*P*-value
	Donors, *N*=48	Patient with sepsis, *N*=10	
PPA	<0.5 (<0.5–0.5)	<0.5	—
PLA	<0.5	2.0 (1.0–2.3)	—
4-HPPA	<0.5	<0.5	—
4-HPAA	<0.5	2,1 (1.7–7.0)	—
4-HPLA	1.3 (1.0–1.6)	4,6 (2.5–12.3)	<0.001
*∑ (PLA, 4-HPAA, 4-HPLA)	1.9 (1.4–2.2)	12.9 (5.2–27.8)	<0.001

Note. *∑ (PLA, 4-HPAA, 4-HPLA), sum of three levels of clinically significant sepsis-associated acids, μM.

lites was significantly higher, amounting to 40% of the total metabolites.

The taxonomic composition of the intestinal contents was quantified using real-time PCR. In patients with sepsis, a quantitative increase of so-called «proinflammatory» microorganisms such as *Proteus vulgaris/mirabilis*, *Staphylococcus aureus*, *Fusobacterium nucleatum*, *Enterobacter* spp., *Klebsiella pneumoniae* was detected. The anaerobic imbalance coefficient (*Bacteroides fragilis group/Faecalibacterium prausnitzii* ratio) was found to be several times higher, amounting to 3750 (400 — 13750) with reference values lower than 100. The levels of lactobacilli and bifidobacteria were also reduced compared to the reference values in more than 60% of patients.

Changes in the concentrations of AMM in the intestinal contents of healthy volunteers and sepsis patients after incubation

The mean concentrations of AMM after incubation are shown in Fig. 3. Control measurements of PLA and 4-HPLA levels after incubation in TM were performed without the addition of intestinal contents. When 25 μM 4-HPLA (Fig. 3, *b*) or PLA (Fig. 3, *b*) was added to normobiotic medium, a decrease in these metabolites and an increase in PPA (P=0.028, the T-Wilcoxon criterion) were observed after 24 hours compared with the control (assays 3 and 2, respectively). Addition of PLA and 4-HPLA to the pathobiota(Fig. 3, *d*, *e*) did not reduce the levels of these acids after 24 hours, PPA was not found at levels above the lower limit of quantification, except in two cases where PPA concentrations were 8 and 15 μM. PLA (P=0.002) and 4-HPLA (P<0.001) levels were significantly higher and PPA (P=0.003) levels were significantly lower in pathobiota samples compared to normobiotic samples.

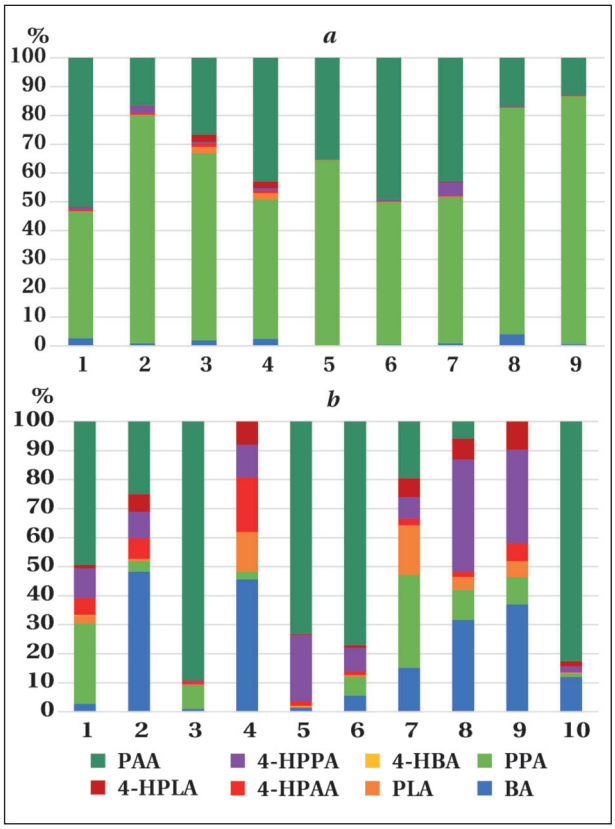

Fig. 2. Composition of microbial metabolites of aromatic amino acids in intestinal contents based on relative acid content.
Note. *a* — in healthy volunteers (*N*=9); *b* — in patients with sepsis (*N*=10).

Discussion

In an *in vitro* experiment, we observed a decrease in the levels of sepsis-associated aromatic microbial metabolites when «healthy» gut microbiota was present. Conversely, we observed an increase in these metabolites when the medium contained pathobiota from sepsis patients. These findings support the hypothesis that the gut microbiota plays a crucial role in the biotransformation of microbial metabolites and the maintenance of homeostasis under normal conditions. Furthermore, our results suggest that this function is impaired in sepsis.

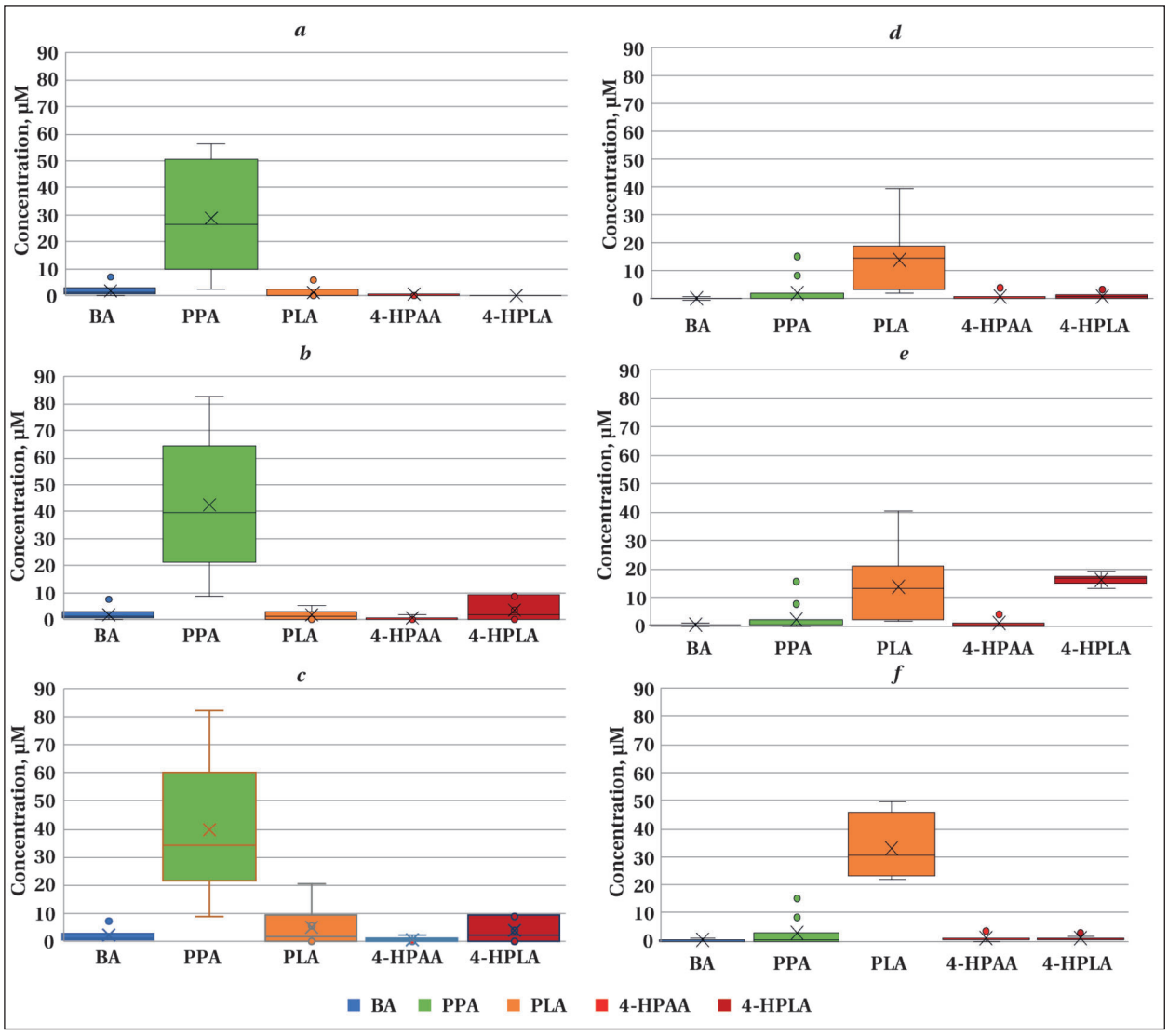

Fig. 3. The levels of microbial metabolites of aromatic amino acids.
Note. Median (IR, 25–75%) in «TGM + normobiota» and «TGM + pathobiota» after 24 h incubation; *a* and *d*: normobiota and pathobiota after incubation without addition of sepsis-associated acids; *b* and *f*: normobiota and pathobiota with added 25 μM 4-HPLA; *c* and *f*: normobiota and pathobiota with added 25 μM PLA.

In addition to the manifold increase in reference values of markers of inflammation and bacterial infection (IL-6, procalcitonin), heart failure (NT-proBNP) and nerve damage (protein S100), reflecting the severity of the patients' condition and the risk of complications [16, 17], we found an almost sevenfold increase in the sum of concentrations of three sepsis-associated serum metabolites, namely PLA, 4-HPAA and 4-HPLA. PLA and 4-HPLA have previously been shown to be metabolites of a number of aerobic and anaerobic bacteria, including the most common pathogens such as Gram-negative bacteria of the Enterobacteriaceae family (e.g., *Escherichia coli, Klebsiella pneumoniae*, etc.) and Gram-positive bacteria (e.g., *Staphylococcus aureus*) [13]. Experimental and clinical studies confirm the biological activity of these metabolites, in particular the inhibition of mitochondrial, neutrophil and platelet function, inhibitory effect on Na^+/K^+ATPase activity [11, 18, 19]. PLA suppressed cell proliferation in rat pancreas, liver and kidney tissue culture and bacterial culture proliferation [20]. Elevated levels of 4-HPAA have been associated with altered bacterial metabolism [21, 22], disruption of the catecholamine synthesis pathway, and development of hemodynamic disturbances in sepsis [10]. The concentration of another metabolite, phenylpropionic acid, one of the end products of microbial metabolism, was significantly reduced or undetectable in the blood of patients with sepsis compared to healthy subjects. This observation is consistent with the fact that only Clostridium sporogenes bacteria were able to produce PPA in the experiment [11, 23]. A positive correlation of one of the phenylpropionic acid precursors, 4-HPPA, with Gram-positive bacteria (including the families *Christensenellaceae*,

Oscillospiraceae, and the genus *Ruminococcus*) representing a healthy microbiome has also been described [6]. The profile of microbial aromatic metabolites in the gut was not identical to that in the serum, but the following trend persisted: sepsis-associated metabolites in healthy individuals did not exceed 5%, whereas their proportion increased manifold and reached 40% in patients with septic shock.

This study was based on the assumption that impaired microbiota composition in sepsis leads to microbiota dysfunction, namely the loss of the ability to utilize excess aromatic metabolites. Indeed, culturing clinically relevant concentrations of 4-HPLA or PLA with normal microbiota was associated with a decrease in the levels of these metabolites and an increase in PLA levels compared to the baseline control, while the pathobiotalacked the ability to biotransform sepsis-associated metabolites. The biochemistry of aromatic acid catabolism by Escherichia coli has been previously studied in vitro in sufficient detail [24, 25]. *Escherichia coli* maintains its ability to grow under aerobic conditions by enzymatic cleavage of phenolic acids to simple compounds in media where aromatic acids are the sole carbon source. The maximum *in vitro* production of PLA and 4-HPLA was observed for *Enterobacteriaceae* and *Staphylococcus aureus*. For example, a 60-fold accumulation of 4-HPLA and 100-fold accumulation of PLA occurred in 24-hour nutrient medium during *Klebsiella* culture compared with the control [12]. Apparently, the biotransformation of metabolites such as PLA and 4-HPLA is performed by healthy human microbiota under the conditions of existing microbial biodiversity, when the excess of metabolites produced as a result of the activity of some bacterial species can be metabolized by other bacterial species according to the «pipeline» principle, resulting in the generation of end products of microbial metabolism, such as PLA [11, 26].

The inability to further metabolize occurs due to changes in the composition and forms of microorganisms under unfavorable conditions and extensive antibiotic therapy. PCR analysis of the taxonomic composition of patients' intestinal contents revealed an anaerobic imbalance, an increase in «proinflammatory», and a decrease in «anti-inflammatory» microorganisms. This finding is consistent with previous studies characterizing the intestinal microbiota of sepsis patients [6, 27, 28]. The microbiota composition changes rapidly within hours of the onset of critical illness [29, 30]. The normal microbiome transforms into an abnormal one dominated by monotonous communities of multidrug-resistant microorganisms [31–34]. The presence of bacterial forms called persisters, which temporarily lose metabolic activity, may contribute to metabolic dysfunction and are challenging to detect using traditional microbiological methods [35, 36]. While a complete transition of the entire population to a persistent state is possible under nutrient starvation [37, 38], we did not specifically investigate this phenomenon.

The experiment showed that redundant sepsis-associated acids in the intestinal contents of healthy humans are partially eliminated by the normobiota, leading to a decrease in the levels (biotransformation) of these acids. The results are consistent with the concept of metabolic interaction potential, based on genomic metabolic reconstructions, which shows that microbial communities contain metabolically interdependent groups. Cooperating groups can efficiently utilize limited resources through metabolite exchange, providing a survival advantage and allowing coexistence in different niches compared to smaller microbial communities [39]. Widespread use of antibiotics disrupts existing metabolic connections and leads to dysfunction of the microbial community as a single organism. Maintaining the biodiversity of the microbiota is an important task because this diversity of species provides continuous biotransformation to the final microbial metabolites that are «useful and safe» for the host.

Conclusion

The accumulation of sepsis-associated metabolites in the blood is not only due to their excessive entry from bacterial growth sites (purulent and inflammatory infection sites), but also largely due to the inability of the gut microbiota to metabolically biotransform these compounds. Comparison of the metabolomic profiles of normobiota and pathobiotain an in vitro experiment showed that when loaded with sepsis-associated metabolites of PLA and 4-HPLA, the microbiota of a healthy individual biotransforms them into the end products of microbial metabolism, whereas the pathobiotaof a septic patient is unable to perform this function. Thus, in sepsis, along with other signs of decompensation of vital functions such as respiration, circulation, brain function, etc., there is a disturbance in microbiota metabolism that contributes to the progression of sepsis and increases the risk of a fatal outcome. Targeting the gut microbiota to eliminate metabolic dysfunction may be a promising strategy for the prevention and treatment of sepsis.

References

1. *Evans L., Rhodes A., Alhazzani W., Antonelli M., Coopersmith C.M., French C., Machado F.R., et al.* Surviving sepsis campaign: international guidelines for management of sepsis and septic shock 2021. *Intensive Care Med.* 2021; 47 (11): 1181–1247. DOI: 10.1007/s00134-021-06506-y. PMID: 34599691.
2. *Zhang Y.-Y., Ning B.-T.* Signaling pathways and intervention therapies in sepsis. *Signal Transduct Target Ther.* 2021; 6 (1): 407. DOI: 10.1038/s41392-021-00816-9. PMID: 34824200.
3. *Быкова К.М., Саввина И.А., Бодарева Н.В., Забродская Ю.М.* Патофизиологические аспекты и комплексная диагностика сепсис-ассоциированной энцефалопатии. Перспективы этиопатогенетической терапии. *Анестезиология и реаниматология.* 2022; (4): 92–98. [*Bykova K.M., Savvina I.A., Bodareva N.V., Zabrodskaya Yu.M.* Pathophysiological aspects and complex diagnosis of sepsis-associated encephalopathy. Prospects for etiopathogenetic therapy. *Russian Journal of Anaesthesiology and Reanimatology/ Anesteziologiya i Reanimatologiya.* 2022; (4): 92–98. (In Russ.)]. DOI: 10.17116/anaesthesiology202204192.
4. *Ковзель В.А., Давыдова Л.А., Карзин А.В., Царенко С.В., Батурова В.Ю., Полупан А.А., Гутников А.И.* Методы экстракорпоральной гемокоррекции при сепсисе (обзор). *Общая реаниматология.* 2023; 19 (2): 68–82. [*Kovzel V.A., Davydova L.A., Karzin A.V., Tsarenko S.V., Baturova V.Yu., Polupan A.A., Gutnikov A.I.* Methods of extracorporeal hemocorrection in sepsis (Review). *General Reanimatology/ Obshchaya Reanimatologya.* 2023; 19 (2): 68–82. (In Russ.)]. DOI: 10.15360/1813-9779-2023-2-2282.
5. *Adelman M.W., Woodworth M.H., Langelier C., Busch L.M., Kempker J.A., Kraft C.S., Martin G.S.* The gut microbiome's role in the development, maintenance, and outcomes of sepsis. *Crit Care.* 2020; 24 (1): 278. DOI: 10.1186/s13054-020-02989-1. PMID: 32487252.
6. *Chernevskaya E., Beloborodova N., Klimenko N., Pautova A., Shilkin D., Gusarov V., Tyakht A.* Serum and fecal profiles of aromatic microbial metabolites reflect gut microbiota disruption in critically ill patients: a prospective observational pilot study. *Crit Care*; 2020; 24 (1): 312. DOI: 10.1186/s13054-020-03031-0. PMID: 32513224.
7. *Xiao K., Sun Y., Song J., Li L., Mao W., Jiang C.* Gut microbiota involved in myocardial dysfunction induced by sepsis. *Microb Pathog.* 2023; 175: 105984. DOI: 10.1016/j.micpath.2023.105984. PMID: 36638851.
8. *Wasyluk W., Zwolak A.* Metabolic alterations in sepsis. *J Clin Med.* 2021; 10 (11): 2412. DOI: 10.3390/jcm10112412. PMID: 34072402.
9. *Sun S., Wang D., Dong D., Xu L., Xie M., Wang Y., Ni T., et al.* Altered intestinal microbiome and metabolome correspond to the clinical outcome of sepsis. *Crit Care.* 2023; 27 (1): 127. DOI: 10.1186/s13054-023-04412-x. PMID: 36978107.
10. *Beloborodova N.V., Sarshor Yu.N., Bedova A.Yu., Chernevskaya E.A., Pautova A.K.* Involvement of aromatic metabolites in the pathogenesis of septic shock. *Shock.* 2018; 50 (3): 273–279. DOI: 10.1097/SHK.0000000000001064. PMID: 29189605.
11. *Beloborodova N.V.* Serum aromatic microbial metabolites as biological markers in intensive care. In: Rajendram, R., Preedy, V.R., Patel, V.B. (eds.). Biomarkers in trauma, injury and critical care. Biomarkers in disease: methods, discoveries and applications. Springer, Cham. 2023; 13: 245–268. DOI: 10.1007/978-3-031-07395-3_64.
12. *Белобородова Н.В., Байрамов И.Т., Оленин А.Ю., Федотчева Н.И.* Экзометаболиты некоторых анаэробных микроорганизмов микрофлоры человека. *Биомедицинская химия.* 2011; 57 (1): 95–105. [*Beloborodova N.V., Bairamov I.T., Olenin A.Iu., Fedotcheva N.I.* Exometabolites of some anaerobic microorganisms of the human microflora. *Biomed Khim.* 2011; 57 (1): 95–105. (In Russ.)]. DOI: 10.18097/pbmc20115701095. PMID: 21516781.
13. *Jenner A.M., Rafter J., Halliwell B.* Human fecal water content of phenolics: the extent of colonic exposure to aromatic compounds. *Free Radic Biol Med.* 2005; 38 (6): 763–772. DOI: 10.1016/j.freeradbiomed.2004.11.020. PMID: 15721987.
14. *Russell W.R., Duncan S.H., Scobbie L., Duncan G., Cantlay L., Calder A,G,, Anderson S.E., et al.* Major phenylpropanoid-derived metabolites in the human gut can arise from microbial fermentation of protein. *Mol Nutr Food Res.* 2013; 57 (3): 523–535. DOI: 10.1002/mnfr.201200594. PMID: 23349065.
15. *Muñoz-González I., Jiménez-Girón A., Martín-Álvarez P.J., Bartolomé B., Moreno-Arribas M.V.* Profiling of microbial-derived phenolic metabolites in human feces after moderate red wine intake. *J Agric Food Chem.* 2013; 61 (39): 9470–9. DOI: 10.1021/jf4025135. PMID: 24010549.
16. *Saito Y., Sato T., Nomoto K., Tsuji H.* Identification of phenol- and p-cresol-producing intestinal bacteria by using media supplemented with tyrosine and its metabolites. *FEMS Microbiol Ecol.* 2018; 94 (9): fiy125. DOI: 10.1093/femsec/fiy125. PMID: 29982420.

17. *Gutiérrez-Díaz I., Fernández-Navarro T., Salazar N., Bartolomé B., Moreno-Arribas M.V., López P., Suárez A., et al.* Could fecal phenylacetic and phenylpropionic acids be used as indicators of health status? *J Agric Food Chem.* 2018; 66 (40): 10438–10446. DOI: 10.1021/acs.jafc.8b. PMID: 30227707.
18. *Жиркова Е.А., Спиридонова Т.Г., Сачков А.В., Елисеенкова Е.А., Брыгин П.А., Никулина В.П., Кашолкина Е.А., с соавт.* Биомаркеры воспаления при острой дыхательной недостаточности у пациентов с ингаляционной травмой. *Анестезиология и реаниматология.* 2022; (5): 23-29. [*Zhirkova E.A., Spiridonova T.G., SachkovA.V., Eliseenkova E.A., Brygin P.A., Nikulina V.P., Kasholkina E.A., et al.* Biomarkers of inflammation in acute respiratory insufficiency in patients with inhalation injury. *Russian Journal of Anaesthesiology and Reanimatology/ Anesteziologiya i Reanimatologiya.* 2022; (5): 23–29. (In Russ.)]. DOI: 10.17116/anaesthesiology202303145.
19. *Козлов И.А., Соколов Д.А.* Оценка биомаркера напряжения миокарда NT-proBNP в реальной клинической практике. *Общая реаниматология.* 2023; 19 (1): 4–12. [*Kozlov I.A., Sokolov D.A.* Assessment of the myocardial stress biomarker NT-proBNP in real clinical practice. *General Reanimatology/ Obshchaya Reanimatologya.* 2023; 19 (1): 4–12. (In Russ.)]. DOI; 10.15360/1813-9779-2023-1-2272.
20. *Dwivedy A.K., Shah S.N.* Effects of phenylalanine and its deaminated metabolites on Na^+,K^+-ATPase activity in synaptosomes from rat brain. *Neurochem Res.* 1982; 7 (6): 717-25. DOI: 10.1007/ BF00965524. PMID: 6289150.
21. *Zhu L., Shao Y.D., Wang J.Y., Lin D.L., Gu C.L., Li Y.H., Gu J.G., et al.* Effect of beta-phenyl lactic acid on platelet aggregation, thrombosis, and plasma cAMP content. *Zhongguo Yao Li Xue Bao.* 1988; 9 (3): 249–251. PMID: 2850712.
22. *Вахитова Т.Я., Чалисова Н.И., Ситкин С.И., Салль Т.С., Шалаева О.Н., Демьянова Е.В., Моругина А.С., с соавт.* Низкомолекулярные компоненты метаболома крови регулируют пролиферативную активность в клеточных и бактериальных культурах. *Доклады академии наук.* 2017; 472 (4): 491–493. [*Vakhitova T.Ya., Chalisova N.I., Sitkin S.I., Sall T.S., Shalaeva O.N., Demyanova E.V., Morugina A.S., et al.* Low molecular weight components of the blood metabolome regulate proliferative activity in cell and bacterial cultures. *Reports of the Academy of Sciences.* 2017; 472 (4): 491–493. (In Russ.)]. DOI: 10.1134/S0012496617010069. PMID: 28429257.
23. *Martiìn M., Gibello A., Fernaìndez J., Ferrer E., Garrido-Pertierra A.* Catabolism of 3- and 4-hydroxyphenylacetic acid by Klebsiella pneumoniae. *J Gen Microbiol.* 1991; 137 (3): 621–628. DOI: 10.1099/00221287-137-3-621.PMID: 1851804.
24. *Calder P.C.* n-3 fatty acids, inflammation, and immunity — relevance to postsurgical and critically ill patients. *Lipids.* 2004; 39 (12): 1147–1161. DOI: 10.1007/s11745-004-1342-z. PMID: 15736910.
25. *Dodd D., Spitzer M.H., Van Treuren W., Merrill B.D., Hryckowian A.J., Higginbottom S.K., Le A., et al.* A gut bacterial pathway metabolizes aromatic amino acids into nine circulating metabolites. *Nature.* 2017; 551 (7682): 648–652. DOI: 10.1038/nature24661. PMID: 29168502.
26. *Díaz E., Ferrández A., Prieto M.A., García J.L.* Biodegradation of aromatic compounds by Escherichia coli. *Microbiol Mol Biol Rev.* 2001; 65 (4): 523–569. DOI: 10.1128/MMBR.65.4.523-569.2001. PMID: 11729263.
27. *Clarkson S.M., Giannone R.J., Kridelbaugh D.M., Elkins J.G., Guss A.M., Michener J.K.* Construction and optimization of a heterologous pathway for protocatechuate catabolism in *Escherichia coli* enables bioconversion of model aromatic compounds. *Appl Environ Microbiol.* 2017; 83 (18): e01313–17. DOI: 10.1128/AEM.01313-17. PMID: 28733280.
28. *Smith E.A., Macfarlane G.T.* Enumeration of human colonic bacteria producing phenolic and indolic compounds: effects of pH, carbohydrate availability and retention time on dissimilatory aromatic amino acid metabolism. *J Appl Bacteriol.* 1996; 81 (3): 288–302. DOI: 10.1111/j.1365-2672.1996.tb04331.x. PMID: 8810056.
29. *Liu Y., Guo Y., Hu S., Wang Y., Zhang L., Yu L., Geng F.* Analysis of the dynamic changes in gut microbiota in patients with different severity in sepsis. *BMC Infect Dis.* 2023; 23 (1): 614. DOI: 10.1186/s12879-023-08608-y. PMID: 37723420
30. *Zhou Y., Luo Y., Wang X., Luan F., Peng Y., Li Y., Ma X., et al.* Early gut microbiological changes and metabolomic changes in patients with sepsis: a preliminary study. *Int Microbiol.* 2023; 26 (4): 1131–1142. DOI: 10.1007/s10123-023-00363-z. PMID: 37145385.
31. *Evans T., Ali U., Anderton R., Raby E., Manning L., Litton E.* Lower gut dysbiosis and mortality in acute critical illness: a systematic review and meta-analysis. *Intensive Care Med Exp.* 2023; 11 (1): 6. DOI: 10.1186/s40635-022-00486-z. PMID: 36732439.
32. *Chanderraj R., Baker J.M., Kay S.G., Brown C.A., Hinkle K.J., Fergle D.J., McDonald R.A., et al.* In critically ill patients, anti-anaerobic antibiotics increase risk of adverse clinical outcomes. *Eur Respir J.* 2023; 61 (2): 2200910. DOI: 10.1183/13993003.00910-2022. PMID: 36229047.

33. *Zanza C., Romenskaya T., Thangathurai D., Ojetti V., Saviano A., Abenavoli L., Robba C., et al.* Microbiome in critical care: an unconventional and unknown ally. *Curr Med Chem.* 2022; 29 (18): 3179–3188. DOI: 10.2174/0929867328666210915115056. PMID: 34525908.
34. *Zaborin A., Smith D., Garfield K., Quensen J., Shakhsheer B., Kade M., Tirrell M., et al.* Membership and behavior of ultra-low-diversity pathogen communities present in the gut of humans during prolonged critical illness. *mBio* 2014; 5 (5): e01361-14. DOI: 10.1128/mBio.01361-14. PMID: 25249279.
35. *Ситкин С.И., Вахитов Т.Я., Демьянова Е.В.* Микробиом, дисбиоз толстой кишки и воспалительные заболевания кишечника: когда функция важнее таксономии. *Альманах клинической медицины.* 2018; 46 (5): 396–425. [*Sitkin S.I., Vakhitov T.Ya., Demyanova E.V.* The microbiome, colon dysbiosis, and inflammatory bowel disease: that moment when function is more important than taxonomy. *Almanac of Clinical Medicine.* 2018; 46 (5): 396–425. (In Russ.)]. DOI: 10.18786/2072-0505-2018-46-5-396-425.
36. *Zhang Z., Cheng L., Ning D.* Gut microbiota and sepsis: bidirectional Mendelian study and mediation analysis. *Front Immunol.* 2023; 14: 1234924. DOI: 10.3389/fimmu.2023. 1234924. PMID: 37662942.
37. *Balaban N.Q., Merrin J., Chait R., Kowalik L., Leibler S.* Bacterial persistence as a phenotypic switch. *Science.* 2004; 305 (5690): 1622–1625. DOI: 10.1126/science.1099390. PMID: 15308767.
38. *Андрюков Б.Г., Ляпун И.Н.* Молекулярные механизмы персистенции бактерий. *Журнал микробиологии, эпидемиологии и иммунобиологии.* 2020; 97 (3): 271–279. [*Andryukov B.G., Lyapun I.N.* Molecular mechanisms of persistence of bacteria. *Journal of microbiology, epidemiology and immunobiology/ Zh. Mikrobiol. Epidemiol. Immunobiol.* 2020; 97 (3): 271–279. (In Russ.)]. DOI: 10.36233/0372-9311-2020-97-3-10.
39. *Orman M.A., Brynildsen M.P.* Inhibition of stationary phase respiration impairs persister formation in *E. coli. Nat Commun.* 2015; 6: 7983. DOI: 10.1038/ncomms8983. PMID: 26246187.
40. *Маркелова Н.Н., Тутельян А.В., Писарев В.М., Гапонов А.М.* Некоторые закономерности формирования персистирующих форм клинических изолятов грамотрицательных бактерий. *Антибиотики и Химиотерапия.* 2018; 63 (7–8): 41–46. [*Markelova N.N., Tutelyan A.V., Pisarev V.M., Gaponov A.M.* Some regularities of persistent forms of clinical isolates of gram-negative bacteria formation. *Antibiotics and Chemotherapy/Antibiotiki i Khimioterapiya.* 2018; 63 (7–8): 41–46. (In Russ.)].
41. *Zelezniak A., Andrejev S., Ponomarova O., Mende D.R., Bork P., Patil K.R.* Metabolic dependencies drive species co-occurrence in diverse microbial communities. *Proc Natl Acad Sci U S A.* 2015; 112 (20): 6449–54. DOI: 10.1073/pnas.1421834112. PMID: 25941371.

Received 27.07.2023
Accepted 31.10.2023

https://doi.org/10.15360/1813-9779-2023-6-13-24

Prognosis for Recovery from a Vegetative State

Yulia I. Vainshenker[1]*, Nikolay V. Tsygan[2,3], Miroslav M. Odinak[2], Igor V. Litvinenko[2]

[1] Institute of experimental medicine,
12 Akad. Pavlov Str., 197376, Saint Petersburg, Russia
[2] Kirov Military Medical Academy,
6 Akad. Lebedev Str., 194044 Saint Petersburg, Russia
[3] Konstantinov St. Petersburg Institute for Nuclear Physics, National Research Center «Kurchatov Institute»,
1 Orlova roshcha mkr., 188300 Gatchina, Leningrad region, Russia
[4] National Research Center «Kurchatov Institute»,
1 Akad. Kurchatova Sq., 123182 Moscow, Russia

For citation: *Yulia.I. Vainshenker, Nikolay V. Tsygan, Miroslav M. Odinak, Igor V. Litvinenko.* Prognosis for Recovery from a Vegetative State. *Obshchaya Reanimatologiya = General Reanimatology.* 2023; 19 (6): 13–24. https://doi.org/10.15360/1813-9779-2023-6-13-24 [In Russ. and Engl.]

*__Correspondence to:__ Yulia I. Vainshenker, juliavajn@mail.ru

Summary

The prognosis for recovery from a vegetative state (VS) remains underdeveloped.

Objective. To determine the feasibility of prognosis for recovery from a vegetative state based on clinical comparison of 18- fluorodeoxyglucose-PET (18FDGPET) and MRI (SCT) data.

Materials and methods. We compared and analyzed retrospectively cerebral PET and MRI (SCT) scans and relevant prognostic criteria (including revised coma recovery scale — CRS-R scores) prospectively during 6–84 months of follow-up in a cohort of 39 VS patients. All VS cases were of different etiologies, lasting for more than 2 months after brain damage (including 18 patients in chronic VS).

Pairwise comparison of groups was used (significance level $P<0.05$) and multiple comparison for three groups with a Bonferroni correction at $P<0.017$ was employed.

Results. Three patterns were identified when comparing 18FDGPET and MRI (SCT) neuro-images: pattern I — the area of functional alterations was larger than the area of structural damage, pattern II — complete matching of areas of structural and functional alterations, III — mixed pattern. Pattern I (69% of cases) was more common than patterns II (18%), and III (13%), $P<0.001$. There were no differences in VS etiology, VC duration, CRS-R scores, patients' gender and age between the groups of patients each falling into one of patterns. The outcome in a group with pattern I patients (all of them recovered from VS) was better than in other two groups exhibiting patterns II or III, each, $P<0.001$. In a group of patients with pattern III the recovery was better than in pattern II (all patients remained in VS), $P=0.018$. The increases in the total CRS-R score values were as follows: 12,1±4,46; Me=12 (4–19), $N=27$ (patients with a pattern I); 0±1,54 (–2–1, $Me=0$, $N=7$ (patients with a pattern II); and 5,20±4,09/ $Me=4$ (1–10), $N=5$ (patients with a pattern III). Significant increases in neurological improvement were revealed in pattern I patients with non-chronic VS versus chronic VS, $P=0.003$.

Conclusion. Clinical comparison of PET/MRI (SCT) data showed certain potential to predict patient's recovery from VS in 87% of cases. A retrospectively confirmed favorable prognosis in patients with pattern I was established in 69% cases, unfavorable (pattern II patients) was defined in 18% cases, regardless of other prognostic criteria, including chronic VS. Therefore, the data confirms the feasibility and clinical relevance of neurophysiological justification as a candidate approach for evaluating the prospect of recovering patients from VS.

Keywords: chronic disorders of consciousness; chronic vegetative state; recovery from a vegetative state; prediction; potential for recovery of consciousness

Conflict of interest. The authors declare no conflict of interest.

Acknowledgments. The authors are grateful to Academician of RAS Svyatoslav V. Medvedev and all staff members of IHB RAS who participated in the examination and treatment of the patients.

Read the full-text English version at www.reanimatology.com

Introduction

Significant advances in emergency medicine in the treatment of acute severe brain injury have been shown to have some drawbacks. With increasing survival comes increasing disability, including the most severe and still poorly understood chronic disorder of consciousness (CDC) [1, 2]. Chronic disorder of consciousness, diagnosed 4 weeks and later after brain injury, refers to the first stages of recovery from coma. It includes the vegetative state (VS), characterized by wakefulness without awareness, and the minimally conscious state (MCS), with minimal signs of conscious behavioral responses, further subdivided into MCS (-) and MCS (+) based on their manifestations. The next stage, emergence from MCS with recovery of functional communication, is not related to CDC [1, 3, 4].

The VS, as well as any stage of recovery from coma, may turn out to be the final stage of recovery of consciousness, although the patient's survival may last for years and decades, which raises many medico-social, economic, as well as ethical prob-

lems [2, 4–6]. In this context, the prediction of outcome, especially in terms of improvement of consciousness, becomes a crucial issue [4, 6, 7]. Over the past two decades, significant progress has been made in diagnosing, predicting, and promoting recovery of consciousness in patients with CDC [8]. However, with an arsenal of prognostic factors and criteria proposed on the basis of virtually all diagnostic modalities used in the study of the brain, many of which are becoming increasingly complex [7–11], there is no reliable pathogenetic and clinically relevant prognosis, nor is there such a treatment [3, 4]. The main prognostic criteria remain clinical and epidemiological [4]. This is largely due to the lack of a universally accepted neurophysiological concept explaining the mechanisms of VS development and recovery [12].

Despite the fact that an empirical approach that does not rely on pathogenesis may undermine the prognostic component of the obtained data [13], multicenter studies and an integrated approach, particularly with the use of non-activation functional neuroimaging [14–16], are expected to provide a breakthrough in prognostication. Previously [17], we proposed using the correlation of structural (MRI, spiral CT) and functional (18FDG-PET) brain abnormalities to determine the potential for recovery of consciousness when considering VS from the perspective of Natalia Bekhtereva's theory of stable pathological state (SPS) of the brain. Although this parameter is critical in determining a valid prognosis [8], the efficacy of such a prediction has not been proven.

The aim of this study was to assess the utility of prediction of recovery from VS based on clinical correlation of 18FDG-PET and MRI (SCT) data.

Materials and Methods

In patients with CDC (VS) admitted for comprehensive diagnosis and treatment in the Department of Anesthesiology and Intensive Care of the Clinic of N. P. Bekhtereva Institute of Human Brain of the Russian Academy of Sciences (IHB RAS) from 2007 to 2016, we performed a retrospective analysis and correlation of 18FDG-PET and MRI (SCT) data, as well as several known prognostic factors, criteria, and follow-up data. All examinations and treatments were carried out with the patients' relatives/guardians' written informed consent. The Ethics Committee and Academic Council of IHB RAS approved the protocol for comprehensive examination and treatment.

We evaluated a consecutive sample of 39 patients with VS who underwent 18FDG-PET and MRI (or spiral CT if MRI was contraindicated) for a detailed assessment of neuropsychiatric status during their first hospitalization at the IHB RAS before specialized treatment, which served as a baseline.

Unknown follow-up was considered a criterion for non-inclusion. Follow-up data were evaluated at 6 months and beyond (up to 7 years) by determining the maximum level of consciousness achieved during this period. The duration of a single hospitalization in the IHB RAS was at least 1 month (usually 1–3 months). Repeated hospitalizations, including multiple hospitalizations with the whole set of examinations, occurred in 26 patients.

Classification of VS according to etiology and duration into chronic (in traumatic etiology >12 months from the onset of brain injury, in non-traumatic etiology >3 months) and non-chronic types, as well as determination of the level of consciousness and its changes according to the Coma Recovery Scale-Revised (CRS-R) were performed in accordance with international guidelines and criteria approved in the Russian Federation [1, 3, 4, 18].

Traumatic VS (VS_t) was diagnosed in 23 of 39 patients (13 women, 26 men; age 29.8 10.5 years (min 14 — max 54, *Me*=27), and non-traumatic VS (VS_{nt}) in 16 patients.

Chronic VS was observed in 18 patients (VS_t 9 and VS_{nt} 9). The actual duration ranged from 18 months to 10 years after brain injury in VSt and from 6 months to 5 years in VS_{nt}.

In the remaining 21 patients (14 VS_t and 7 VS_{nt}), the actual time of VS was >2 months (up to 12 months for VS_t, up to 3 months for VSnt) after the brain injury. For clarity, it was further referred to as non-chronic VS.

The cause of VSnt was hypoxic-ischemic and anoxic brain injury in 13 patients, inflammatory in 2 patients, and toxic in 1 patient. TBI was severe in all 23 patients with VSt (severe brain contusion with/without brain compression in 23 patients, diffuse axonal damage grade II–III in 20 patients), 17 of whom underwent various neurosurgical procedures. Prior to admission to the IHB RAS, all 39 patients received intensive care in specialized hospitals for at least 2 months from the time of the brain injury and were subsequently hospitalized either for life-threatening complications or (less frequently) for rehabilitation. The rest of the time, patients remained at home or in care facilities. Various complications were recorded in all patients during the first 6 months of VS (purulent/septic in 39, paroxysmal sympathetic hyperactivity syndrome in 39, hypertensive hydrocephalus in 17, epileptic syndrome in 18, and others). MRI (SCT) revealed progressive brain atrophy of varying degrees in the thalamus, subcortical nuclei, and cerebellum in all 18 patients with chronic VS; no change (improvement) in consciousness was documented from the time of coma recovery. In 11 patients, a benzodiazepine test [12] was performed. All patients were in critical condition with compensated vital functions when admitted to IHB RAS.

MRI was performed on 1.5 Tesla (General Electric) before 2009 and 3 Tesla (Philips Achieva 3T)

since 2009. Sequences used: T2VI (weighted images); T2-FLAIR WI; T1 WI non-contrast and, if necessary, with contrast enhancement (Gadadiomide from Omniscan). Spiral CT was performed on a Gemini TF Base scanner (Philips, Netherlands). 18FDG-PET was performed with a PC2048-15B (Scanditronix) or Gemini TF Base (Philips) PET scanner.

The functional status of brain regions was determined using the glucose metabolic rate (GMR) with evaluation of images in each image acquisition by visual and semi-quantitative methods. The value of GMR within the physiological range [19] was defined as «normal», and the value outside the reference values (regardless of intensity) was defined as «abnormal». The study was performed in a standardized manner under identical conditions. The correlation (congruency/non-congruency) of the areas of structural (MRI, SCT) and functional (PET) abnormalities in separate brain regions was checked visually. In particular, areas of functional impairment (PET) and areas of structural lesions (1.5T MRI or 3T MRI or SCT) were identified and then matched based on the topographic anatomy of the brain.

The congruence of functional and structural abnormalities was confirmed if the anatomical localization of the lesion coincided (with precision down to the details of individual structures such as gyrus, subcortical nuclei, brainstem, determined by generally accepted known anatomical landmarks) and if the area of abnormalities differed by no more than 15–20%. Image fusion using high-end software was carried out in some cases (when the area of abnormality was small) for clarification and quantitative comparison of lesion areas on PET and MRI (SCT) images. In cases where it was possible to perform repeated (multiple) PET scans, changes in metabolic abnormalities between consecutive PET scans were identified if the increase/decrease in metabolism exceeded the physiological variation of this parameter for the corresponding structure (usually 7–15% [19]) and/or the change in area of GMR abnormalities exceeded 20–25%.

Treatment options for patients were not considered. Treatment was based on clinical need, which is generally consistent with current guidelines and protocols [3, 4, 20, 21]. In addition, diagnosis and treatment of low-grade infection were performed [22], and high-dose multi-pattern botulinum therapy (IncobotulinumtoxinA) was used to treat generalized spasticity and dystonia [23].

Clinical data were analyzed with Statistica for Windows V11.0. Non-parametric methods were used. Frequency variables were compared using χ^2 and χ^2 with Yates correction (for small groups), Fisher's criterion. To evaluate quantitative parameters, means, errors of means, standard deviations, data range (min-max), medians, descriptive statistics (absolute and relative frequencies, ratios) were calculated. Quantitative parameters were compared using Mann–Whitney, Wald, median χ^2 criteria. Pairwise comparisons of groups were performed (differences were considered significant at $P<0.05$). For additional confirmation of some correlations, multiple comparisons of groups were performed with Bonferroni correction for three groups; differences at $P<0.017$ were considered significant. Spearman's rank correlation coefficients were calculated.

Results

Clinical correlation of PET and MRI (SCT) data revealed the following 3 variants of brain damage (without taking topography into account).

Variant I was identified when the area of energy metabolism disturbance exceeded the area of structural damage. In addition to a gross decrease (up to absence) of metabolism directly in the areas of structural damage, perifocal and/or visually preserved brain areas also showed varying degrees of metabolic abnormalities (Fig.)

Variant II was confirmed when the area of energy metabolism disorder was completely equal to or smaller than the area of structural damage (Fig.)

Variant III (mixed) was characterized by a combination of variants I and II in different anatomical structures. This variant was recognized in cases that did not fall under variants I and II.

The frequency of the three variants of PET/MRI (SCT) correlations, as well as the characteristics of VS corresponding to these variants with the follow-up data on change of consciousness are shown in the Table.

Variant I was significantly more frequent than II ($P<0.001$) and III ($P<0.001$). The frequency of variants II and III did not differ ($P=0.54$). Patients classified into the different correlation variants did not differ in gender ($P=0.79$ or more), age ($P=0.47$ or more), duration of VS (non-chronic/chronic) ($P=0.74$ or more), occurrence of VS of different etiology (traumatic/non-traumatic) ($P=0.29$ or more), total CRS-R score ($P=0.88$ or more). Inflammatory epilepsy was characteristic of all patients with variant III.

The outcome for variant I (all recovered from VS) was better than for variant II ($P<0.001$) and variant III ($P<0.001$), and for variant III better than for variant II (all remained in VS) ($P=0.018$).

The best outcome in terms of increase in total SRS-R score was also with variant I (vs II, $P<0.001$, vs III, $P=0.001$) and the worst with variant II (less increase in total score than variant III, $P=0.035$). Outcomes were better with variant I ($P<0.001$) than with variant II for both chronic and non-chronic VS, and with variant III for non-chronic VS ($P<0.001$).

In patients with variant I, the increase in total CRS-R score at baseline was less in chronic VS than in non-chronic VS ($P=0.003$). In variant II, the increase in score did not differ according to the duration of VS ($P=0.84$), while in variant III there was

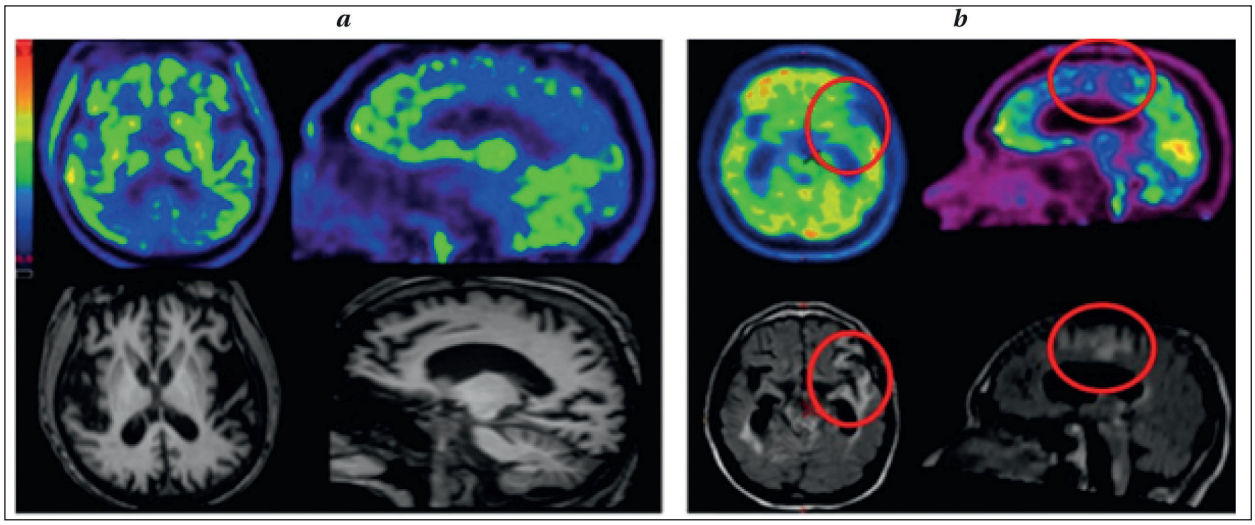

Fig. Standardized evaluation and comparison of individual 18F-FDG PET images (top row) and MRI/CT (bottom row) for prognostic purposes.
Note. *a* — variant I: areas of reduced glucose metabolism (PET) are significantly more extensive than corresponding areas of structural damage (MRI, T1). *b* — variant II: areas of reduced glucose metabolism (PET) coincide with areas of structural damage (CT). At the time of examination, both patients are in chronic traumatic VS.

a trend toward a greater increase in cases of chronic VS (P=0.052).

In a multiple comparison of groups with Bonferroni correction, all outcome parameters were better in patients with variant I than in patients with variant II and III (P<0.017). The worse outcome in variant II compared to variant III was observed only as a trend in «remained in VS/recovered from VS», which is the key prognostic parameter.

Thus, variant I (69% of patients) was prognostically favorable. In a pairwise comparison of the groups, the differences in outcome were significant for variant II (18% of patients) and III (13% of patients). The differences in the course of neurological recovery in these patients were indirectly confirmed by the trend toward worsening of the key index in multiple comparisons with few observations. This allowed us to consider variant II as prognostically unfavorable (Fig.), and variant III as equivocal. Taking into account the above, the accuracy of prognosis (favorable/unfavorable) was actually 87%, of which the prognosis was favorable in 69% of patients, unfavorable in 18%, and equivocal in 13%.

Changes in PET parameters in combination with clinical characteristics were analyzed in 26 of 39 patients in VS.

In the variant I group, 21 patients (12 VS_t, 9 VS_{nt}) were followed up with improvement of consciousness. In all patients, normalization of energy metabolism (PET) was observed over time, consisting of reduction of the area of abnormal metabolism (usually beyond the area of structural damage) and/or improvement of GMR. In 18 patients (chronic and non-chronic VS of various etiologies), PET changes were recorded before and/or simultaneously with the appearance of behavioral signs of awareness. In addition, in one of these patients, clinical and neuroimaging parameters obtained at the time of improvement in consciousness were compared with postmortem morphological data (acute cardiac death), which has been reported in detail separately [23]. In the other three patients (all with chronic VS of different etiology), the initial improvement in GMR did not exceed the level of physiological variability, but became evident after clinical changes. In all patients, GMR improvement did not occur in all brain regions and was not immediate. Initially, when the metabolic disorders persisted, the improvement of this parameter occurred gradually with the improvement of consciousness (in our observations, during repeated courses of treatment). If patients' consciousness did not change or even worsened over time (compared to the previous examination), GMR did not change and sometimes decreased. Changes in the energy metabolism of all or some brain regions were manifested in the evolution of neurological symptoms and/or electrophysiological parameters [23].

In the variant II group, 4 patients who remained in VS were followed up. In 2 patients (VS_t), PET data and level of consciousness did not change over time. In the third patient (VS_t), an episode of minimal improvement was observed, when inconclusive and transient eye fixation occurred without changes in PET parameters. At the insistence of the relatives, treatment was discontinued and only nursing care was provided. One year later, in the control study, the level of consciousness corresponded to VS. There were negative changes (compared to baseline data) in the CRS-R score with an increase in the area of structural and functional damage.

The fourth patient, who had already been in VS for 5 years at the time of admission to the IHB

Table. Variants of PET/MRI (CT) correlation: frequency, characteristics, and outcomes of VS.

Parameter, units	Values in compared groups,			*P*		
	I	II	III	I / II	I/ III	III/ II
Frequency, *N* (%)	27 (69)	7 (18)	5 (13)	<0.001; <0.017	<0.001; <0.017	>0.05; >0.017
Characteristics of VS cases						
Sex (female/male), *N*	9 : 18	2 : 5	2 : 3	>0.05; >0.017	>0.05; >0.017	>0.05; >0.017
Age, years *M*±σ (min–max), *[Me]*	30.44±9.85 (17–54), [27]	31.28±13.90 (15–54), [26]	24.40±9.15 (14–39), [23]	>0.05; >0.017	>0.05; >0.017	>0.05; >0.017
VS_{nc} : VS_c, *N*	14 : 13	4 : 3	3 : 2	>0.05; >0.017	>0.05; >0.017	>0.05; >0.017
VS_t : VS_{nt}, *N*	15:12	4:3	4:1	>0.05; >0.017	>0.05; >0.017	>0.05; >0.017
CRS-R , total score, *M*±σ (min–max), *[Me]*	4.11±1.37 (1–6), [4]	4.0±0.82 (3–5), [4]	3.80±1.64 (2–6), [3]	>0.05; >0.017	>0.05; >0.017	>0.05; >0.017
Follow-up: △ CRS-R, *M*±σ (min–max) [Me]						
All VS cases	12.1±4.46 (4–19), [12]	0±1.54 (–2–1), [0]	5.20±4.09 (1–0), [4]	<0.001; <0.017	<0.01; <0.017	<0.05; >0.017
VS_{nc}	14.28±4.45 (7–9), [15]	0.25±1.15 (–2–1), [0]	4.33±4.93 (1–10), [2]	<0.001; <0.017	<0.001; <0.017	>0.05; >0.017
VS_c	9.7±3.19 (4–14), [11]	0.33±0.58 (0–1), [0]	6.50±3.53 (4–9), [6.5]	<0.001; <0.017	>0.05; >0.017	>0.05; >0.017
P-value for VS_{nc} / VS_c	<0.01	>0.05	>0.05*	—	—	—
Follow-up: maximal consciousness						
Remained in VS: Recovered from VS, All VS cases, *N*	0 : 27	7 : 0	2 : 3	<0.001; <0.017	<0.001; <0.017	<0.05; >0.017*
MCS(-) : MCS(+) : EMCS						
All VS cases, *N*	7 : 14 : 6	0 : 0 : 0	2 : 1 : 0	n/p	n/p	n/p
VS_{nc}, *N*	1 : 8 : 5	0 : 0 : 0	1 : 0 : 0	n/p	n/p	n/p
VS_c, *N*	6 : 6 : 1	0 : 0 : 0	1 : 1 : 0	n/p	n/p	n/p

Note. MCS — minimally conscious state; EMCS — emergence from minimally conscious state; VS — vegetative state; VS_c — chronic vegetative state; VS_{nc} — non-chronic vegetative state; VS_t — vegetative state of traumatic etiology; VS_{nt} — vegetative state of non-traumatic etiology; CRS-R — Coma Recovery Scale Revised; △CRS-R — increase in CRS-R score; n/p — not performed. Statistical significance level *(P)* for pairwise comparison of groups: <0.001 — strong difference; <0.01 — marked difference; <0.05 — difference; >0.05 — no difference; >0.05* — trend for difference (*P*=0.052). Additionally with Bonferroni correction for the three groups: <0.017 — significant difference; >0.017 — no difference; >0.017* — trend for difference (*P*=0.018). The exact *P*-values are shown in the text.

RAS, had brain areas with reduced GMR outside the structural damage according to the history data in the stage of non-chronic VS. The result of the benzodiazepine test suggested a favorable prognosis [12], which was the reason for initiating intensive pharmacotherapy. Brain metabolism recovered to normal and remained unchanged according to the results of repeated PET scans. However, the expected improvement in consciousness never occurred until the patient's death.

In the variant III, a patient was observed in chronic VS. Over time, the area of reduced GMR decreased and consciousness improved to MCS(-). In the following three years of survival, despite treatment attempts, the level of consciousness and PET parameters did not change.

Data on energy metabolism of individual brain regions were not evaluated in this study.

The results of the application of some prognostic factors and criteria were reported. Only 17% of 18 patients with chronic VS remained in this state (1 VS_t and 2 VS_{nt}), contrary to expectations. All (18/18) patients with chronic VS had signs of brain atrophy, 78% (14/18) had absent or extremely weak pupillary reaction to light, 44% (8/18) had the «rabbit snout» sign. No significant differences were found in the etiology of VS, with 22% (5/23) of patients with VS_t and 25% (5/23) with VSnt remaining in VS, *P*=0.87. The mean total CRS-R score remained <6 in all 39 patients, with no significant differences between those who later remained in VS (3.63±0.74 (3–5, *Me*=3.5, *N*=8)) and those who recovered to MCS (4.16±1.39 (1–6, *Me*=4, *N*=31), *P*=0.21. The prognosis according to benzodiazepine test results (accurately determined in 10 of 11 patients) was poor in 8 but confirmed in only one (for variant II); favorable in 2 but confirmed in one (for variant I).

Discussion

Most studies on predicting outcome in VS do not specifically define criteria for functional recovery, return to normal life (which is the strategic goal of rehabilitation), and even recovery from VS [4]. We focused on the latter, i. e., defining the potential to achieve at least MCS, which expands the possibilities for further treatment.

The baseline characteristics and medical histories of the patients with VS were generally not different from those reported in the literature [24]. However, our patients had some specific features related to the duration and outcome of VS. During the first 4 weeks after brain injury, the prognosis

for recovery from VS is considered «cautious» (although the prognosis for VS is less favorable than for MCS) [3, 4].

In the patients studied, the duration of impaired consciousness exceeded 2 months, and almost half of them had chronic VS, which significantly reduced their chances of improving consciousness [3, 4]. Moreover, cases of chronic VS corresponded to the so-called permanent VS (no change in chronic VS_t and VS_{nt} for more than 6 and 3 months, respectively), when recovery is highly unlikely, which is a reason to consider discontinuing life support [4].

Therefore, a rather high percentage of patients with improved consciousness attracts attention, which, on the other hand, served as a reference point for evaluating the accuracy of the proposed prognostic method. Consciousness improved in 77% (30/39) of the patients, with 71% (15/21) in non-chronic VS and 83% (15/18) in chronic VS. These results, as well as the proportion of patients with a confirmed favorable prognosis (favorable in 69%, unfavorable in 18%), are more positive than those reported by several other investigators. In comparison, the prognostic significance of the benzodiazepine test, according to its developers, was confirmed in 76% of VS cases, of which only 28% had a favorable prognosis [12]. Other data suggest that only 20% of patients with chronic VS can be expected to improve their level of consciousness [5].

Traumatic etiology of VS is considered to be prognostically more favorable than non-traumatic (the most unfavorable being anoxic) [4, 25]. According to the literature, the frequency of recovery from VS was independent of the etiology of the brain injury. This is consistent with the results of a recent multicenter study to identify predictors of short-term outcome [15].

All patients had cerebral and extracerebral complications in the early and later periods after brain injury [4, 26]. Most had CRS-R scores <6 points [18, 27], many, especially in chronic VS, had the «rabbit snout» phenomenon and absent pupillary response to light [24], which are considered negative prognostic signs. While some investigators believe that clinical assessment of CDC is fundamental for prognostication [28], it is worth noting that even the absence of all brainstem reflexes during prolonged continuous lung ventilation is not an obligatory attribute of brain death, nor does it exclude the presence of awareness (the so-called «responsive unawakefulness syndrome») [29].

All patients with VS had a variety of structural brain damage, including damage to the corpus callosum, brainstem (including dorsolateral oral areas), or corona radiata, and damage to the left (dominant) or both frontal lobes, all of which have a negative prognostic value [3]. In chronic VS (regardless of etiology), all patients had marked brain atrophy [30], sometimes involving the thalamus and cerebellum [25]. All of these structural changes were found in patients with variant I neuroimaging correlations, thus reducing their prognostic value. Furthermore, brain regions known to be uniquely associated with consciousness have not been identified [11, 29].

A number of factors considered positive, such as young age [4, 25] and early advanced treatment [31], were only implemented in variant I, although they occurred with equal frequency in all variants, including variant II. This suggests that they may be more important in predicting survival or survival time than neurological recovery.

In line with the notion that disorders of consciousness are mainly determined by functional rather than structural brain abnormalities [32], many neurophysiological prognostic criteria based on electrophysiological parameters, PET and functional MRI data have been proposed [7, 8, 10, 12, 13]. After analyzing the literature data, we conclude that the detection of patterns more expected in MCS and emergence from MCS are mostly considered positive in VS. Their detection may be of diagnostic value (given the high risk of erroneous clinical diagnosis of VS [1, 3, 4, 18]) or may serve as a predictor of recovery from VS, reflecting the spontaneous or induced [33] reorganization of the persistently impaired functional state of the brain [34].

Neurophysiological parameters were recently found to be generally better predictors of the transition from VS to MCS than from VS/MCS to emergence from MCS. However, their prognostic value has often not been confirmed [35]. For example, P300 (evoked brain potentials) [35, 15] and fMRI activation patterns, which are classic from a neurological point of view, have not proven their «favorability» [35]. Electrophysiological parameters, whose ineffectiveness we have previously shown, were not evaluated [23], but it should be noted that the benzodiazepine test [12] had no prognostic value in patients with variant I.

Although the usual prognostic criteria proved to be of little value in predicting recovery from VS in variant I, it should be stressed that they mostly focus on a rather short period from the time of brain injury, whereas markers of late recovery have not yet been identified [7]. On the other hand, since in variant I the extent of recovery from non-chronic VS was greater than from chronic VS, it is possible that all (or some) of the criteria known from the literature are essential for predicting the extent of recovery of consciousness and/or function. This assumption, which is in line with current requirements [4], warrants further investigation with a data set for pathogenetic therapy.

Most patients, especially in chronic VS, have only reached MCS levels when consciousness improved. However, the fact of transition from VS to

MCS increases not only the likelihood of further recovery but also the availability of treatment [4, 36]. We believe that the improvement of patients' consciousness (especially in chronic/permanent VS) is related to the applied therapeutic approaches, which, as well as the prognosis, are based on Natalia Bekhtereva's theory of the stable pathological state (SPS) of the brain. Evidence of the effectiveness of these methods was reported earlier [22, 23].

From the perspective of the above-mentioned theory [17, 37], VS seems to be the result of activation of the brain's protective response, which, after stabilization, is transformed into a new entity, i.e., SPS. Without going into the underlying mechanisms, we emphasize that the SPS cannot be destroyed, but only destabilized and unbalanced, which is clinically reflected (in VS patients) in the transition to the next level of consciousness, which in turn represents a new SPS, and so on. Visualization of brain regions with impaired functional state outside of structural lesions (evidence of SPS) means that there is a potential for improvement of consciousness, which is prognostically positive (variant I), while the absence of such regions (variant II) corresponds to an unfavorable prognosis. Variant III, which was identified due to the high sensitivity and low specificity of PET [1, 19], later transformed into variant I or II, especially after appropriate treatment.

Confidence in the above concepts is crucial. In the pairwise comparison of the groups, the differences in the results in patients with all variants of the neuroimaging correlations were found to be significant. However, from a formal point of view, it is important to identify only the favorable variant I, which predominates in the patient population. No significant differences were found for the key parameter (recovery from VS) for variants II and III in the intergroup comparison with Bonferroni correction, but a trend towards differences was revealed, probably due to the small number of such patients.

Based on the SPS theory of Natalia Bekhtereva, specific characteristics of the PET method and documented follow-up data, we concluded that variant II is prognostically unfavorable and variant III is equivocal.

In the available literature, we did not find similar prognostic approaches or results, suggesting a potential for improvement of consciousness in most cases of VS. The frequency of the three prognostic variants may change as the number of observations increases. However, given the available data on brain energy metabolism in CDC, no fundamental changes are expected.

Typically, energy metabolism abnormalities in VS are described on PET as larger in area and more severe than those in MCS, and MCS as more extensive than recovery from MCS [1, 12]. When correlated with MRI, the area of abnormal metabolism decreases to the limits of the structural lesion area as consciousness improves [38]. In fact, this «common» description corresponds to variant I, confirming its frequency (69% according to our data). On the contrary, there are only a few confirmed cases of VS in which the cerebral cortex metabolism appears to be relatively preserved [1, 32]. This corresponds to the less common variant II (18%).

«Unusual» cases of VS (in variant II) give reason to believe that PET does not prove the presence of consciousness. It can be explained by the unique characteristics of brain neuroplasticity [32]. However, there is a lack of information in the literature about «normal» neuroplasticity (in variant I).

Based on the follow-up of patients classified as variant I (death upon improvement of consciousness) [23], it can be assumed that «typical» improvement of consciousness is associated with activation of axonogenesis and so-called functional neurogenesis with the appearance of scattered newly formed cells in those brain regions where functional improvement occurs (clinically and according to PET data). In variant II, if activation of neurogenesis and axonogenesis occurs, it is most likely aberrant. Further research is needed, but the structural and functional changes noted above in variant I do not contradict the theory of SPS, but only broaden the scope of its application.

From a clinical point of view, the following aspects are important A favorable prognosis (potential for recovery of consciousness) may go unrealized or even become unfavorable for many reasons, including inadequate therapy, as demonstrated by the history of our patients.

Many patients who recovered from MCS remained severely disabled, especially when recovering from chronic long-term VS. According to the data of international studies [24, 39], this was due, among other things, to «medical neglect».

Patients with CDC frequently experience inadequate palliative care, poor rehabilitation, and even segregation in the treatment of chronic diseases [39, 41], owing to a variety of neurological complications and comorbidities [40]. This does not contribute to the improvement of patients' general condition and consciousness.

Despite the lack of a widely accepted approach to the treatment of VS, we believe it is reasonable to classify patients with variants I and III (favorable and uncertain prognosis, regardless of VS duration) into a «target group» for adequate observation and reasonable therapeutic measures.

Given the good prognosis, the inclusion of variant I in the «target group» is self-explanatory. Despite the uncertain prognosis, the inclusion of variant III in this group is also justified. However, only 5 patients had variant III, according to our data. Consciousness improved in three of them,

and they recovered from VS: two reached MCS (-) and one reached MCS (+).

Unfortunately, only one of these three patients had follow-up PET scans when their consciousness improved or stopped improving during their survival years. All patients with variant III, on the other hand, had inflammatory epilepsy, which could have influenced the change in metabolic parameters during the PET scan [22].

The presented analysis of PET/MRI (SCT) data demonstrated the ability to predict recovery from VS in 87% of cases with either a favorable (69%, variant I) or unfavorable (18%, variant II) prognosis, regardless of other factors and criteria. In contrast, the examination of functional and structural brain abnormalities, unlike several published studies [1, 14], was based on the standard evaluation of individual PET and MRI/SCT images used for routine diagnostics. The utilization of scanners of different models to evaluate both structural and functional changes in the brain of patients does not impact the accuracy of the semi-quantitative assessment of the correlation between the volumes of structural and functional brain lesions [42–44]. This approach, which takes into account the variability in localization and volume of brain lesions in patients with VS [1, 12], greatly facilitates the translational aspect of research.

Functional neuroimaging is now required in addition to standardized clinical assessment and EEG when investigating patients with CDC [18]. 18FDG-PET is considered one of the most informative imaging techniques for studying brain function [1, 12, 14].

Additionally, other factors are important: all necessary tomographs are readily available, MRI and SCT can be used interchangeably if there are contraindications to MRI, and visual comparison of data is straightforward. However, a model based on non-activation fMRI, which has a similar accuracy rate (88%) in predicting the potential for regaining consciousness within a year, can only be utilized if there are no contraindications to MRI and if the structural brain damage is minimal (less than 30%). Furthermore, this model relies on three key epidemiological criteria (etiology, timing, age) [16].

Limitations. Firstly, we cannot guarantee that the prognostic criteria generated will be relevant for patients in the earlier stage of VS, specifically within 2 months after the brain injury. Additionally, it is uncertain whether the unfavorable prognosis (variant II) will remain consistent as medical technology advances.

This study did not evaluate the significance of criteria based on non-activation fMRI or laboratory data. The study did not examine the potential timing of improvement in consciousness due to the involvement of different clinical factors including complications, treatment, and nutrition.

Conclusion

We determined three prognostic variants of neuroimaging correlations reflecting the potential for emerging from VS during the period of more than 2 months after brain injury based on the results of standard evaluation and correlation of individual 18FDG PET and MRI (SCT) images of the brain used in routine diagnostics of CDC and considering VS from the position of N. P. Bekhtereva's theory of stable pathological state of the brain. Variant I involves functional abnormalities that outnumber structural abnormalities and has a favorable prognosis (69% of cases). Variant II has a complete overlap of these abnormalities and an unfavorable prognosis (18%), whereas variant III has a «mixed» presentation and uncertain prognosis (13%).

A retrospective analysis of prognosis based on neuroimaging correlation variants revealed that it predicted recovery from VS in 87% of cases (69% and 18% in variants I and II, respectively) independent of other prognostic criteria, including chronic VS.

Given the pathophysiologic validity, availability, and ease of assessment, it is reasonable to use PET/MRI (SCT) prognostication in clinical practice, with patients in VS with I and III variants assigned to the «target group» for active monitoring and implementation of relevant therapeutic strategies.

References

1. *Пирадов М.А.* (ред.) Хронические нарушения сознания. 2-е изд., перераб. и доп. М.: Горячая линия-Телеком; 2021: 288. [*Piradov M.A.* (ed.) Chronic disorders of consciousness. 2nd ed., revised and updated M.: Hotline-Telecom; 2020: 288. (in Rus.)]. DOI: 10. 25780/006. ISBN 978-5-9912-0856-7.
2. *Schnakers C., Monti M.M.* Towards improving care for disorders of consciousness. *Nat Rev Neurol*. 2020; 16 (8): 405–406. DOI: 10.1038/s41582-020-0358-y. PMID: 32273598
3. *Giacino J.T., Katz D.I., Schiff N.D., Whyte J., Ashman E.J., Ashwal S., Barbano R., et al.* Practice guideline update recommendations summary: Disorders of consciousness: Report of the Guideline Development, Dissemination, and Implementation Subcommittee of the American Academy of Neurology; the American Congress of Rehabilitation Medicine; and the National Institute on Disability, Independent Living, and Rehabilitation Research. *Neurology*. 2018; 91 (10): 450–460. DOI: 10.1212/WNL.0000000000005926. PMID: 30089618.
4. *Royal College of Physicians.* Prolonged disorders of consciousness following sudden onset brain injury: National clinical guidelines. Report of a working party 2020. London: RCP; 2020: 200. ISBN 978-1-86016-793-5. URL: https://bit.ly/38rdU5q (accessed on/ дата обращения: 12.12.2021).
5. *Giacino J.T., Katz D.I., Schiff N.D., Whyte J., Ashman E.J., Ashwal S., Barbano R., et al.* Comprehensive systematic review update summary: Disorders of consciousness: Report of the Guideline Development, Dissemination, and Implementation Subcommittee of the American Academy of Neurology; the American Congress of Rehabilitation Medicine; and the National Institute on Disability, Independent Living, and Rehabilitation Research. *Neurology*. 2018; 91 (10): 461–470. DOI: 10.1212/WNL.0000000000005928. PMID: 30089617.
6. *Fins J.J., Bernat J.L.* Ethical, palliative, and policy considerations in disorders of consciousness. *Neurology*. 2018; 91 (10): 471–475. DOI: 10.1212/WNL.0000000000005927. PMID: 30089621.
7. *Estraneo A., Trojano L.* Prognosis in disorders of consciousness. In: Schnakers C., Laureys S. (ed.) Coma and disorders of consciousness, second edition. Cham: Springer International Publishing; 2018: 17–36. DOI: 10.1007/978-3-319-55964-3_2. ISBN: 978-3-319-55964-3
8. *Edlow B.L., Claassen J., Schiff N.D., Greer D.M.* Recovery from disorders of consciousness: mechanisms, prognosis and emerging therapies. *Nature Reviews Neurology*. 2021; 17 (3): 135–156. DOI: 10.1038/s41582-020-00428-x.1.
9. *Bagnato S., D'Ippolito M.E., Boccagni C., De Tanti A., Lucca L.F., Nardone A., Salucci P., et al.* Sustained axonal degeneration in prolonged disorders of consciousness. *Brain Sci*. 2021; 11 (8): 1068. DOI: 10.3390/brainsci11081068. PMID: 34439687.
10. *Comanducci A., Boly M., Claassen J., De Lucia M., Gibson R.M., Juan E., Laureys S., et al.* Clinical and advanced neurophysiology in the prognostic and diagnostic evaluation of disorders of consciousness: review of an IFCN-endorsed expert group. *Clinical Neurophysiol*. 2020; 131 (11): 2736–2765. DOI: 10.1016/j.clinph.2020.07.015. PMID: 32917521.
11. *Snider S.B., Edlow B.L.* MRI in disorders of consciousness. *Curr Opin Neurol*. 2020; 33 (6): 676–683. DOI: 10.1097/WCO.0000000000000873. PMID: 33044234.
12. *Кондратьева Е.А., Авдюнина И.А., Кондратьев А.Н., Улитин А.Ю., Иванова Н.Е., Петрова М.В., Лугинина Е.В., с соавт.* Определение признаков сознания и прогнозирования исхода у пациентов в вегетативном состоянии. *Вестник РАМН*. 2016; 71 (4): 273–280. [*Kondratieva E.A., Avdunina I.A., Kondratyev A.N., Ulitin A.U., Ivanova N.E., Petrova M.V., Luginina E.V., et al.* Vegetative state: difficulties in identifying consciousness and predicting outcome. *Vestn Ross Acad Med Nauk*. 2016; 71 (4): 273–280. (in Russ).]. DOI: 10.15690/vramn728. PMID: 29297644.
13. *Threlkeld Z.D., Bodien Y.G., Rosenthal E.S., Giacino J.T., Nieto-Castanon A., Wu O., Whit-*

field-Gabrieli S., et al. Functional networks reemerge during recovery of consciousness after acute severe traumatic brain injury. *Cortex*. 2018; 106: 299–308. DOI: 10.1016/j.cortex.2018.05.004. PMID: 29871771.

14. *Cavaliere C., Kandeepan S., Aiello M., Ribeiro de Paula D., Marchitelli R., Fiorenza S., Orsini M., et al.* Multimodal neuroimaging approach to variability of functional connectivity in disorders of consciousness: a PET/MRI pilot study. *Front Neurol*. 2018; 9: 861. DOI: 10.3389/fneur.2018.00861. PMID: 30405513.
15. *Estraneo A., Fiorenza S., Magliacano A., Formisano R., Mattia D., Grippo A., Romoli A.M., et al., IBIA DoC-SIG.* Multicenter prospective study on predictors of short-term outcome in disorders of consciousness. *Neurology*. 2020; 95 (11): 1488–1499. DOI: 10.1212/WNL.0000000000010254. PMID: 32661102.
16. *Song M., Yang Y., He J., Yang Z., Yu S., Xie Q., Xia X., et al.* Prognostication of chronic disorders of consciousness using brain functional networks and clinical characteristics. *eLife*. 2018; 7: 36173. DOI: 10.7554/eLife.36173. PMID: 30106378.
17. *Vainshenker Yu.I., Ivchenko I.M., Korotkov A.D., Melyucheva L.A., Kataeva G.V., Medvedev S.V.* The vegetative state as a manifestation of a stable pathological state. *Human Physiology*. 2010; 36 (1): 118–120. DOI: 10.1134/s0362119710010160.
18. *Kondziella D., Bender A., Diserens K., van Erp W., Estraneo A., Formisano R., Laureys S., et al., EAN Panel on Coma, Disorders of Consciousness.* European Academy of Neurology guideline on the diagnosis of coma and other disorders of consciousness. *Eur J Neurol*. 2020; 27 (5): 741–756. DOI: 10.1111/ene.14151. PMID: 32090418.
19. *Катаева Г.В., Коротков А.Д., Мельничук К.В.* Паттерны относительных оценок регионарного мозгового кровотока и скорости метаболизма глюкозы в здоровом мозге человека. *Медицинская визуализация*. 2007; 2: 84–92. [*Kataeva G.V., Korotkov A.D., Melnichuk K.V.* Patterns of relative evaluations of regional cerebral blood flow and cerebral metabolism of glucose in a brain of a normal person. *Medical imaging/ Meditsinskaya Vizualizatciya*. 2007; 2: 84–92. (in Russ.)]. URL: https://elibrary.ru/download/elibrary_11746472_36186959.pdf. (дата обращения/accessed 15.01.2022).
20. *Гельфанд Б.Р., Заболотских И.Б. (ред.).* Интенсивная терапия. Национальное руководство. 2-е изд., перераб. и доп. М.: ГЭОТАР-Медиа; 2017: 928. ISBN 978-5-9704-4161-9. [*Gelfand B.R., Zabolotskikh I.B.* (ed.). Intensive care. National guidelines. 2nd ed., rev& exp. M.: GEOTAR-Media; 2017: 928. ISBN 978-5-9704-4161-9. (in Russ.)] URL: https://www.rosmedlib.ru/book/ISBN9785970441619.html (Дата обращения/ Accessed: 15.01.2022).
21. *Giacino J.T., White J., Nakase-Richardson R., Katz D.I., Arciniegas D.B., Blum S., Day K., et al.* Minimum competency recommendations for programs that provide rehabilitation services for persons with disorders of consciousness: a position statement of the American Congress of rehabilitation medicine and the National Institute on Disability, independent living and rehabilitation research traumatic brain injury model systems. *Arch Phys Med Rehabil*. 2020; 101 (6): 1072–89. DOI: 10.1016/j.apmr.2020.01.013. PMID: 32087109.
22. *Zinserling V., Vainshenker Y.I.* Hidden encephalitis in prolonged disorders of consciousness. In: Zinserling V. Infectious lesions of the central nervous system. Cham.: Springer; 2022: 271–279. DOI: 10.1007/978-3-030-96260-9. ISBN 978-3-030-96259-3.
23. *Вайншенкер Ю.И., Цинзерлинг В.А., Мелючева Л.А. Боброва В.В., Коротков А.Д., Ивченко И.М., Цыган Н.В.* с соавт. Центральные эффекты мультипаттерной ботулинотерапии при посткоматозных длительных бессознательных состояниях. *Вестник Российской Военно-медицинской академии*. 2019; 2 (66): 78–87. [*Vainshenker Yu.I., Zinserling V.A., Melyucheva L.A. Bobrova V.V., Korotkov A.D., Ivchenko I.M., Tsygan N.V., et al.* Central effects of multipattern botulinum therapy in patients with prolonged postcomatous unconsciousness. *Bulletin of the Russian Military Medical Academy/ Vestnik Rossiyskoy Voenno-*

Meditsinskoy Akademii. 2019; 2 (66): 78–87. (in Russ.)]. DOI: 10.17816/brmma25924.

24. *Dolce G., Sazbon L. (ed)*. The post-traumatic vegetative state. Stuttgart, New York: Thieme. 2002: 158. ISBN: 1588901165.
25. *Vargas A.G.A., Morales C.E., Machado C.C.* Clinical and imaging description of patients with prolonged consciousness disorders. *Rev Cubana Neurol Neurocir*. 2020; 10 (3): 1–21. URL: https://www.medigraphic.com/pdfs/revcubneuro/ cnn2020/cnn203a.pdf. (Accessed/Дата обращения: 12.12.2021).
26. *Estraneo A., Loreto V., Masotta O., Pascarella A. Trojano L.* Do medical complications impact long-term outcomes in prolonged disorders of consciousness? *Arch Phys Med Rehabil*. 2018; 99 (12): 2523-31.e3. DOI: 10.1016/j.apmr.2018.04.024. PMID: 29807003.
27. *Lucca L.F., Lofaro D., Pignolo L., Leto E., Ursino M., Cortese M.D., Conforti D., et al.* Outcome prediction in disorders of consciousness: the role of coma recovery scale revised. *BMC Neurology*. 2019; 19 (1): 68. DOI: 10.1186/s12883-019-1293-7. PMID: 30999877.
28. *Hermann B., Goudard G., Courcoux K., Valente M., Labat S., Despois L., Bourmaleau J., et al.; Pitié-Salpétrière hospital Neuro-ICU*. Wisdom of the caregivers: pooling individual subjective reports to diagnose states of consciousness in brain-injured patients, a monocentric prospective study. *BMJ Open*. 2019; 9 (2): e026211. DOI: 10.1136/bmjopen-2018-026211. PMID: 30792234.
29. *Machado C.* Jahi McMath, a new disorder of consciousness. *Rev. Latinoam. Bioet*. 2021; 21 (1): 137–154. DOI: 10.18359/ rlbi.5635.
30. *Weiss N., Galanaud D., Carpentier A., Tezenas de Montcel S., Naccache L., Coriat P., Puybasset L.* A combined clinical and MRI approach for outcome assessment of traumatic head injured comatose patients. *J Neurol*. 2008; 255 (2): 217–223. DOI: 10.1007/s00415-008-0658-4. PMID: 18283406.
31. *Seel R.T., Douglas J., Dennison A.C., Heaner S., Farris K., Rogers C.* Specialized early treatment for persons with disorders of consciousness: program components and outcomes. *Arch Phys Med Rehabil*. 2013; 94 (10): 1908–1923. DOI: 10.1016/j.apmr.2012.11.052. PMID: 23732166.
32. *Gosseries O., Di H., Laureys S., Boly M.* Measuring consciousness in severely damaged brains. *Annu Rev Neurosci*. 2014; 37: 457–478. DOI: 10.1146/annurev-neuro-062012-170339. PMID: 25002279.
33. *Cheng L., Cortese D., Monti M.M., Wang F., Riganello F., Arcuri F., Di H., et al.* Do sensory stimulation programs have an impact on consciousness recovery? *Front. Neurol*. 2018; 9: 826. DOI: 10.3389/fneur.2018.00826. PMID: 30333789.
34. *Vainshenker Y.I., Melucheva L.A., Bobrova V.V., Starchenko M.G.* EEG reflection of clinical effects dynamics during botulinum toxin therapy of movement disorders under long-term consciousness disorders. *Human Physiology*. 2018; 44 (2): 216–225. DOI: 10.1134/s036211971801019x.
35. *Kotchoubey B., Pavlov Y.G.* A systematic review and meta-analysis of the relationship between brain data and the outcome in disorders of consciousness. *Front. Neurol*. 2018; 9: 315. DOI: 10.3389/fneur.2018.00315. PMID: 29867725.
36. *Dolce G., Arcuri F., Carozzo S., Cortese M.D., Greco P., Lucca L.F., Pignolo L., et al.* Care and neurorehabilitation in the disorder of consciousness: a model in progress. *Scientific World Journal*. 2015; 2015: 463829. DOI: 10.1155/2015/463829. PMID: 25893211.
37. *Бехтерева Н.П., Камбарова Д.К., Поздеев В.К.* Устойчивое патологическое состояние при болезнях мозга. Л.: Медицина; 1978: 240. [*Bekhtereva N.P., Kambarova D.K., Pozdeev V.K.* Stable pathological condition in brain diseases. L.: Medicine; 1978: 240. (in Russ.)].
38. *Aubinet C., Murphy L, Bahri M.A., Larroque S.K., Cassol H., Annen J., Carrière M., et al.* Brain, behavior, and cognitive interplay in disorders of consciousness: a multiple case study. *Front Neurol*. 2018; 9: 665. DOI: 10.3389/fneur.2018. 00665. PMID: 30154755.
39. *Fins J.J., Wright M.S., Bagenstos S.R.* Disorders of consciousness and disability law. *Mayo Clin Proc*. 2020; 95 (8): 1732–1739. DOI: 10.1016/j.mayocp.2020.02.008. PMID: 32753147.
40. *Zhang B., Huang K., Karri J., O'Brien K., DiTommaso C., Li S.* Many faces of the hidden souls: medical and neurological complications and comorbidities in disorders of consciousness.

Brain Sci. 2021; 11 (5): 608. DOI: 10.3390/brainsci11050608. PMID: 34068604.

41. *Goss A. L., Creutzfeldt C.J.* Prognostication, ethical issues, and palliative care in disorders of consciousness. *Neurologic Clinics.* 2022; 40 (1): 59–75. DOI: 10.1016/j.ncl.2021.08.005. PMID: 34798975.
42. *Guo H., Song X., Vandorpe R., Zhang Y., Chen W., Zhang N., Schmidt M. H., et al.* Alzheimer's disease neuroimaging initiative. Evaluation of common structural brain changes in aging and Alzheimer disease with the use of an MRI-based brain atrophy and lesion index: a comparison between T1WI and T2WI at 1.5T and 3T. *AJNR Am J Neuroradiol.* 2014; 35 (3): 504–512. DOI: 10.3174/ajnr.A3709. PMID: 23988753.
43. *Wittens M.M.J., Allemeersch G.-J., Sima D.M., Naeyaert M., Vanderhasselt T., Vanbinst A.-M., Buls N., et al.* Inter- and intra-scanner variability of automated brain volumetry on three magnetic resonance imaging systems in Alzheimer's disease and controls. *Front Aging Neurosci.* 2021; 13: 746982. DOI: 10.3389/fnagi.2021.746982. PMID: 34690745.
44. *Souvatzoglou M., Ziegler S. I., Martinez M. J., Busch R., Dzewas G., Schwaiger M., Bengel F.* Standardised uptake values from PET/CT images: comparison with conventional attenuation-corrected PET. *Eur J Nucl Med Mol Imaging.* 2007; 34 (3): 405–412. DOI: 10.1007/s00259-006-0196-1. PMID: 16953402.

Received 26.12.2022
Accepted 15.09.2023

https://doi.org/10.15360/1813-9779-2023-6-25-38

Significance of Corticospinal, Associative and Inter-Hemispheric Tracts for the Development of Posttraumatic Hemiparesis

Eduard L. Pogosbekian[1,2]*, Elena V. Sharova[1], Liudmila M. Fadeeva[2], Marina V. Shtern[3], Evgenia V. Aleksandrova[2], Natalia E. Zakharova[2], Igor N. Pronin[2]

[1] Institute of Higher Nervous Activity and Neurophysiology, RAS, 54 Butlerova Str., 117485 Moscow, Russia
[2] N. N. Burdenko National Medical Research Center of Neurosurgery, Ministry of Health of Russia, 16 Tverskaya-Yamskaya 4th Str., 125047 Moscow, Russia
[3] Federal Research and Clinical Center of Intensive Care Medicine and Rehabilitology, 25 Petrovka Str., Bldg. 2, 107031 Moscow, Russia

For citation: *Eduard L. Pogosbekian, Elena V. Sharova, L. M. Fadeeva, Marina V. Shtern, Evgenia V. Aleksandrova, N. E. Zakharova, Igor N. Pronin.* Significance of Corticospinal, Associative and Inter-Hemispheric Tracts for the Development of Posttraumatic Hemiparesis. *Obshchaya Reanimatologiya = General Reanimatology.* 2023; 19 (6): 25–38. https://doi.org/10.15360/1813-9779-2023-6-25-38 [In Russ. and Engl.]

***Correspondence to:** Eduard L. Pogosbekian, epogosbekyan@nsi.ru

Summary

Motor disorders are among the most common consequences of severe craniocerebral injury (traumatic brain injury — TBI). Deeper insight into pathophysiological mechanisms of these disorders is important both from a theoretical point of view and in terms of improving neurorehabilitation approaches.

The aim of the study was to investigate the correlation of right–sided posttraumatic hemiparesis severity with composite characteristics of fractional anisotropy (FA) in the segments of the corpus callosum (CC), corticospinal tract (CST) and the inferior fronto-occipital fasciculus (IFO) at different stages of traumatic disease (acute, subacute and long-term periods).

Material and methods. Cases of 43 patients with TBI were analyzed (28 men and 15 women aged 13 to 59 years, mean age 28±9 years). Forty patients were diagnosed with severe TBI with diffuse axonal damage, three patients had moderate severity TBI. Long-term follow up included continuous clinical and neurological examination with evaluation of patient's level of consciousness using the CRS-R scale, and the degree of motor deficits in right-sided hemiparesis using a five-point scale. During three post-TBI periods (up to 1 month, from 1 to 6 months, and from 6 to 12 months), patients were examined using diffusion tensor MRI (DTI), tractography and FA. Motor, cortico-spinal tracts and IFO were divided by measurement grid, correlations between FA and scores of right-sided hemiparesis were calculated for each segment.

Results. FA correlations ($P<0.05$) with the severity of hemiparesis were established not only for CST motor-specific segments, but also for some CC and IFO segments. In the early period of TBI significant correlations with hemiparesis severity were found not only in the contralateral CST segments, but also in the ipsilateral ones. Significant differences in FA in the related CC and CST segments were found between the groups with good and limited motor recovery: at all stages after TBI, FA was higher in patients with successful recovery.

Conclusion. The results of the study provide better insight into pathophysiological mechanisms of post-traumatic motor disorders development, therefore favoring optimization of therapeutic strategies.

Keywords: TBI; tractography; hemiparesis; fractional anisotropy

Conflict of interest. The authors declare no conflict of interest.

Financing of the study. The study was conducted within the Ministry of Education and Science of the Russian Federation state assignment for 2021–2023.

Read the full-text English version at www.reanimatology.com

Introduction

Severe traumatic brain injury (TBI), which causes damage to various parts of the brain including the cortex, subcortical structures and neural pathways, is a common type of brain disorder [1, 2]. Approximately 75% of individuals affected by TBI experience motor impairments such as reduced muscle strength (limb paresis), increased muscle tone and coordination problems. Motor deficits are a major contributor to post-traumatic disability [3]. It is therefore important to investigate the underlying mechanisms of motor impairments after brain injury and to develop effective strategies for their rehabilitation. This research is important both from a scientific perspective and in terms of improving neurorehabilitation approaches.

In a series of previous studies fMRI responses during independent and passive (with the help of another person) performance of clenching-unclenching of the fingers of the hand in healthy people, as well as in patients with different severity of right and left hemiparesis after traumatic brain injury [4–7] were investigated. A stereotyped and reproducible motor fMRI response (mainly related to corticospinal tract activity) was demonstrated when this motor test was performed in healthy subjects, while its

variability increased as the severity of the motor defect (manifested as hemiparesis) worsened. The analysis of the involvement of cortical and subcortical brain structures that are not normally active, matched with the topographical neuroanatomy of the motor system, allowed to formulate the hypothesis that, together with the motor cortex of the hemisphere ipsilateral to the movement [8], non-pyramidal tracts and subcortical structures comprising the extrapyramidal system may act as «functional backup» in post-traumatic hemiparesis [9, 10]. These ideas evolved into the study of fMRI connectivity within the functional motor system, including frontal and motor cortical areas associated with movement, as well as a significant number of subcortical nuclei and the cerebellum as «zones of interest» [11]. It was found that as the severity of hemiparesis increases, functional fMRI connectivity in the corticospinal tract (CST) system weakens [12], but some connectivity in the frontal-motor network increases. The increase in the level of bilateral cortical motor and paleostriatal connections in severe hemiparesis can also be considered as a possible compensatory mechanism for motor impairment [11].

However, all the data presented above are based on the results of the analysis of functional parameters. At the same time, the crucial role of brain pathways, and especially the CCT, in ensuring voluntary human movement is well known [13]. Recent studies using neuroimaging techniques have consistently demonstrated the relationship between the integrity of this tract and the presence and severity of hemiparesis after stroke or severe TBI [14, 15]. Meanwhile, tractography data in recent years have expanded traditional understanding of importance of the corpus callosum (CC) [16, 17] and the inferior frontal-occipital tracts (IFOT) [18, 19] in the execution of voluntary movement in both normal and pathological conditions.

In this regard, this study aims to clarify the importance of CST, CCT and IFOT in the severity of post-traumatic hemiparesis. Considering the current neurophysiological ideas about the evolution of neurotrauma [20] and its phases [3], it is reasonable to evaluate the importance of these tracts at different time points following traumatic injury.

Literature analysis reveals various approaches to assessing the state of these tracts. It is possible to estimate average FA values [21], referred to as tractometry in some publications. Sometimes researchers examine FA values in individual manually labeled white matter regions [22]. A more accurate assessment of white matter status can be obtained by estimating FA profiles along tracts [23, 24] or by using the TBSS algorithm [25] and similar methods [26], where tracts are projected onto the white matter «skeleton» and then voxel-wise statistics are calculated for the groups studied. We believe that the method of estimating profiles along tracts is not suitable for studying the CC, since this structure has numerous branches in different parts of the brain, and the concepts of «beginning» and «end» do not apply to it. The TBSS voxel-wise method is not appropriate for measuring patients with severe traumatic brain injury because they often have serious brain deformities due to surgery, hydrocephalus, and increased intracranial pressure. Edema, hemorrhage, diffuse axonal damage — all of these make it impossible to construct a correct white matter «skeleton» in TBI patients and to perform further group analysis.

The authors [27] created a mask for each patient that excluded areas of post-stroke edema when analyzed with the TBSS method. This approach might allow group analysis of patients with severe TBI, but it would exclude the most damaged white matter regions of interest from the statistics.

Therefore, in this study, we decided to use a non-standard, original, patent-pending algorithm for segmentation of the tracts under study and their subsequent analysis.

The aim of the study was to reveal the correlation between the severity of right post-traumatic hemiparesis and the fractional anisotropy characteristics of CCT, CST and IFOT segments during different phases (acute, subacute and chronic) of traumatic disease.

Materials and Methods

The study was conducted in the Department of Radiology and Radioisotope Diagnostic Methods of the Burdenko Neurosurgical Center of the Ministry of Health of the Russian Federation.

It was an observational and retrospective study, analyzing data collected from September 2011 to January 2020. Patients were studied in the acute (up to 1 month), subacute (1 to 6 months), and chronic (6 to 12 months) phase after TBI.

The main observation group consisted of 43 patients with TBI (28 males and 15 females, aged 13 to 59 years, mean age 28 ± 9 years).

All patients had suffered a TBI with variable brain damage and were treated in the Neurotraumatology department of the Burdenko Neurosurgical Center of the Ministry of Health of the Russian Federation. Among them, 40 patients were diagnosed with severe brain injury with diffuse axonal damage (DAD), while the remaining three had moderate closed TBI. For more information on specific traumatic injuries, see Table 1.

On admission to the hospital, the severity of the disease was assessed using the Glasgow Coma Scale (GCS) [28] (Table 2).

The Glasgow Outcome Scale (GOS) [29] was used to assess the success of recovery six months after the injury: 10 patients received a score of 5 points, 11 patients were assessed 4 points, 11 patients

Table 1. Injuries in traumatic brain injury.

Injury	Number of patients
DAI	25
DAI+SDH	9
DAI+focal contusion	6
Traumatic brain injury without MRI-visible brain damage	3

Note. DAI — diffuse axonal injury; SDH — subdural hematoma.

had 3 points, 10 patients scored 2 points, and one patient received a score of 1 point.

Each patient underwent a thorough repeated clinical and neurological examination, including an assessment of current level of consciousness using the CRS-R scale [30] and the severity of movement impairment using the five-point hemiparesis scale [31], where the most severe hemiparesis corresponds to low points (1–2) and its absence to 5.

The study included patients who either had no hemiparesis or had right hemiparesis following a traumatic injury., which can greatly influence a person's future quality of life.

Exclusion criteria:

1) Refusal of the patient or his/her legal representative to sign an informed consent for participation in the study,

2) Inability to undergo an MRI study due to the presence of implants, intracranial pressure sensors, braces, clips, etc,

3) Serious condition including hemodynamic instability, elevated blood pressure, decompensated heart failure, acute infection, etc.

4) Patient's death occurring within one year of the traumatic injury.

Table 3 displays data pertaining to the severity of right hemiparesis throughout the follow-up period.

Magnetic resonance diffusion tensor imaging (DTI) was conducted on all patients with traumatic injuries. In the acute phase, 28 patients underwent the procedure once. In the subacute phase, 22 patients were included, with 4 of them being examined twice. The time interval between examinations ranged from 8 to 77 days. In the chronic phase, 20 patients were scanned, with 7 of them being scanned twice and one being scanned three times. The time intervals between scans ranged from 120 to 511 days. Among the patients, 8 were scanned at least once in each of the acute, subacute, and chronic phases. There were 4 patients who were scanned in the acute and subacute phases only, 6 patients scanned in the subacute and chronic phases only, and 3 patients scanned in the acute and chronic phases only. Furthermore, 14 patients were scanned in the acute phase only, 5 patients were scanned in the subacute phase only, and 4 patients were scanned in the chronic phase only.

The control group for the DTI patients consisted of data from a similar study involving 22 healthy volunteers (14 men and 8 women) with ages ranging from 21 to 55 years, and a mean age of 30±10 years.

The scans were conducted using a 3.0 Tesla magnetic field strength tomograph (3.0 T Signa HDxt, General Electric USA) with an eight-channel head coil utilizing a diffusion tensor MRI (DTI) protocol. The protocol included routine MR imaging in T1, T2, T2 FLAIR (T2 with water signal suppression), gradient echo (T2*, 2D, 3D, or SWAN), and diffusion-weighted imaging (DWI) modes to diagnose traumatic lesions or intracranial hemorrhage. The diffusion tensor MRI in the DTI protocol was performed using a spin echo — echo planar imaging (SE EPI) sequence with the following parameters: TR=8000 ms, TE_{min}=96 ms, 33 diffusion gradient directions, diffusion weight b=0, 1000 s/mm², two repetitions, reconstruction matrix 256×256; slice thickness/gap 4/0 mm, field of view 240 mm, voxel size 1.9×1.9×4 mm³, and a scan duration of 3 minutes and 40 seconds in one projection.

The original diffusion MR image analysis algorithm used is illustrated in Fig. 1.

Importantly, clinical and DTI correlations took into account the level of localization of the tract segment corresponding to the determined correlation coefficient value, i.e. brainstem, subcortical nuclei, and cortex (Fig. 2). Correlations of 0.6 and higher were considered to be the most interesting.

We used the Wilcoxon test and ROC analysis in Matlab to perform a nonparametric group comparison of FA values for individual tract segment localizations. The severity of right hemiparesis at

Table 2. Severity of patients with traumatic brain injury on admission.

Parameter	Values												
GCS score, points	3	4	5	6	7	8	9	10	11	12	13	14	15
Number of patients	1	6	3	6	4	1	5	0	1	0	0	0	3

Table 3. Severity of right hemiparesis at different follow-up time points.

Severity, points	Number of tests in different phases		
	Acute	Subacute	Chronic
1	14	3	4
2	2	9	3
3	2	4	4
4	2	3	4
5	7	5	12

Note. The severity of hemiparesis according to manual muscle testing system [31]: 5 — full range of movement and almost normal strength with maximal resistance; 4 — mild hemiparesis; 3 — moderate hemiparesis; 2 — severe hemiparesis; 1 — gross hemiparesis (barely noticeable muscle contractions).

the end of treatment was used to divide patients into two groups. Patients with a score of two points or less were assigned to the first group («non-recovered»), while the remainder were assigned to the second group («recovered»).

DTI data from the control group were used at various stages of the study, including template creation and statistical analysis of parameters.

A box-and-whisker plot was generated for selected tract segments that showed a significant correlation between fractional anisotropy (FA) and hemiparesis severity. This plot showed the distribution of FA values between the « recovery « and «non-recovery» patient groups during the chronic phase of TBI. In addition, the plot showed the distribution of FA values in the corresponding tract (or its segment) in a group of healthy volunteers. Using ROC analysis, we determined and plotted the optimal FA value that could discriminate between the «recovered» and «non-recovered» patient groups.

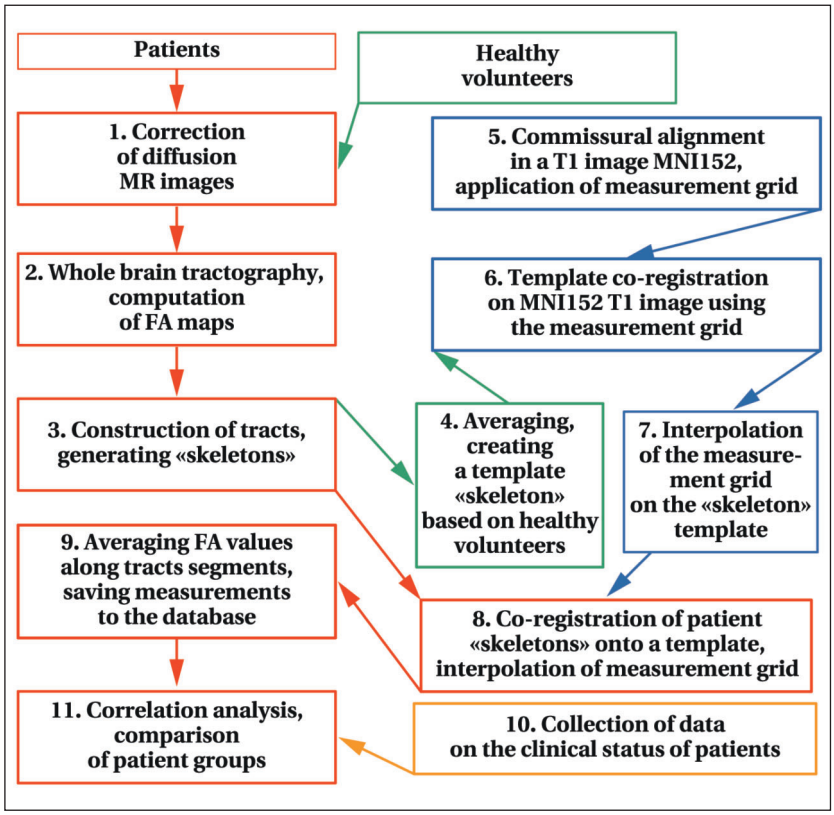

Results

During the visual matching, the tracts analyzed in all patients and healthy volunteers closely aligned with the template image used to mark the measurement areas. Consequently, no subjects were excluded from the study due to errors in the data acquisition algorithm.

Table 4 shows the highest correlation values between the severity of right hemiparesis and FA of the tract segments studied in acute TBI. The correlation coefficient *(r)* values for different segments of the left corticospinal tract (responsible for voluntary motor activity in the right hand) ranged from 0.61 to 0.64, indicating a moderate level of congruency between these parameters. Furthermore, these segments included both cortical (paracentral lobule) and subcortical (thalamus and caudate nu-

Fig. 1. Stages of DTI data analysis.
Note. The red color indicates steps using patient MRI data, the green color indicates steps using healthy volunteer MRI data only, the blue color indicates MNI152 template only, and the orange color indicates patient clinical assessment data. Step explanations:

1. Diffusion image correction included removing Gibbs artifacts and thermal noise, and correcting eddy current artifacts with FSL eddy (http://fmrib.ox.ac.uk/fsl/) and Mrtrix3 (https://www.mrtrix.org/) software.

2. Whole brain tracts were calculated in Mrtrix3 using the HARDI CSD method [32] with default settings and a stopping criterion of 10 million fibers. Mrtrix3 was also used to compute metric fractional anisotropy maps.

3. Construction of corticospinal (CST), inferior fronto-occipital (IFOT), and corpus callosum (CCT) tracts for each subject in TrackVis (http://trackvis.org/). The combination of these tracts was dubbed the «skeleton», with the tracts connecting the brain's margins in three orthogonal directions: interhemispheric, frontal-occipital, and cortical-brainstem. Based on the findings of previous studies [33, 34], seven leads were conventionally identified in the CCT.

4. The averaged «skeleton» was built using the ANTs software package's script antsMultivariateTemplateConstruction2 (http://stnava.github.io/ANTs/).

5. In MNI152 space, the template T1 image was rotated so that the anterior and posterior commissures were on the same section in axial projection.

6, 7, 8. The averaged skeleton was co-registered to the template T1 image using affine and nonlinear transformations with the ANTs software package's antsRegistrationSyN.sh utility. The same utility was used to co-register the patient «skeletons» to the image averaged over the group of healthy volunteers. The measurement grid used to divide the tracts into segments was made up of 18×18×18 mm^3 cells. If one of the CCT's seven leads was analyzed, the central part of the CCT, delimited by a parallelepiped of 5×2×3 cells, was counted as one measurement block.

9, 11. The average FA values for each tract segment were collected and saved, and statistical analysis was carried out using Matlab R2018b software (http://www.mathworks.com/). For each tract segment, two value vectors were saved, including the average FA values of that tract segment for each patient and the assessment of right hemiparesis. These vectors were used to compute the Spearman rank correlation. In the table of final correlations, only values with a multiple value-adjusted significance level of $P<0.05$ were included. The total number of segments analyzed for each tract (approximately 100) was included in the correction. On the template T1 image, the cells of the tract segments with statistically significant correlations were displayed.

Table 4. Correlation of right hemiparesis severity with fractional anisotropy for segments of different tracts in the acute traumatic brain injury.

Tract	FA (min–max–average)	Hemisphere	Level	*r (p)*	95% CI of the correlation (min–max)	Adjacent anatomical structure
Splenium of CC	0.22–0.54 0.37±0.09	left	Subcortical nuclei	0.86 (2×10^{-7})	0.68–0.93	Superior temporal gyrus. Lateral ventricle. Gyrus supramarginalis
CC	0.22–0.54 0.37±0.09	left	Subcortical nuclei	0.86 (4×10^{-7})	0.67–0.93	Superior temporal gyrus. Lateral ventricle
CC	0.16–0.39 0.31±0.05	left	Cortex	0.69 (0.00014)	0.33–0.85	Posterior middle frontal gyrus. Superior frontal gyrus.
Anterior CC	0.16–0.40 0.31±0.05	left	Cortex	0.68 (0.00018)	0.32–0.85	Posterior middle frontal gyrus. Superior frontal gyrus
Splenium of CC	0.27–0.54 0.37±0.08	right	Subcortical nuclei	0.66 (0.0005)	0.24–0.87	Superior temporal gyrus. Lateral ventricle. Inferior parietal gyrus
Left CST	0.32–0.63 0.45±0.08	left	Cortex	0.64 (0.0020)	0.21–0.84	Paracentral lobule. Posterior cingulate gyrus
Left CST	0.36–0.69 0.58±0.09	left	Subcortical nuclei	0.62 (0.0009)	0.27–0.82	Thalamus
Left CST	0.31–0.6 0.47±0.08	left	Cortex	0.61 (0.0010)	0.23–0.81	Lateral ventricle. Caudate nucleus
Right CST	0.30–0.67 0.53±0.10	right	Subcortical nuclei	0.60 (0.0012)	0.24–0.82	Amygdala. Ventral intermediate medulla. Hippocampus

cleus) components of the left corticospinal tract (Fig. 3, I).

However, more significant correlations with hemiparesis severity (ranging from 0.66 to 0.86) were found both for the CC as a whole and for its individual segments (Table 4). Relatively low r values were found for the right part of the splenium of the CC (lateral ventricle and inferior parietal gyrus, *r*=0.66) and the left anterior CC (superior frontal gyrus, *r*=0.68). The most significant correlation (0.86) was found for the left part of the splenium of the CC located near the lateral ventricle and superior supramarginal gyrus. The highest r values were associated with subcortical CC areas.

Moreover, we observed a correlation of approximately 0.6 between the severity of right hemiparesis and the fractional anisotropy (FA) of subcortical segments of the right corticospinal tract (CST) ipsilateral to the hemiparesis (Table 4, Fig. 3, III).

In subacute TBI, the number of correlations of hemiparesis severity with DTI data exceeding 0.6 (Table 5) was significantly lower than in the acute

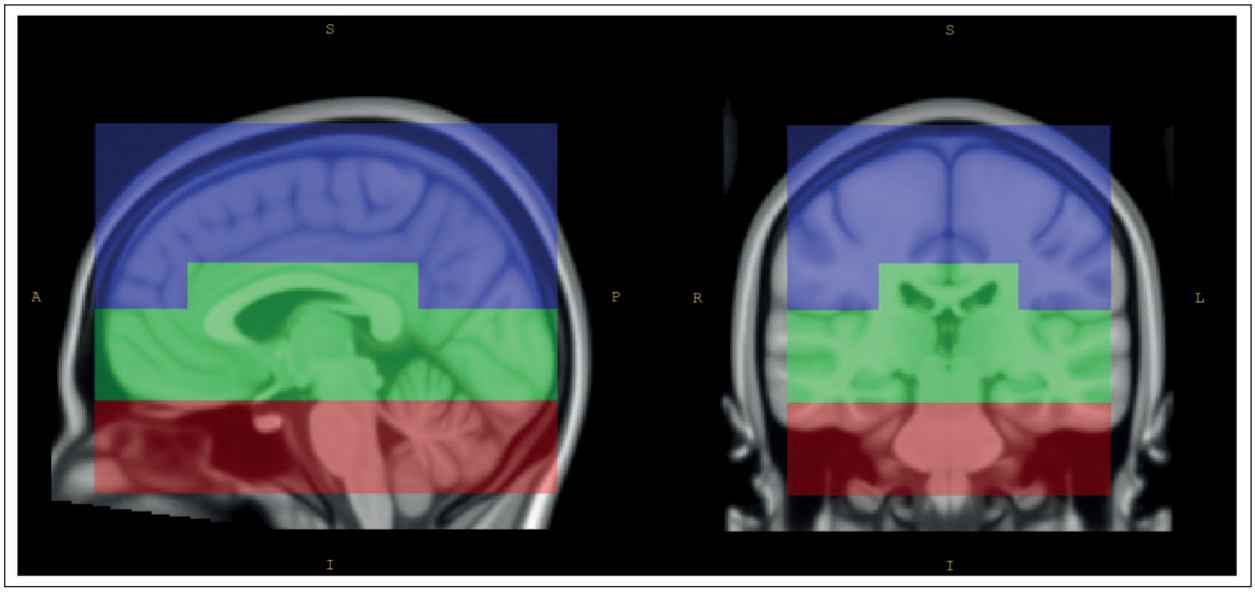

Fig. 2. Three levels of anatomical location of clinical-DTI correlations: brainstem (red), subcortical nuclei (green), and cortex (blue).

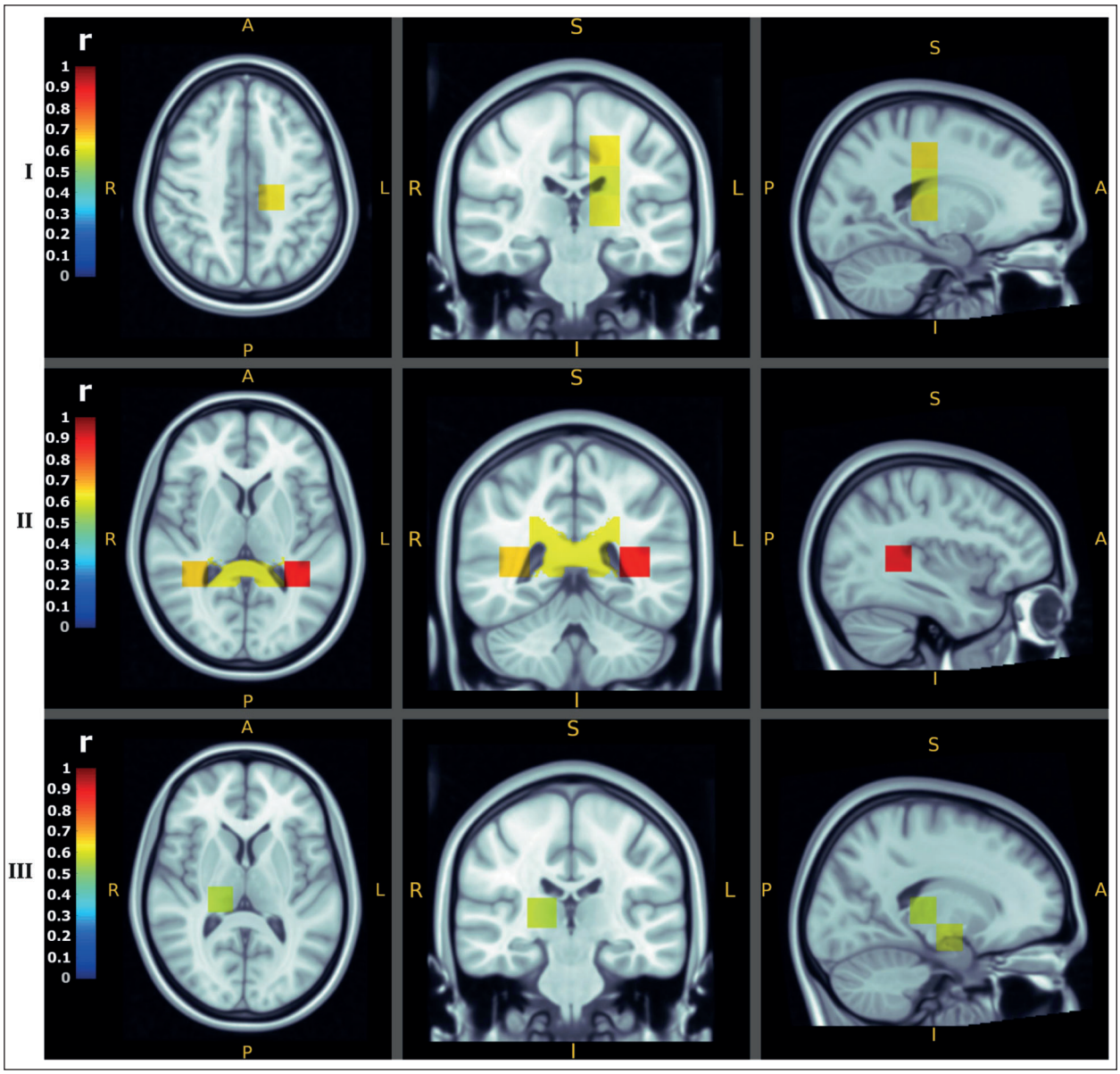

Fig. 3. Zones of correlation between severity of right hemiparesis and fractional anisotropy of segments of left CST (I), splenium of corpus callosum (II), and right CST (III) in acute TBI.
Note. In Figures 3–5, the color scale on the left reflects the values of the correlation coefficient.

phase (Table 4); their values ranged from 0.6 to 0.71. Meanwhile, only one parameter was related to the cortical segment of the left CST (Fig. 4, I), while the other two were associated with the subcortical segments of the anterior part and especially with the splenium of the CC. Together with them, we revealed the previously missing correlation between the severity of hemiparesis and the status of the central segment of the left inferior fronto-occipital tract adjacent to the hippocampus (Fig. 4, II).

In chronic TBI, the correlation of hemiparesis severity with the status of conduction pathways was less strong, with maximum r values not exceeding 0.68 and mainly ranging from 0.53 to 0.58 (Table 6). The CSTs of both hemispheres were absent among the tracts with significant correlations. However, the «representation» of cortical projections of the corpus callosum (mainly its right anterior part) was preserved (Fig. 5, I). In addition, we found a correlation with FA for the central segment of the right IFOT, but not for the left one (Fig. 5, II).

The important directions of this study included the impact of FA of the tracts correlating with hemiparesis severity at different phases of traumatic disease on the recovery of motor function in the chronic phase.

Fig. 6 shows the plots of FA for splenium of CC in acute TBI (Fig. 3, II), the cortical segment of the left CST in subacute phase (Fig. 4, I), and for the FA of anterior CC in the chronic phase (Fig. 5, I).

According to this correlation, the vast majority of FA parameters for different tracts were lower than normal in the examined patients at all stages of the study. The magnitude of the reduction was

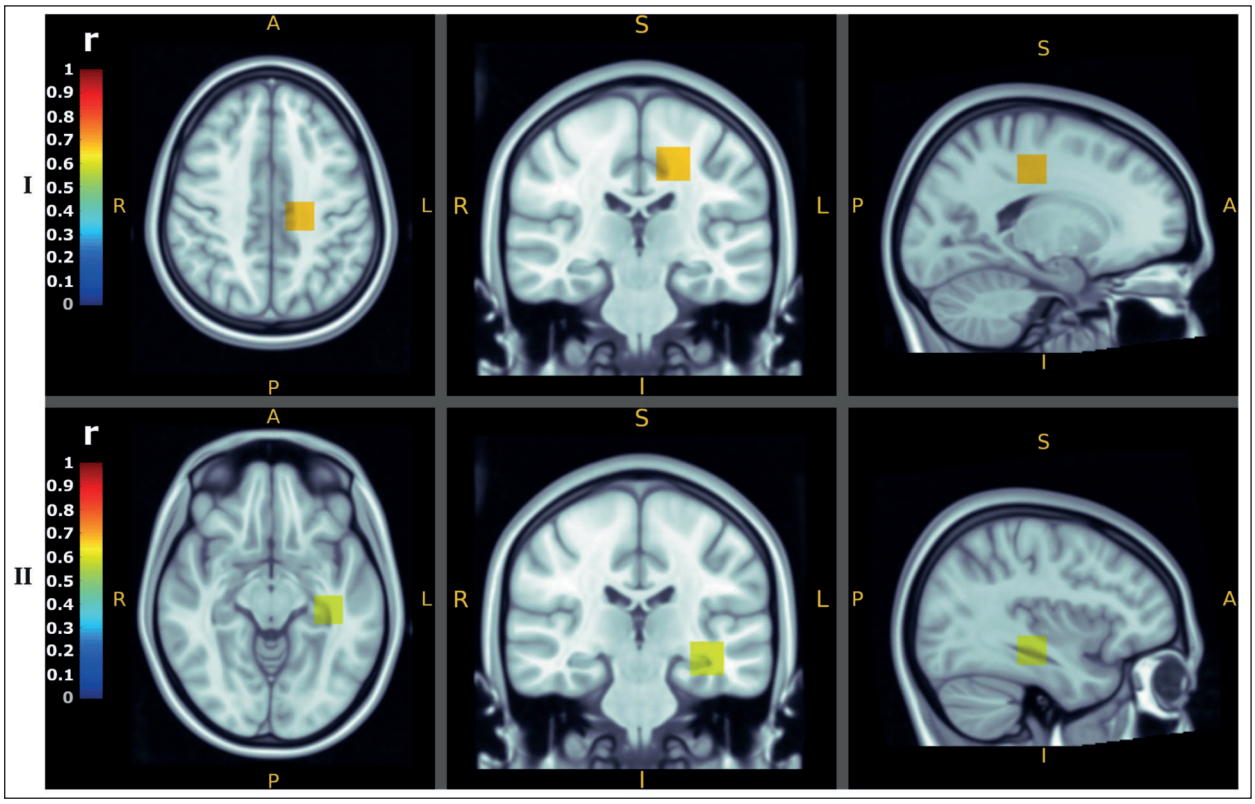

Fig. 4. Zones of correlation between the severity of right hemiparesis and fractional anisotropy of segments of the left CST (I) and left IFOT (II) in subacute traumatic brain injury.

Table 5. Correlations of severity of right hemiparesis with fractional anisotropy of segments of different tracts in chronic TBI.

Tract	Hemisphere	Level	*r*	Adjacent anatomical structures
CCT	Right	Cortex	0.68	Superior frontal gyrus Posterior middle frontal gyrus Posterior cingulate gyrus
Anterior CCT	—	Subcortical nuclei	0.58	Anterior cingulate cortex
Middle CCT	Right	Cortex	0.58	Anterior cingulate gyrus Superior frontal gyrus Posterior middle frontal gyrus
Right IFOT	Right	Subcortical nuclei	0.56	Inferior lateral ventricle Amygdala Putamen Insula Hippocampus
Anterior CCT	Right	Cortex	0.56	Anterior cingulate gyrus Superior frontal gyrus Posterior middle frontal gyrus
Middle CCT	—	Subcortical nuclei	0.53	Anterior cingulate gyrus

directly related to the severity and persistence of the motor deficits.

Figures 6 B and C show typical variants of FA values distribution in the study groups. Thus, in patients with subacute TBI (from 1 to 6 months), FA values for the cortical segment of the left CST less than 0.4 were associated with no further reduction of right hemiparesis, whereas higher values of this parameter were associated with further regression of this motor defect (nonparametric Wilcoxon test, *P*=0.02). DTIs performed in the chronic phase show similar FA ratios for the right anterior segment of the corpus callosum (*P*=0.03 when comparing groups using the Wilcoxon test) (Fig. 6, C). The selective comparison of parameters in the study groups revealed that the average FA values in «non-recovery» patients were 68-78% of the normal values of the specific segment at all stages of the study.

In «recovery» patients, the tracts with segmental FA values within or above the normal range were found only in the acute phase. These tracts included subcortical segment of splenium of CC (Fig. 6, A), as well as cortical and subcortical parts of the left corticospinal tract.

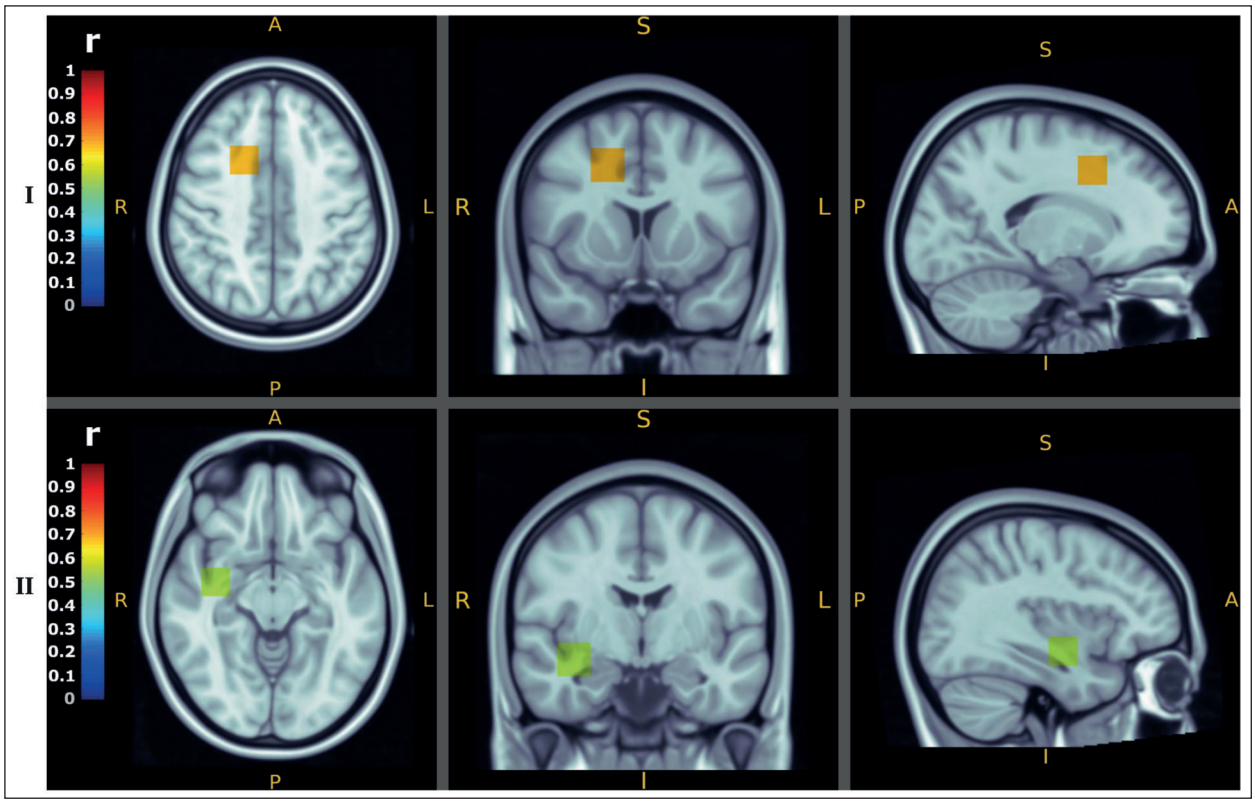

Fig. 5. Zones of correlation between the severity of right hemiparesis and fractional anisotropy of the right anterior CCT segments (I) and right IFOT (II) in the chronic traumatic brain injury.

Table 6. Correlations between right hemiparesis severity and fractional anisotropy of segments of different tracts in the chronic traumatic brain injury.

Tract	FA (min–max–average)	Hemisphere	Level	*r* (*P*-value)	95% CI of the correlation (min–max)	Adjacent anatomical structure
CCT	0.15–0.41 0.31±0.08	right	Cortex	0.68 (0.0002)	0.20–0.86	Superior frontal gyrus. Posterior middle frontal gyrus. Posterior cingulate gyrus
Anterior CCT	0.14–0.40 0.32±0.06	—	Subcortical nuclei	0.58 (0.0017)	0.04–0.82	Anterior cingulate gyrus
Middle CCT	0.16–0.45 0.32±0.08	right	Cortex	0.58 (0.003)	0.04–0.85	Anterior cingulate gyrus. Superior frontal gyrus. Posterior middle frontal gyrus
Right IFOT	0.22–0.39 0.33±0.04	right	Subcortical nuclei	0.56 (0.008)	0.10–0.80	Inferior lateral ventricle. Amygdala. Putamen. Insula. Hippocampus
Anterior CCT	0.14–0.43 0.32±0.07	right	Cortex	0.56 (0.005)	0.05–0.80	Anterior cingulate gyrus. Superior frontal gyrus. Posterior middle frontal gyrus
Middle CCT	0.25–0.49 0.36±0.07	—	Subcortical nuclei	0.53 (0.005)	0.07–0.79	Anterior cingulate gyrus

Discussion

We used a non-conventional algorithm to measure cerebral white matter FA in patients with traumatic brain injury. The MR images of some of them showed severe brain damage and signs of cerebral oedema, which made it difficult to mark the measurement zones. The advantage of the algorithm used was its automation, which minimized the dependence of the result on the expertise of the researcher. The successful application of the developed algorithm suggests its usefulness for the other studies.

The results of this study demonstrate a dynamic, time-dependent correlation between the severity of right post-traumatic hemiparesis and FA of the

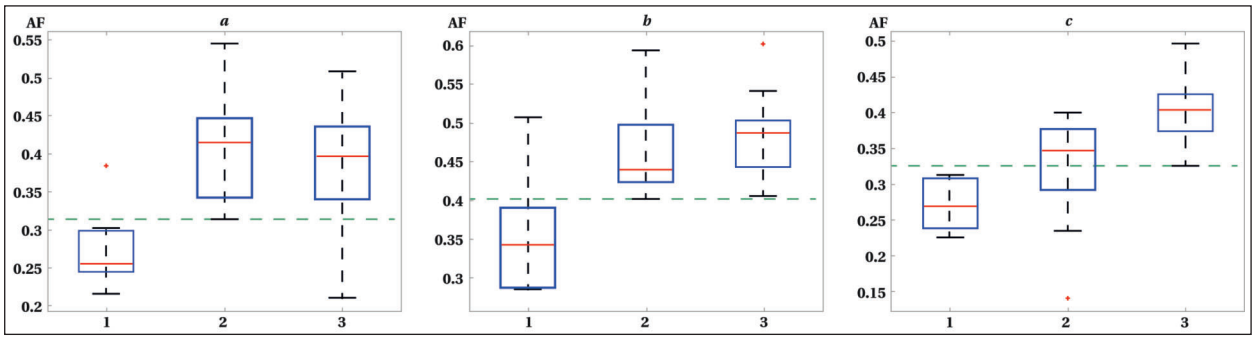

Fig. 6. Fractional anisotropy of segments of individual tracts in patients with different degree of motor function recovery and in healthy subjects.

Note. *a* — FA of the subcortical segment of the splenium of CC in the acute phase. *b* — FA of the subcortical segment of the left CST in the subacute phase. *c* — FA of the right anterior CC in chronic traumatic brain injury. 1 — patients with right hemiparesis 1 and 2 points on the manual muscle testing scale [31] in chronic traumatic brain injury («not recovered»); 2 — patients with right hemiparesis 3, 4 and 5 points in chronic traumatic brain injury («recovered»); 3 —healthy subjects. The green dotted line is the optimal threshold value calculated using ROC-analysis and discriminating between groups of patients.

cerebral tracts, supporting the idea of the staged development of traumatic brain disease [3].

FA of the corticospinal tract contralateral to the hemiparesis has been shown to correlate significantly with motor deficits in acute and subacute TBI, which in turn is consistent with classical neuroanatomy [13, 35]. However, even in the acute phase, a similar correlation was found for ipsilateral hemiparesis and the right corticospinal tract. Furthermore, the correlation between the segments of different tracts of this hemisphere and the degree of hemiparesis increased up to the chronic phase of TBI. This suggests that the hemisphere ipsilateral to the defect is likely to be involved in neuroplastic compensatory processes. The active role of the 'healthy' hemisphere in these processes is well known in stroke, which is usually caused by unilateral hemispheric damage [36, 15].

In TBI with diffuse, often bilateral brain damage, our previous studies [10, 5] have shown that the severity of ipsilateral hemiparesis is most evident in mild cases of paresis (4 points), where there is predominantly unilateral hemispheric damage or no damage at all. This significance cannot be ruled out in patients with marked hemiparesis but without focal lesions.

We have found that there is a dynamic relationship between cerebral structures and the severity of hemiparesis that changes over time. In the acute phase of TBI, the correlation is stronger in the deeper (subcortical) parts of the brain, while in the chronic phase it shifts to the cortical areas. The presence of significant correlations in the acute phase, specifically damage to subcortical structures, can be attributed to the continuous functional activity of the extrapyramidal system. This system is responsible for controlling motor functions and muscle tone and is in constant functional interaction with the pyramidal system. These correlations can be considered as an early compensation for motor disorders during the post-traumatic depression of the functional activity of the corticospinal tract (CST). As the traumatic injury progresses to subacute and chronic stages, the role of subcortical formations decreases, and the activity of cortical areas involved in movement production becomes the main manifestation of neuroplastic mechanisms.

Aside from the well-established importance of movement-specific corticospinal tracts in the acute phase, significant correlations with the severity of hemiparesis have also been discovered for some areas of the corpus callosum, which persist even in chronic TBI. The importance of interhemispheric interaction of the brain sensorimotor areas in providing motor function has previously been demonstrated using both functional methods [37, 12, 38] and DTI data [16, 17]. The hypogenesis of the corpus callosum and the corresponding decrease in FA in children with spastic diplegia have been found to correlate with the severity of motor impairments and to be an accurate indicator of motor deficits [39]. The results of our study directly confirm this fact in TBI.

Furthermore, our study revealed correlations between the severity of right hemiparesis and segments of the inferior fronto-occipital fasciculus (IFOT), with the left segment being significant in the subacute phase and the right segment in the chronic phase. Although this tract is not directly related to motor function, current ideas about multicomponent neural networks supporting different types of activity suggest that it may be involved in the sensorimotor integration required for movement execution. A study [40] found that therapeutic translingual stimulation improved motor functions as well as increased the initially reduced FA of several non-motor brain tracts, including the left inferior frontal-occipital tract, in children with cerebral palsy. The authors believe that the IFOT, a ventral associative pathway that connects the frontal

lobe to the occipital and parietal lobes via the temporal lobe and the insula [41], is involved in mixed sensorimotor integration because of its middle component. Changes in its FA correlated with hemiparesis severity in our study as well, and it is one of the «areas of interest» of neural networks such as DMN, relevance, and speech networks [42]. While the CST's cortical and subcortical segments are part of the sensorimotor neural network, which ensures the direct act of executing a voluntary movement, the DMN, relevance, and speech networks are associated with more sophisticated components of movement organization, such as memory, motivation and behavior integration, sensory integration, spatial navigation, and others.

According to the obtained data, we can assume that the importance of structural and functional interactions of sensorimotor neuronal networks is more obvious in the development of motor disorders in the acute phase, while in the subacute and especially in the chronic phase, the persistence and severity of these disorders depend more on the preservation of anatomical connections of more global (integral) neuronal networks.

In general, the results of our study confirm the literature data on the diagnostic usefulness of tractography (and in particular fractional anisotropy values) in the development and regression of motor disorders such as hemiparesis, both in stroke [43] and in traumatic brain injury [44]. Moreover, the dynamic changes in the correlations between FA parameters and hemiparesis severity in different phases of TBI can serve as a rationale for the use of DTI in neurorehabilitation, both for diagnostic purposes and for studying the different mechanisms of recovery from motor disorders of different etiologies [45, 46].

Conclusion

We found that post-traumatic right motor dysfunction is associated not only with damage to the left CST, but also with disruption of interhemispheric interaction due to damage to the tracts of the corpus callosum.

In the subacute and especially in the chronic phase of TBI, a correlation has been demonstrated between the severity of right hemiparesis and the topography of the bilateral IFOTs, which are nonspecific with respect to motor function. This could indicate the involvement of these tracts, the CST and the ipsilateral hemiparesis in the compensation of the motor defect.

The obtained specific quantitative characteristics of structural and clinical correlations, as well as FA values in cases with different success rates of motor recovery, should be considered in the management of patients with traumatic brain injury.

References

1. *Потапов А.А., Данилов Г.В., Сычев А.А., Захарова Н.Е., Пронин И.Н., Савин И.А., Ошоров А.В., с соавт.* Клинические и магнитно-резонансные томографические предикторы длительности комы, объема интенсивной терапии и исходов при черепно-мозговой травме. *Журнал «Вопросы нейрохирургии» имени Н.Н. Бурденко.* 2020; 84 (4): 5–16. [*Potapov A.A., Danilov G.V., Sychev A.A., Zakharova N.E., Pronin I.N., Savin I.A., Oshorov A.V., et al.* Clinical and MRI predictors of coma duration, critical care intensity and outcomes in traumatic brain injury. *Burdenko's Journal of Neurosurgery / Zhurnal Voprosy Neirokhirurgii Imeni N.N. Burdenko.* 2020; 84 (4): 5–16. (in Russ.). DOI: 10.17116/neiro2020840415.
2. *Лихтерман Л.Б., Кравчук А.Д., Охлопков В.А.* Учение о последствиях черепно-мозговой травмы Часть I. Дефиниции, классификация, клиническая и количественно-томографическая синдромология. *Клинич. разбор в общей медицине.* 2021; 5: 25–29. [*Lichterman L. B., Kravchuk A.D., Okhlopkov V. A.* Theory about traumatic brain injury effects. Part I. Definitions, classification, clinical signs and quantitative tomography. *Clinical Analysis in General Medicine/Klinichesky Razbor v Obshchey Meditcine.* 2021; 5: 25–29. (in Russ.)]. DOI: 10.47407/kr2021.2.5.00067.
3. *Лихтерман Л.Б., Кравчук А.Д., Охлопков В.А., Могила В.В., Лихтерман Б.Л.* Периодизация клинического течения черепно-мозговой травмы. *Неврология и Ревматология. (при. к Журн. Consilium Medicum.* 2019; 1: 56–60. [*Lichterman L.B., Kravchuk A.D., Okhlopkov V.A., Grave V.V., Lichterman B.L.* Periodization of clinical course of head injury. *Neurology and Rheumatoloy (Suppl Consilium Medicum.* 2019; 1: 56–60. (in Russ.)]. DOI: 10.26442/2414357X. 2019.1.190275.
4. *Болдырева Г. Н., Шарова Е.В., Жаворонкова Л.А., Челяпина М.В., Дубровская Л.П., Симонова О.А., Корниенко В.Н.* ФМРТ и ЭЭГ реакции мозга здорового человека при активных и пассивных движениях ведущей рукой. *Журнал высшей нервной деятельности им. ИП Павлова.* 2014; 64 (5): 488–488. [*Boldyreva G.N., Sharova E.V., Zhavoronkova L.A., Chelyapina M.V., Dubrovskaya L.P., Simonova O.A., Kornienko V. N.* EEG and fMRI reactions of a healthy brain at active and passive movements of the leading hand. *I.P.*

Pavlov Journal of Higher Nervous Activity/Zh Vyssh Nerv Deiat I P Pavlova. 2014; 64 (5): 488–488. (in Russ.)]. DOI: 10.7868/S004446 7714050049.

5. *Болдырева Г.Н., Ярец М.Ю., Шарова Е.В., Жаворонкова Л.А., Купцова С.В., Челяпина-Постникова М.В., Машеров Е.Л., с соавт.* Особенности фМРТ-реакций мозга при двигательных нагрузках у пациентов с легким посттравматическим гемипарезом. *Журнал высшей нервной деятельности им. ИП Павлова*. 2020; 70 (5): 579–589. [*Boldyreva G.N., Yaretz M.Y., Sharova E.V., Zhavoronkova L.A., Kuptsova S.V., Chelyapina-Postnikova M.V., Masherov E.L., et al.* Features of fMRI brain reactions in motor load by patients with mild posttraumatic hemiparesis. *I.P. Pavlov Journal of Higher Nervous Activity/Zh Vyssh Nerv Deiat I P Pavlova*. 2020; 70 (5): 579–589. (in Rus.)]. DOI: 10.31857/ S0044467720050044.
6. *Мухина Т.С., Шарова Е. В., Болдырева Г.Н., Жаворонкова Л.А., Смирнов А.С., Куликов М.А., Пронин И.Н.* Особенности нейроанатомии активного движения руки у пациентов с тяжелой черепно-мозговой травмой (анализ данных функциональной магнитно-резонансной томографии). *Неврология, нейропсихиатрия, психосоматика*. 2017; 9 (1): 27–33. [*Mukhina T.S., Sharova E. V., Boldyreva G.N., Zhavoronkova L.A., Smirnov A.S., Kulikov M.A., Pronin I.N.* The neuroanatomy of active hand movement in patients with severe traumatic brain injury: analysis of functional magnetic resonance imaging data. *Neurology, Neuropsychiatry, Psychosomatics/ Nevrologiya Neiropsikhiatriya, Psikhosomatika*. 2017; 9 (1): 27–33. (in Russ.)]. DOI: 10.14412/2074-2711-2017-1-27-33.
7. *Жаворонкова Л.А., Морареску С.И., Болдырева Г.Н., Шарова Е.В., Купцова С.В., Смирнов А.С., Машеров Е.Л. с соавт.* ФМРТ-реакции мозга при выполнении двигательных нагрузок у пациентов с черепно-мозговой травмой. *Физиология человека*. 2018; 44 (5): 5-13. [*Zhavoronkova L.A., Morarescu S.I., Boldyreva G.N., Sharova E.V., Kuptsova S.V., Smirnov A.S., Masherov E.L., et al.* fMRI reactions in motor tasks performed by patients with traumatic brain injury. *Human Physiology/ Fiziologiya Cheloveka*. 2018; 44 (5): 5–13. (in Russ.)]. DOI: 10.1134/S0131164 618050168.
8. *Советов А.Н.* Восстановительные и компенсаторные процессы в центральной нервной системе. Москва: Медицина; 1988: 141. [*Sovietov A.N.* Restorative and compensatory processes in the central nervous system. Moscow: Medicine; 1988: 141. (in Russ.)]. ISBN 5-225-00124-6.
9. *Шарова Е.В., Болдырева Г.Н., Лысачев Д.А., Дзюбанова Н.А., Жаворонкова Л.А., Смирнов А.С., Погосбекян Э.Л., с соавт.* О функциональной и диагностической значимости типа фМРТ-ответа при двигательных нагрузках у пациентов с травматическим повреждением мозга. *Медицинская визуализация*. 2021; 25 (4): 31–46. [*Sharova E.V., Boldyreva G.N., Lysachev D.A., Dzyubanova N.A., Zhavoronkova L.A., Smirnov A.S., Pogosbekian E.L., et al.* Functional and diagnostic significance of the fMRI-response type to motor loads in patients after traumatic brain damage. *Medical Visualization/ Meditsinskaya Vizualizatsia*. 2021; 25 (4): 31–46. (In Russ.)]. DOI: 10.24835/1607-0763-1003.
10. *Шарова Е.В., Болдырева Г.Н., Лысачев Д.А., Куликов М.А., Жаворонкова Л.А., Челяпина-Постникова М.В., Попов В.А. с соавт.* ЭЭГ-корреляты пассивного движения руки у пациентов с черепно-мозговой травмой при сохранном двигательном фМРТ-ответе. *Физиология человека*. 2019; 45 (5): 30–40. [*Sharova E.V., Boldyreva G.N., Lysachev D.A., Kulikov M.A., Zhavoronkova L.A., Chelyapina-Postnikova M.V., Popov V.A., et al.* EEG correlates of passive hand movement in patients with traumatic brain injury with preserved motor fMRI response. *Human Physiology/ Fiziologiya Cheloveka*. 2019; 45 (5): 30–40. (in Russ.)]. DOI: 10.1134/S01311 64619050175.
11. *Штерн М.В., Шарова Е.В., Жаворонкова Л.А., Долгих В.Т., Кузовлев А.Н., Пронин И.Н.* Методика фМРТ анализа двигательной функциональной системы у пациентов после тяжелой черепно-мозговой травмы. *Общая реаниматология*. 2023; 19 (2): 51–59. [*Stern M.V., Sharova E.V., Zhavoronkova L.A., Dolgikh V.T., Kuzovlev A.N., Pronin I.N.* Methodical approach to fMRI assessment of motor connectome in patients after severe traumatic brain injury. *General Reanimatology/Obshchaya Reanimatologya*. 2023; 19 (2): 51–59. (in Russ. and Engl.)]. DOI: 10.15360/1813-9779-2023-2-2297.
12. *Sharova E. V., Mukhina T. S., Boldyreva G. N., Zhavoronkova L. A., Chelyapina M. V., Smirnov A. S., Pronin I. N.* FMRI analysis of the motor network functional connections at rest and with motor load in healthy people and patients with STBI. *J Neurol Stroke*. 2018; 8 (2): 91–92. DOI: 10.15406/ jnsk.2018.08.00287.

13. *Welniarz Q., Dusart I., Roze E.* The corticospinal tract: evolution, development, and human disorders. *Deve Neurobiol.* 2017; 77 (7): 810–829. DOI: 10.1002/dneu.22455. PMID: 27706924.
14. *Jang S. H.* The role of the corticospinal tract in motor recovery in patients with a stroke: a review. *NeuroRehabilitation.* 2009; 24 (3): 285–290. DOI 10.3233/NRE-2009-0480. PMID: 19458437.
15. *Бархатов Ю.Д., Кадыков А.С.* Прогностические факторы восстановления нарушенных в результате ишемического инсульта двигательных функций. *Анналы клинической и экспериментальной неврологии.* 2017; 11 (1): 80–89. [*Barkhatov Yu.D., Kadykov A.S.* Prognostic factors for recovery of motor dysfunction following ischemic stroke. *Annals of Clinical and Experimental Neurology/Annaly Klinicheskoy i Eksperimentalnoy Nevrologii*. 2017; 11 (1): 80–89. (in Russ.)]. eLIBRARY ID: 28944105.
16. *Stewart J.C., Dewanjee P., Tran G., Quinlan E.B., Dodakian L., McKenzie A., Cramer S.C.* Role of corpus callosum integrity in arm function differs based on motor severity after stroke. *NeuroImage Clin.* 2017; 14: 641–647. DOI: 10.1016/j.nicl. 2017.02.023. PMID: 28348955.
17. *Takeuchi N., Izumi S.-I.* Maladaptive plasticity for motor recovery after stroke: mechanisms and approaches. *Neural plast.* 2012; 2012: 359728. DOI: 10.1155/2012/359728. PMID: 22792492.
18. *Sarubbo S., Tate M., De Benedictis A., Merler S., Moritz-Gasser S., Herbet G., Duffau H.* Mapping critical cortical hubs and white matter pathways by direct electrical stimulation: an original functional atlas of the human brain. *Neuroimage.* 2020; 205: 116237. DOI: 10.1016/j.neuroimage.2019.116237. PMID: 31626897.
19. *Spencer A.P.C., Brooks J.C.W., Masuda N., Byrne H., Lee-Kelland R., Jary S., Chakkarapani E.* Motor function and white matter connectivity in children cooled for neonatal encephalopathy. *NeuroImage Clin.* 2021; 32: 102872. DOI: 10.1016/j.nicl.2021.102872. PMID: 34749285.
20. *Гриндель О.М.* Электроэнцефалограмма человека при черепно-мозговой травме. Москва: Наука; 1988. [*Grindel O.*M. Electroencephalogram of a person with a traumatic brain injury. Moscow: Nauka; 1988. (in Russ.)]. ISBN 5-02-005268-X.
21. *Lebel C., Caverhill-Godkewitsch S., Beaulieu C.* Age-related regional variations of the corpus callosum identified by diffusion tensor tractography. *Neuroimage.* 2010; 52 (1): 20–31. DOI: 10.1016/j.neuroimage.2010.03.072. PMID: 20362683.
22. *Zakharova N., Kornienko V., Potapov A., Pronin I.* Neuroimaging of traumatic brain injury. Springer International Publishing Switzerland: 2014; ISBN 978-3-319-04354-8.
23. *Colby J.B., Soderberg L., Lebel C., Dinov I.D., Thompson P.M., Sowell E.R.* Along-tract statistics allow for enhanced tractography analysis. *Neuroimage*. 2012; 59 (4): 3227-3242. DOI: 10.1016/j.neuroimage.2011.11.004. PMID: 22094644.
24. *Shirazi Y., Oghabian M.A., Batouli S.A.H.* Along-tract analysis of the white matter is more informative about brain ageing, compared to whole-tract analysis. *Clin Neurol Neurosurg.* 2021; 211: 107048. DOI: 10.1016/j.clineuro. 2021.107048. PMID: 34826755.
25. *Smith S.M., Jenkinson M., Johansen-Berg H., Rueckert D., Nichols T. E., Mackay C. E., Watkins K.E., et al.* Tract-based spatial statistics: voxelwise analysis of multi-subject diffusion data. *Neuroimage.* 2006; 31 (4): 1487-1505. DOI: 10.1016/j.neuroimage.2006.02.024. PMID: 16624579.
26. *Chen Z., Zhang H., Yushkevich P. A., Liu M., Beaulieu C.* Maturation along white matter tracts in human brain using a diffusion tensor surface model tract-specific analysis. *Front Neuroanat.* 2016; 10: 9. DOI: 10.3389/fnana. 2016.00009. PMID: 26909027.
27. *Owen M., Ingo C., Dewald J.P.A.* Upper extremity motor impairments and microstructural changes in bulbospinal pathways in chronic hemiparetic stroke. *Front Neurol.* 2017; 8: 257. DOI: 10.3389/fneur.2017.00257. PMID: 28659855.
28. *Teasdale G., Jennett B.* Assessment of coma and impaired consciousness: a practical scale. *Lancet.* 1974; 2 (7872): 81–84. DOI: 10.1016/s0140-6736 (74)91639-0. PMID: 4136544.
29. J*ennett B., Bond M.* Assessment of outcome after severe brain damage. *Lancet.* 1975; 1 (7905): 480–484. DOI: 10.1016/S0140-6736 (75)92830-5. PMID: 46957.
30. *Мочалова Е.Г., Легостаева Л.А., Зимин А.А., Юсупова Д.Г., Сергеев Д.В., Рябинкина Ю.В., Бодин Е. с соавт.* Русскоязычная версия пересмотренной шкалы восстановления после комы — стандартизированный метод оценки пациентов с хроническими нарушениями сознания. *Журнал неврологии и психиатрии.* 2018; 118 (3–2): 25–31. [*Mochalova E.G., Legostaeva L.A., Zimin A.A., Yusupova D.G., Sergeev D.V., Ryabinkina Yu.V., Bodin E. et al.* The Russian version of Coma Recovery Scale-revised — a standardized method for assessment of patients with disorders of con-

sciousness. Journal of Neurology and Psychiatry/ *Zhurnal Nevrologii i Psikhiatrii imeni S.S. Korsakova*. 2018; 118 (3–2): 25–31. (in Russ.)]. DOI: 10.17116/jnevro20181183225-31.
31. *McPeak L.A.* Physpiatric history and examination in: Physical Medicine and Rehabilitation, Braddom, R. (ed.). WB Saunders Company; 1996: 3–42.
32. *Tax C.M.W., Jeurissen B., Vos S.B., Viergever M.A., Leemans A.* Recursive calibration of the fiber response function for spherical deconvolution of diffusion MRI data. *Neuroimage*. 2014; 86: 67–80. DOI: 10.1016/j.neuroimage.2013.07.067. PMID: 23927905.
33. *Witelson S.F.* Hand and sex differences in the isthmus and genu of the human corpus callosum: a postmortem morphological study. *Brain*. 1989; 112 (Pt 3): 799–835. DOI: 10.1093/brain/112.3.799. PMID: 2731030.
34. *Sharova E.V., Pogosbekyan E.L., Korobkova E.V., Zaitsev O., Zakharova N., Chelyapina M.V., Fadeeva L.M., et al.* Inter hemispheric connectivity and attention in patients with disorders of consciousness after severe traumatic brain injury. *J Neurol Stroke*. 2018; 8 (4): 245–253. DOI: 10.15406/jnsk.2018. 08.00319.
35. *Белова А.Н., Григорьева В.Н., Сушин В.О., Белова Е.М., Исраелян Ю.А., Шейко Г.Е.* Анатомо-функциональные особенности кортикоспинальных трактов и их роль в восстановлении двигательных функций после повреждений головного мозга. *Вестник восстановительной медицины*. 2020; 1 (95): 9–18. [*Belova A.N., Grigorieva V.N., Sushin V.O., Belova E.M., Israelyan Yu.A., Sheiko G.E.* Anatomical and functional features of corticospinal tracts and their role in restoring motor functions after brain injury. *Bulletin of Rehabilitation Medicine/Vestnik Vosstanovitelnoy Meditciny*. 2020; 1 (95): 9–18. (in Russ.)].
36. *Volz L.J., Rehme A.K., Michely J., Nettekoven C., Eickhoff S.B., Fink G.R., Grefkes C.* Shaping early reorganization of neural networks promotes motor function after stroke. *Cereb Cortex*. 2016; 26 (6): 2882–2894. DOI: 10.1093/cercor/bhw034. PMID: 26980614.
37. *Ковязина М.С., Балашова Е.Ю.* О некоторых аспектах межполушарного взаимодействия в двигательных функциях у детей в норме и с синдромом Дауна. *Вестник Московского университета. Серия* 14. *Психология*. 2008; (4): 54–66. [*Kovyazina M.S., Balashova E.Yu.* Some characteristics of the interhemispheric coordination in motor functions in normal child development and Down syndrome. *Bulletin of the Moscow University. Series* 14. *Psychology*/ *Vestnik Moskovskogo Universiteta. Seriya* 14. *Psikhologiya*. 2008; (4): 54–66. (in Russ.)].
38. *Min Y.-S., Park J.W., Park E., Kim A.-R., Cha H., Gwak D.W., Jung S.-H., et al.* Interhemispheric functional connectivity in the primary motor cortex assessed by resting-state functional magnetic resonance imaging aids long-term recovery prediction among subacute stroke patients with severe hand weakness. *J Clin Med*. 2020; 9 (4): 975. DOI: 10.3390/jcm9040975. PMID: 32244596.
39. *Зыкин П.А., Ялфимов А.Н., Александров Т.А., Краснощекова Е.И., Ткаченко Л.А., Середа В.М., Насыров Р.А.* Особенности развития мозолистого тела мозга детей по данным МРТ. *Педиатр*. 2018; 9 (1): 37–48. [*Zykin P.A., Yalfimov A.N., Alexandrov T.A., Krasnoshchekova E.I., Tkachenko L.A., Sereda V.M., Nasyrov R.A.* Developmental features of corpus callosum in children revealed by MRI. *Pediatrician*/*Pediatr*. 2018; 9 (1): 37–48. (in Russ.)]. DOI: 10.17816/PED9137-48.
40. *Анпилогова К.С., Чегина Д.С., Игнатова Т.С., Ефимцев А.Ю., Труфанов Г.Е.* Структурная реорганизация проводящих путей белого вещества головного мозга у пациентов со спастической диплегией после транслингвальной нейростимуляции. *Трансляционная медицина*. 2021; 8 (4): 27–34. [*Anpilogova K.S., Chegina D.S., Ignatova T.S., Efimtsev A.Yu., Trufanov G.E.* Structural reorganization of the white matter pathways of the brain in patients with spastic diplegia after translingual neurostimulation. *Translational Medicine/Translyacionnaya Meditsina*. 2021; 8 (4): 27–34. (in Russ.).]. DOI: 10.18705/2311-4495-2021-8-4-27-34.
41. *Потапов А.А., Горяйнов С.А., Жуков В.Ю., Пицхелаури Д.И., Кобяков Г.Л., Пронин И.Н., Меликян З.А.* Длинные ассоциативные пути белого вещества головного мозга: современный взгляд с позиции нейронаук. *Вопросы нейрохирургии им. НН Бурденко*. 2014; 78 (5): 66–77. [*Potapov A.A., Goryainov S.A., Zhukov V.Yu., Pithelauri D.I., Kobyakov G.L., Pronin I.N., Melikyan Z.A.* The Long-associative pathways of the white matter: modern view from the perspective of neuroscience. *Burdenko's Journal of Neurosurgery* / *Zhurnal Voprosy Neirokhirurgii Imeni N.N. Burdenko*. 2014; 78 (5): 66–77. (in Russ)].
42. *Shirer W.R., Ryali S., Rykhlevskaia E., Menon V., Greicius M.D.* Decoding subject-driven cognitive states with whole-brain connectivity patterns. *Cereb Cortex*. 2012; 22 (1): 158–165. DOI: 10.1093/cercor/bhr099. PMID: 21616982.

43. *Okamoto Y., Ishii D., Yamamoto S., Ishibashi K., Wakatabi M., Kohno Y., Numata K.* Relationship between motor function, DTI, and neurophysiological parameters in patients with stroke in the recovery rehabilitation unit. *J Stroke Cerebrovasc Dis*. 2021; 30 (8): 105889. DOI: 10.1016/j.jstrokecerebrovasdis.2021.105889. PMID: 34062310.
44. *Voelbel G.T., Genova H.M., Chiaravalotti N.D., Hoptman M.J.* Diffusion tensor imaging of traumatic brain injury review: implications for neurorehabilitation. *NeuroRehabilitation*. 2012; 31 (3): 281–293. DOI: 10.3233/NRE-2012-0796. PMID: 23093455.
45. *Song J., Young B.M., Nigogosyan Z., Walton L.M., Nair V.A., Grogan S. W., Tyler M.E., et al.* Characterizing relationships of DTI, fMRI, and motor recovery in stroke rehabilitation utilizing brain-computer interface technology. *Front Neuroeng*. 2014; 7: 31. DOI: 10.3389/fneng.2014.00031. PMID: 25120466.

Received 17.07.2023
Accepted 23.10.2023

https://doi.org/10.15360/1813-9779-2023-6-39-47

Evolution of Techniques and New Protocols for Lung Ultrasound Examination in COVID-19 Pneumonia Patients

Ivan S. Shcheparev[1]*, Boris A. Teplykh[1], Galina S. Kireeva[1], Denis N. Protsenko[2,3], Denis V. Kotsyubinsky[1], Oleg Yu. Bronov[1], Eleonora A. Balanyuk[2,3]

[1] N. I. Pirogov National Medical Surgical Center, Ministry of Health of Russia, 70 Nizhnyaya Pervomayskaya Str., 105203 Moscow, Russia
[2] City Clinical Hospital № 40, Moscow City Health Department, 7 Kasatkina Str., 107014 Moscow, Russia
[3] Moscow Multispecialized Clinical Center «Kommunarka», Moscow City Health Department, 8 Sosensky Stan Str.. Kommunarka settlement, 108814 Russia

For citation: *Ivan S. Shcheparev, Boris A. Teplykh, Galina S. Kireeva, Denis N. Protsenko, Denis V. Kotsyubinsky, Oleg Yu. Bronov, Eleonora A. Balanyuk.* Evolution of Techniques and New Protocols for Lung Ultrasound Examination in COVID-19 Pneumonia Patients. *Obshchaya Reanimatologiya = General Reanimatology.* 2023; 19 (6): 39–47. https://doi.org/10.15360/1813-9779-2023-6-39-47 [In Russ. and Engl.]

***Correspondence to:** Ivan S. Shcheparev, is22@list.ru

Summary

Competent triage of patients with COVID-19 pneumonia is not only about efficient allocation of hospital resources, but also about making timely decisions that can ultimately save the patient's life. When healthcare facility is overloaded, computed tomography to assess the severity of COVID-19-associated pneumonia in each individual case is not always possible. Alternative solutions, however, are opted.

The aim of the study was to develop Lung UltraSound (LUS) protocols with high diagnostic potential for assessing the severity of pneumonia caused by COVID-19, which can be reliably used instead of CT during triage in an emergency setting.

Materials and methods. We conducted a retrospective analysis of data on 161 hospitalized patients with confirmed pneumonia caused by COVID-19, subjected to both CT and LUS within 24 hours after hospitalization. Three consecutive LUS protocols, including two LUS developed by the NMHC (National Medical Surgical Center) authors, were tested to choose the most reliable protocol for assessing the severity of lung damage in pneumonia caused by COVID-19 (based on correlation with chest CT results). We also checked the applicability of LUS for the prognosis of the disease.

Results. Moderate (<50% CT) and severe (>50% CT) lung damage can be distinguished when using both — the 16-zone and 12-zone LUS NMHC scanning protocols. The AUC for the ROC curves was almost identical: 0.83 (95% CI: 0.75–0.90 and 0.81 (95% CI: 0.73–0.88) for the 16-zone and 12-zone LUS NMHC protocols, respectively. The 16-zone LUS NMHC had an optimal threshold of 20 scores with a sensitivity of 67% and a specificity of 82%, while the 12-zone LUS NMHC provided an optimal threshold of 15 scores with the same sensitivity but lower specificity — only 73%. Neither the 16-zone nor the 12-zone NMHC LUS protocols could predict the outcome.

Conclusion. The newly developed 16- and 12-zone LUS NMHC scanning protocols for patients with pneumonia caused by COVID-19 proved to be easy to implement, demonstrating a strong correlation with CT results. The 16-zone LUS NMHC protocol is probably more relevant for triage of patients with more than 50% of pulmonary tissue involvement based on CT data. Both protocols can be useful in emergency settings and in medical institutions with limited or no access to CT.

Keywords: lung ultrasound; LUS score; COVID-19; pneumonia

Conflict of interest. The authors declare no conflict of interest.

Read the full-text English version at www.reanimatology.com

Introduction

Following the first few months of the COVID-19 pandemic, it has become clear that public health systems are struggling to allocate limited resources during an unprecedented increase in hospitalizations [1]. One of the most difficult tasks is still triaging and identifying patients who require hospitalization. Although PCR testing is still the gold standard for SARS-CoV-2 diagnosis, chest CT is the preferred diagnostic modality for determining disease severity in confirmed cases [2, 3]. Several studies [4, 5] have shown that CT has a diagnostic value in asymptomatic infected patients. However, limited radiology resources and strict decontamination protocols following COVID-19 examinations have jeopardized CT's widespread availability and efficacy [6–8].

Lung ultrasound (LUS) has been proposed as an effective diagnostic tool [11, 12] and is a feasible and inexpensive diagnostic option for COVID-19 pneumonia. Despite its controversial diagnostic value, LUS eventually gained widespread clinical use [13, 14]. The variability of the LUS protocols used and the lack of reproducibility for different

operators [2] undermine the validity of using LUS in the triage of COVID-19 pneumonia patients.

Another issue with LUS is the lack of standardized reporting and interpretation systems [15]. The Pirogov National Medical and Surgical Center discovered early in the pandemic that the standard descriptive LUS protocol had moderate to low diagnostic value and was unacceptably time-consuming in triaging patients with COVID-19.

Therefore, the aim of the study was to propose new LUS protocols with high diagnostic performance for determining the severity of lung injury in COVID-19 pneumonia that could be used instead of CT scanning in patient triage in the acute care setting.

Furthermore, to our knowledge, this is the first study to report the results of different LUS protocols performed in the same patients with confirmed COVID-19.

Materials and Methods

We performed a retrospective study using lung ultrasound data from 161 patients with COVID-19 hospitalized between March and May 2021.

This study was approved by the Local Ethical Committee of the Pirogov National Medical and Surgical Center (Protocol No. 11, dated October 26, 2021) and conducted in accordance with the Declaration of Helsinki. Because the data were collected retrospectively and processed anonymously, informed consent was not considered necessary by the Local Ethics Committee of the Pirogov National Medical and Surgical Center.

Patients were initially admitted to the intensive care unit (ICU), and both chest CT and LUS were performed within 24 h of admission.

The diagnosis of COVID-19 was confirmed either by a positive PCR test for SARS-CoV-2 or by a combination of clinical manifestations and radiological signs of infection, even with a negative PCR test on admission.

The exclusion criteria were suspected bacterial infection based on laboratory or radiological findings that developed before admission.

Chest CT evaluation. All enrolled patients underwent chest CT as part of the routine local protocol for suspected COVID-19 pneumonia. A 64-channel Brilliance (Philips Healthcare, Cleveland, OH, USA) or GE Revolution Evo CT scanner was used. The acquisition parameters were 120 kV and 90 mA (±25%). The slice thickness for the lung reconstruction was 1.25 mm. The «lung» filter was used. The extent of lung damage was assessed using a semiquantitative visual CT scoring system (Table 1) based on the volume and characteristics of lung tissue damage (ground-glass opacities and/or consolidation) [16]:

- CT-0, no abnormalities
- CT-1, lung tissue damage <25%
- CT-2, lung tissue damage 25–50%
- CT-3, lung tissue damage 50–75%
- CT-4, lung tissue damage >75%.

Lung UltraSound scales and interpretation. Sonosite Edge II (Fujifilm Sonosite, USA) and Logiq E (GE Healthcare, China) ultrasound devices were used, and a convex transducer was used in the study. The basic mode was «abdominal» and the scan depth was 11–13 cm.

SPSS IBM version 22 (SPSS Inc., Chicago, IL, USA) was used for statistical analysis. As appropriate, demographic, clinical, and endpoint variables were presented as means and standard deviations (SD), medians and interquartile ranges (IQR), or numbers (percentages).

To determine the distribution of data, the Shapiro–Wilk test was used. Depending on the normality of the distribution, ANOVA or Mann–Whitney and Kruskal–Wallis *U* criteria were used for comparative analysis.

Spearman's correlation coefficient was used to assess the correlation between data obtained by

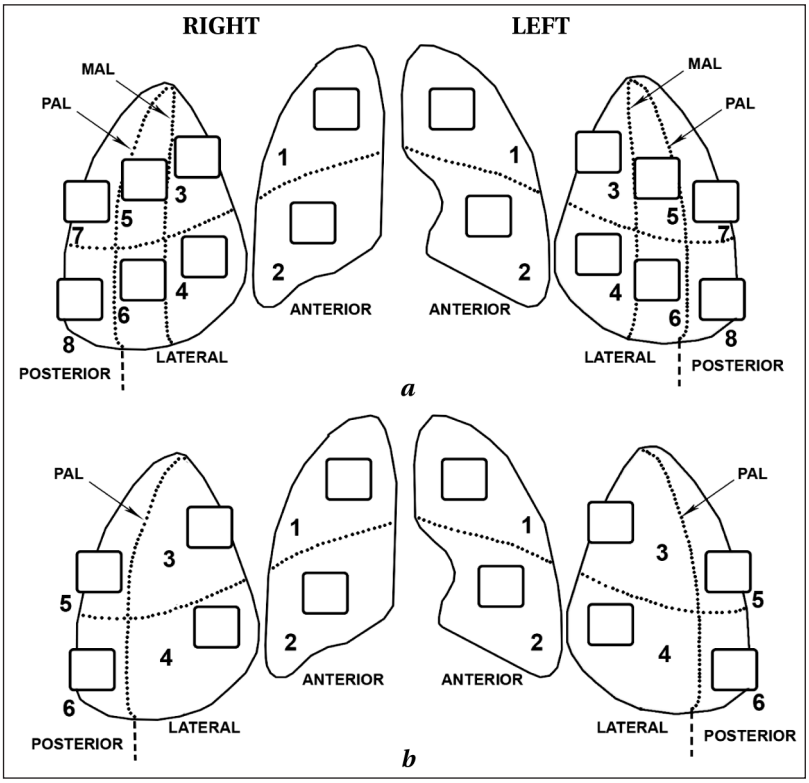

Fig. 1. Lung scheme for the 16-zone LUS and LUS NMHC protocols *(a)* and the 12-zone LUS NMHC protocol *(b)*.
Note. MAL stands for middle axillary line and PAL stands for posterior axillary line. Author's drawing.

Table 1. Scoring protocols for determining the severity of lung damage in COVID-19-induced pneumonia according to LUS results.

Points	Protocol Criteria		
	16-zone LUS	**16-zone LUS NMHC**	**12-zone LUS NMHC**
0	Normal lung profile without pleural deformities. Single (<3) B-lines are acceptable	A-lines occupy 100% of the tested area, up to 2 lines per the field of view are allowed. B-lines cannot be confluent or bright, A-lines should be clearly visible against them.	A-lines occupy 100% of the tested area, up to 2 lines per the field of view are allowed. B-lines cannot be confluent or bright, A-lines should be clearly visible against them.
1	Moderate interstitial syndrome, up to 5 B-lines per the field of view. Deformed pleural line.	A-lines occupy >50% of the intercostal spaces per the field of view **or** A-lines occupy 100% of the tested area with multiple B-lines that are clearly visible against the A-lines	A-lines occupy >50% of the intercostal spaces per the field of view **or** A-lines occupy 100% of the tested area with multiple B-lines that are clearly visible against the A-lines
2	Significant interstitial syndrome, subpleural consolidations less than 15 mm*	A-lines occupy <50% of the intercostal spaces per the field of view. **or** The ratio of B-lines to A-lines is 1:1 with subpleural consolidation less than 15 mm	A-lines occupy <50% of the intercostal spaces per the field of view. **or** The ratio of B-lines to A-lines is 1:1 with subpleural consolidation less than 15 mm
3	Large consolidation of more than 15 mm*	Large consolidation greater than 15 mm with or without pleural effusion	Large consolidation greater than 15 mm with or without pleural effusion

Note. * — A threshold value of 15 mm was adopted to differentiate between subpleural and large consolidations [18] detected during ultrasound examination.

LUS and chest CT protocols (as well as between different LUS protocols).

ROC curves were used to compare LUS's ability to discriminate the severity of lung damage detected by CT and predict outcome.

The optimal threshold was determined using the Youden index. The feasibility of using LUS and CT scores for individualized prognosis was evaluated using multivariable logistic regression.

Availability of data and materials. The data are not publicly available because they contain sensitive information about the study participants. Anonymized data supporting the findings of this study are available from the author, I. S. Shcheparev, upon request.

Results

A total of 161 patients with COVID-19 who underwent both chest CT and LUS at hospitalization were included in the study. Their demographic and clinical data are presented in Table 2. The mean duration of symptoms from onset to hospitalization was 10 days (IQR, 3–10).

Of the 161 patients admitted, 59 (36.6%) ultimately required invasive mechanical ventilation and 7 (4.3%) required noninvasive mechanical ventilation. A total of 137 patients (85%) spent at least 1 day in the ICU, with a median length of stay of 5 days (IQR, 3–10). The median length of hospital stay was 8 days (IQR, 3–15).

An example of matched LUS and CT images of a patient with COVID-19 pneumonia used for evaluation is presented in Fig. 2.

In May 2020, the 16-zone LUS protocol together with chest CT was performed in 18 patients (11.1%),

Table 2. Baseline characteristics of hospitalized patients with COVID-19.

Parameter	Value (*N*=161)
Men, n (%)	67 (41.6)
Women, n (%)	94 (58.4)
Age, years	69.2±14.6
SpO_2, %	85.0±12.6
Time from onset of symptoms to hospitalization, days	10 [3–10]
C-reactive protein, mg/L (*N*=154)	97.5 [42.3; 158.5]
NEWS scale, points (*N*=137)	4.8±2.9
LUS protocols used, *N* (%)	161 (100)
16-zone LUS, *N* (%)	18 (11.1)
16-zone LUS NMHC, *N* (%)	143 (88.8)
12-zone LUS NMHC, *N* (%)	143 (88.8)

while the 16-zone LUS NMHC and 12-zone LUS NMHC protocols were performed sequentially in the remaining 143 patients (88.8%) between March and May 2021. The reason for the small number of patients evaluated by the initially developed descriptive 16-zone LUS was due to several pitfalls of the protocol that were discovered during its clinical application. These included:

1. The high heterogeneity of lung damage observed with the ultrasound transducer made it difficult to count the exact number of B-lines.

2. The presence of areas of intact lung tissue together with large confluent B-lines, which did not allow reliable and clear differentiation of Grade 1 or Grade 2 criteria.

3. Personal protective equipment, including goggles, and their frequent change, which contributed to distractions that interfered with accurate assessment of the ultrasound result.

LUS scores measured using the 16-zone LUS NMHC or 12-zone LUS NMHC protocols in patients

with varying degrees of CT lung damage differed significantly ($P<0.001$) (Table 3, Fig. 3), with the median LUS score for the 12-zone protocol tending to be several points lower in all patients graded by CT.

A strong positive correlation was found between 16-zone LUS NMHC results and the severity (%) of lung damage on CT (Spearman correlation coefficient $R=0.79$, $P<0.001$) (Fig. 3, *a*), and 12-zone LUS and the severity of lung damage on CT, $R=0.78$, $P<0.001$) (Fig. 3, *c*).

Both the 16-zone and 12-zone LUS NMHC protocols showed good performance in discriminating between moderate (less than 50% of lung tissue volume on CT) and severe (>50%) lung damage (Figure 4). The AUC of the ROC curves were almost identical: 0.83 (95% CI, 0.75–0.90) and 0.81 (95% CI, 0.73–0.88) for the 16-zone LUS NMHC and 12-zone LUS NMHC protocols, respectively. The 16-zone LUS NMHC had an optimal threshold of 20 points with a sensitivity of 67% and a specificity of 82%, whereas the 12-zone LUS NMHC had an optimal threshold of 15 points with the same sensitivity but a lower specificity of only 73%.

Seventy-six patients died, 74 (97%) before day 30, 2 patients (3%) after day 30 of treatment, 64 patients were discharged, and outcome data were not available for 3 patients. The AUC of the ROC curves for the 16-zone LUS NMHC (0.67; 95% CI, 0.58–0.76) and 12-zone LUS (0.68; 95% CI, 0.59–0.77) protocols demonstrated moderate ability to predict outcome, as did the AUC for CT (0.65; 95% CI, 0.56-0.74) (Fig. 5). The optimal threshold for 16-zone LUS NMHC and 12-zone LUS NMHC was 12 and 10 points, respectively, with unacceptable specificity of 53 and 55%.

Male sex, older age, and greater percentage of lung damage detected on CT scan on admission were predictors of unfavorable prognosis (Table 4).

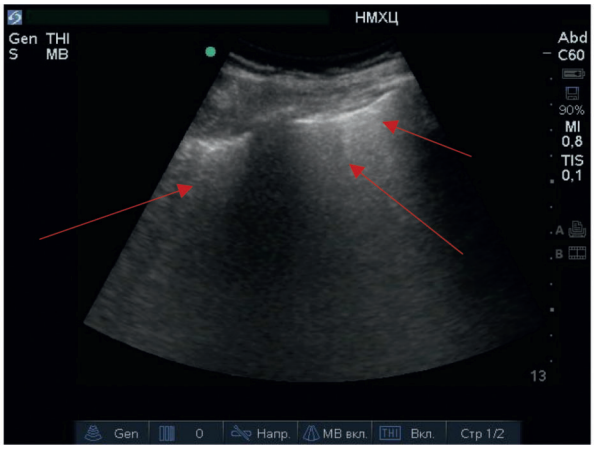

a

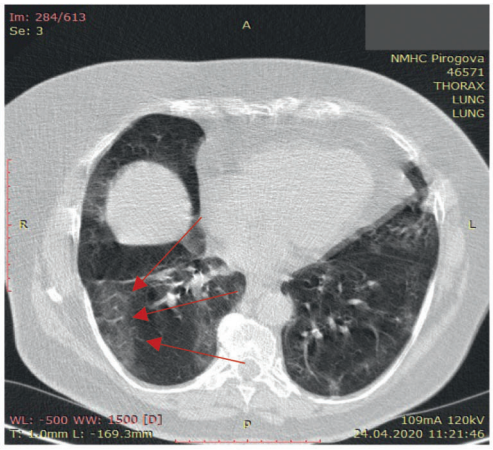

b

Fig. 2. Example of paired LUS and CT images.
Note. LUS image shows *(a)* multiple confluent B-lines without clearly visible A-lines («corresponds to grade 2»); CT image shows *(b)* a large ground glass-like opacity area.

Discussion

Although LUS cannot be considered the diagnostic modality of choice for patients with COVID-19

Table 3. Correspondence of chest CT scores and LUS scores according to protocols used.

CT scale, points	LUS scale, points				
	Number of patients and protocol options				
	N	16-zone LUS	*N*	16-zone LUS NMHC	12-zone LUS NMHC
0	5	4 (0–0.4)	54	6 (5.7–8.1)	5 (5.0–7.0)
1	4	11 (4.3–15.7)	21	14 (10.4–15.9)	11 (8.7–12.9)
2	1	—	38	21.5 (20.0–23.0)	17.5 (16.0–18.3)
3	8	26.5 (21.7–31.3)	29	23 (21.0–24.5)	18 (16.3–19.1)
4	0	—	1	—	—
0–2*	10	9 (3.0–10.8)	113	12 (11.5–14.5)	10 (9.5–11.8)
3–4**	8	27 (22.6–31.1)	30	22.5 (20.7–24.2)	18 (16.1–18.9)

Note. * <50% of lung damage; ** >50% of lung damage. Data presented as median (interquartile range).

Table 4. Analysis of predictors of mortality in patients with COVID-19.

Parameter	Odds ratio (95% CI)	*P*-value
Male sex	2.13(1.25–3.62)	0.005
Age	1.05 (1.02–1.08)	0.002
Days before hospitalization	1.03 (0.96–1.11)	0.36
SpO_2 on admission	0.98 (0.95–1.02)	0.38
Lung damage on CT, %	0.98 (0.96–0.99)	0.04

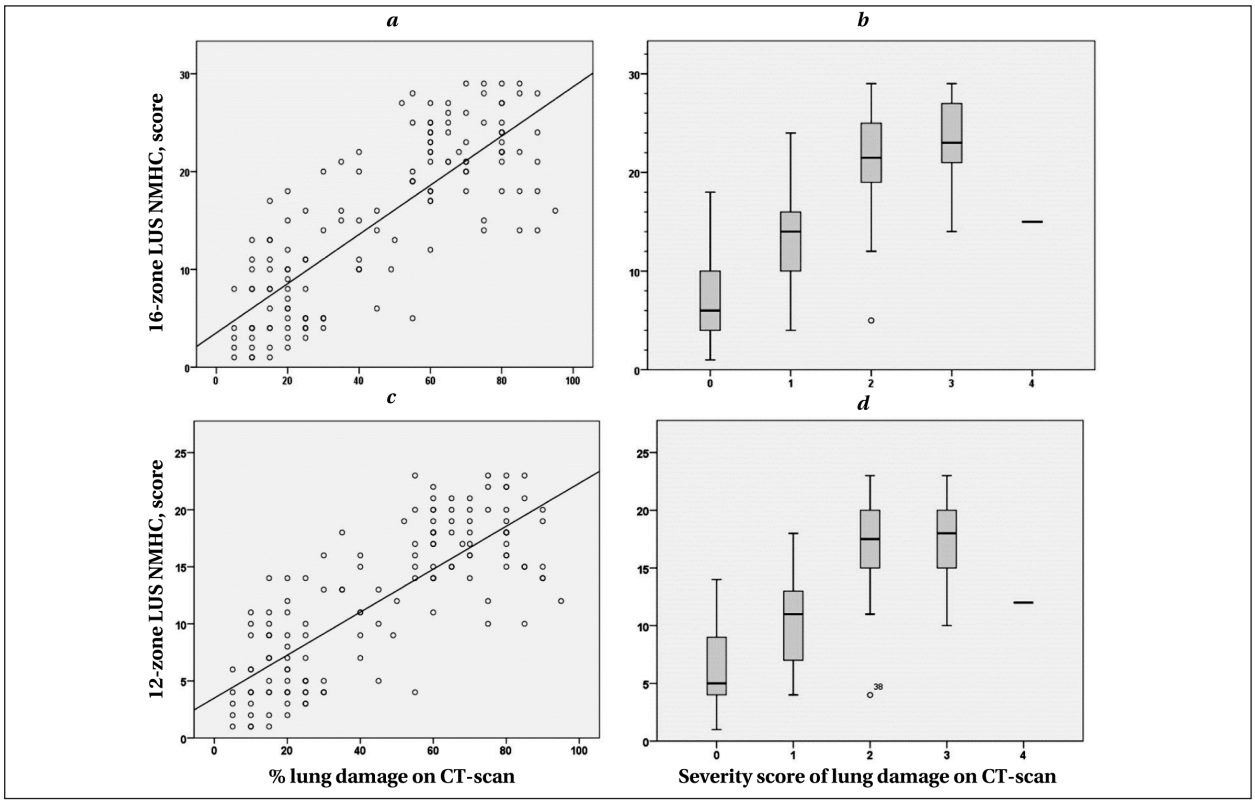

Fig. 3. Correlation of lung damage severity (%) based on CT data with 16-zone *(a)*, 12-zone *(c)* LUS NMHC results; correlation of lung damage severity (scores) based on CT data with 16-zone *(b)*, 12-zone *(d)* LUS NMHC results.

pneumonia, it has been shown to be a reliable tool for patient triage in mass hospitalizations and with limited CT capacity [19, 20]. LUS is relatively easy to use [21] and can be performed at the patient's bedside, minimizing the number of healthcare providers in contact with the patient. However, difficulties can arise in its interpretation in assessing the severity of lung injury and thus in selecting the best treatment strategy. Reliable LUS assessment protocols can be of great value as a diagnostic tool, especially in acute care settings and healthcare facilities with limited access to CT scans. The only systematic review and meta-analysis on this topic concluded that the diagnostic concordance between LUS and

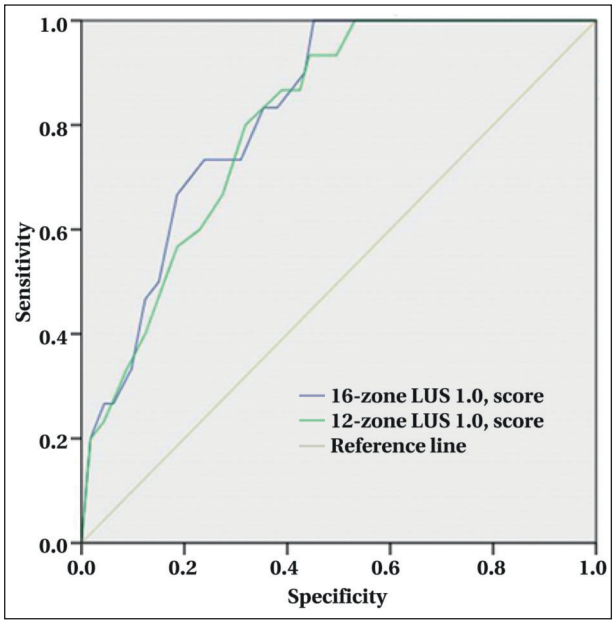

Fig. 4. ROC curve comparison for 16-zone and 12-zone LUS NMHC protocols in patients with >50% lung damage on CT.

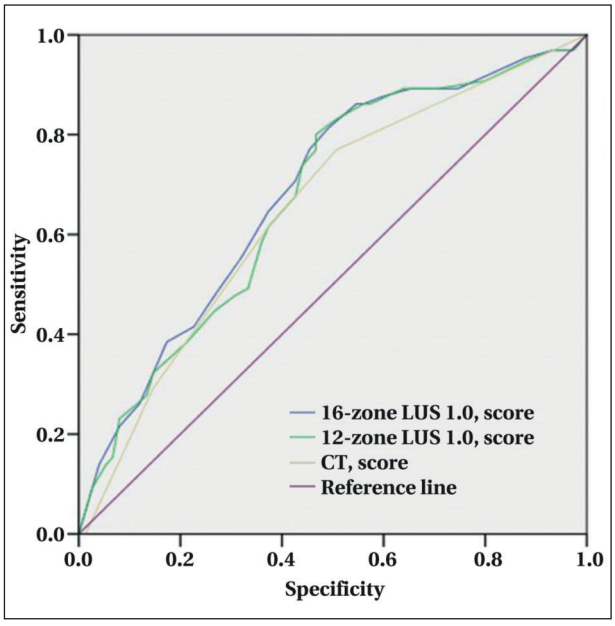

Fig. 5. Comparison of ROC curves for 16-zone, 12-zone LUS NMHC and CT protocols in patients with >50% lung damage on CT.

CT for the diagnosis of lung injury in COVID-19 is high [5]. The quality of the evidence reviewed was considered low; however, LUS has great potential as an alternative to CT in emergency or critical care settings.

Three protocols for LUS evaluation of patients with confirmed COVID-19 were developed and tested. First, a 16-zone LUS protocol was based on the calculation of B-lines, degree of interstitial changes, and size of the subpleural consolidations. The other two protocols, the modified 16-zone LUS NMHC and 12-zone LUS NMHC, were based on the evaluation of A-lines, and B-lines were of secondary importance. It was found that the first LUS protocol was associated with several technical problems related to the evaluation of the results obtained; thus, its implementation did not provide a reliable evaluation and convenience of performance. This protocol was used in 18 patients, and in this limited sample, an increase in the score was noted along with an increase in the CT severity score, which was consistent with the results of the other two protocols tested later in 143 patients.

The 16 zone LUS NMHC and 12 zone LUS NMHC protocols have been proposed as more feasible and reliable scoring systems. Similar LUS protocols have been described in several studies [22, 23]; however, the ratio of vertical to horizontal artifacts was used instead of A-line scoring. In the literature, visible A-lines are not described as a separate feature along with B-lines in the field of view of the ultrasound transducer. We hypothesize that the appearance of A-lines in front of B-lines is only possible with a certain amount of intact lung tissue and that the interpretation of such images does not follow any known guidelines or evaluation protocols.

Therefore, we hypothesized that the evaluation of A-lines instead of the ratio of vertical to horizontal artifacts would be diagnostically significant and easier to perform than in previously described protocols [22, 23].

According to known data, many authors tend to use the 12-zone LUS protocol [23–29]. However, the present study showed that the modified 16-zone LUS NMHC protocol was «slightly better» than the 12-zone LUS NMHC protocol. The performance of the 16-zone LUS NMHC and 12-zone LUS NMHC protocols had a strong correlation with the severity of lung damage on CT, which adds to similar findings from other studies [5, 24, 25, 30–32]. Meanwhile, LUS NMHC with 16 zones was more accurate in differentiating less/more than 50% lung injury. This may support the use of the 16-zone LUS NMHC protocol in the acute care setting to determine prognosis and the need for ICU admission.

Both protocols had moderate prognostic performance with a specificity of 53% for the 16-zone LUS NMHC and 55% for the 12-zone LUS NMHC. There are conflicting data regarding the prognostic value of LUS. In two observational studies [26, 28], a higher LUS score using the 12-zone protocol was not a predictor of mortality. On the contrary, Heldeweg et al [27] showed that a higher LUS score using the 12-zone protocol had a strong association with mortality and ICU stay of more than 30 days.

In this study, the 12-zone LUS NMHC protocol scores were recalculated from the 16-zone LUS NMHC protocol data, which does not allow direct comparison of the data with previous studies.

The main limitations of the study were its retrospective design and the fact that it was not designed to test the hypothesis of clinical equivalence between LUS and CT but rather to test the correlation between these techniques.

Another difficulty was the initial use of a 16-zone LUS protocol, which «evolved» from a local descriptive LUS protocol for non-COVID-19 pneumonia, the continued use of which was abandoned due to a number of technical problems; hence, the small patient sample size. However, the total sample size (161 patients) was larger than that in most published papers, and the two developed LUS evaluation protocols were tested in the same patients.

Conclusion

The developed 16-zone and 12-zone NMHC LUS protocols in patients with COVID-19-associated pneumonia proved to be feasible and strongly correlated with CT findings. The results of the 16-zone and 12-zone NMHC LUS protocols were not predictive of the outcome. Both protocols can probably be adapted for the triage of patients with confirmed COVID-19, especially in the acute care setting and in healthcare facilities with limited or no access to CT.

References

1. *Conti S., Ferrara P., Fornari C., Harari S., Madotto F., Silenzi A., Zucchi A., et al.* Estimates of the initial impact of the COVID-19 epidemic on overall mortality: evidence from Italy. *ERJ Open Res.* 2020; 6 (2): 00179–2020. DOI: 10.1183/ 23120541.00179-2020. PMID: 32613013.
2. *Rubin G.D., Ryerson C.J., Haramati L.B., Sverzellati N., Kanne J.P., Raoof S., Schluger N.W., et al.* The role of chest imaging in patient management during the COVID-19 pandemic: a multinational Consensus Statement from the Fleischner Society. *Chest.* 2020; 158 (1): 106–116. DOI: 10.1016/j.chest.2020. 04.003. PMID: 32275978.
3. ACR. ACR Recommendations for the use of chest radiography and computed tomography (CT) for suspected COVID-19 infection. American College of Radiology. Available at https: //www.acr.org/Advocacy-and-Economics/ACR-Position-Statements/Recommendations-for-Chest-Radiography-and-CT-for-Suspected-COVID19-Infection. March 22, 2020; Accessed: April 2, 2020.
4. *Hu Z., Song C., Xu C., Jin G, Chen Y., Xu X., Ma H.,et al.* Clinical characteristics of 24 asymptomatic infections with COVID-19 screened among close contacts in Nanjing, China. *Sci China Life Sci.* 2020; 63 (5): 706–711. DOI: 10.1007/s11427-020-1661-4. PMID: 32146694.
5. *Wang Y., Liu Y., Liu L., Wang X., Luo N., Ling L.* Clinical outcome in 55 patients with severe acute respiratory syndrome Coronavirus 2 who were asymptomatic at hospital admission in Shenzhen, China. *J Infect Dis.* 2020; 221 (11): 1770–1774. DOI: 10.1093/infdis/jiaa119. PMID: 32179910.
6. Yan C., Lin J., Xu Y. Recommendations for coronavirus disease 2019 (COVID-19) prevention and infection control in the radiology department: Chinese experience. Clin Imaging. 2021; 69: 33–36. DOI: 10.1016/j.clinimag. 2020.06.044. PMID: 32652455.
7. *Qu J., Yang W., Yang Y., Qin L, Yan F.* Infection control for CT equipment and radiographers' personal protection during the Coronavirus disease (COVID-19) outbreak in China. *AJR Am J Roentgenol.* 2020; 215 (4): 940–944: DOI: 10.2214/AJR.20. 23112. PMID: 32352309.
8. *Stogiannos N., Fotopoulos D., Woznitza N., Malamateniou C.* COVID-19 in the radiology department: what radiographers need to know. *Radiography* (Lond) 2020; 26 (3): 254–263. DOI: 10.1016/j.radi.2020.05.012. PMID: 32532596.
9. *Mayo P.H., Copetti R., Feller-Kopman D., Mathis G., Maury E., Mongodi S., Mojoli F. et al.* Thoracic ultrasonography: a narrative review. *Intensive Care Med.* 2019; 45 (9): 1200–1211. DOI: 10.1007/s00134-019-05725-8. PMID: 31418060.
10. *Buonsenso D., Pata D., Chiaretti A.* COVID-19 outbreak: less stethoscope, more ultrasound. *Lancet Respir Med.* 2020; 8 (5): e27. DOI: 10.1016/S2213-2600 (20)30120-X. PMID: 32203708.
11. *Cheung J.C.-H., Lam K.N.* POCUS in COVID-19: pearls and pitfalls. *Lancet Respir Med.* 2020; 8 (5): e34. DOI: 10.1016/ S2213-2600 (20)30166-1. PMID: 32275856.
12. *Soldati G., Smargiassi A., Inchingolo R., Buonsenso D., Perrone T., Briganti D.F., Perlini S., et al.* Is there a role for lung ultrasound during the COVID-19 pandemic? *J Ultrasound Med.* 2020; 39 (7): 1459–1462. DOI: 10.1002/jum. 15284. PMID: 32198775.
13. *Volpicelli G., Lamorte A., Villén T.* What's new in lung ultrasound during the COVID-19 pandemic. *Intensive Care Med.* 2020; 46 (7): 1445–1448. DOI: 10.1007/s00134-020-06048-9. PMID: 32367169.
14. *Peixoto A.O., Costa R.M., Uzun R., Fraga A.M.A., Ribeiro J.D., Marson F.A.L.* Applicability of lung ultrasound in COVID-19 diagnosis and evaluation of the disease progression: a systematic review. *Pulmonology.* 2021: 27 (6): 529–562. DOI: 10.1016/j.pulmoe.2021.02.004. PMID: 33931378.
15. *Schultz M.J., Sivakorn C., Dondorp A.M.* Challenges and opportunities for lung ultrasound in novel Coronavirus disease (COVID-19). *Am J Trop Med Hyg.* 2020; 102 (6): 1162–1163. DOI: 10.4269/ajtmh.20-0323. PMID: 32333546.
16. *Inui S., Fujikawa A., Jitsu M., Kunishima N., Watanabe S., Suzuki Y., Umeda S., et al.* Chest CT findings in cases from the cruise ship *Diamond Princess* with Coronavirus disease (COVID-19). *Radiol Cardiothorac Imaging.* 2020; 2 (2): e200110. DOI: 10.1148/ryct. 2020200110. PMID: 33778566.
17. *Лахин Р.Е., Жирнова Е.А., Щеголев А.В., Йованикич О., Меньков И.А., Салухов В.В., Чугунов А.А.* Ультразвук легких у пациентов с пневмонией, вызванной COVID-19: сравнение с данными компьютерной томографии. Обсервационное проспективное клиническое исследование. *Вестник интенсивной*

терапии имени А.И. Салтанова. 2021; 2: 82–93. [*Lakhin R.E, Zhirnova E.A., Shchegolev A.V., Jovanikić O., Zheleznyak I.S., Menkov I.A., Salukhov V.V., Chugunov A.A.* Lung ultrasound in COVID-19 pneumonia: comparison with computed tomography. An observation prospective clinical trial. *Ann Crit Care /Vestnik Intensivnoy Terapii im AI Saltanova*. 2021; 2: 82–93. (in Russ.)]. DOI: 10.21320/1818-474X-2021-2-82-93.

18. *Dargent A., Chatelain E., Kreitmann L., Quenot J.-P., Cour M., Argaud L.* COVID-LUS study group. Lung ultrasound score to monitor COVID-19 pneumonia progression in patients with ARDS. *PLoS* One. 2020; 15 (7): e0236312. DOI: 10.1371/journal.pone.0236312. PMID: 32692769.
19. *Smith M.J., Hayward S.A., Innes S.M., Miller A.S.C.* Point-of-care lung ultrasound in patients with COVID-19 — a narrative review. *Anaesthesia*. 2020; 75 (8): 1096–1104. DOI: 10.1111/anae.15082. PMID: 32275766.
20. *Lichter Y., Topilsky Y., Taieb P., Banai A., Hochstadt A., Merdler I., Oz A.G., et al.* Lung ultrasound predicts clinical course and outcomes in COVID-19 patients. *Intensive Care Med*. 2020; 46 (10): 1873–1883. DOI: 10.1007/s00134-020-06212-1.PMID: 32860069.
21. *Arbelot C., Neto F.L.D., Gao Y., Brisson H., Chunyao W., Lv J., Barbas C.S.V., et al;* APECHO Study Group. Lung ultrasound in emergency and critically ill patients: number of supervised exams to reach basic competence. *Anesthesiology*. 2020; 132 (4): 899–907. DOI: 10.1097/ALN.0000000000003096. PMID: 31917702.
22. *Bitar Z.I., Shamsah M., Maadarani O.S., Bamasood O.M., Bitar A.Z., Alfoudri H.* Lung ultrasound and sonographic subpleural consolidation in COVID-19 pneumonia correlate with disease severity. *Crit Care Res Pract.* 2021; 6695033. DOI: 10.1155/2021/6695033. PMID: 33425386.
23. *Ökmen K., Yýldýz D.K., Soyaslan E.* Comparison of lung ultrasonography findings with chest computed tomography results in coronavirus (COVID-19) pneumonia. *J Med Ultrason* (2001). 2021; 48 (2): 245–252. DOI: 10.1007/s10396-021-01081-7. PMID: 33638057.
24. *Wang M., Luo X., Wang L., Estill J., Lv M., Zhu Y., Wang Q., et al.* A Comparison of lung ultrasound and computed tomography in the diagnosis of patients with COVID-19: a systematic review and meta-analysis. *Diagnostics (Basel)*. 2021; 11 (8): 1351. DOI: 10.3390/diagnostics 11081351. PMID: 34441286.
25. *Ottaviani S., Franc M., Ebstein E., Demaria L., Lheure C., Debray M.P., Khalil A.,et al.* Lung ultrasonography in patients with COVID-19: comparison with CT. *Clin Radiol*. 2020; 75 (11): 877.e1-877.e6. DOI: 10.1016/j.crad.2020.07.024. PMID: 32854921.
26. *Persona P., Valeri I., Zarantonello F., Forin E., Sella N., Andreatta G., Correale C., et al.* Patients in intensive care unit for COVID-19 pneumonia: the lung ultrasound patterns at admission and discharge. An observational pilot study. *Ultrasound J.* 2021; 13 (1): 10. DOI: 10.1186/s13089-021-00213-x. PMID: 33624222.
27. *Heldeweg M.L.A., Lopez Matta J.E., Haaksma M.E., Smit J.M., Elzo Kraemer C.V., de Grooth H.-J., de Jonge E., et al.* Lung ultrasound and computed tomography to monitor COVID-19 pneumonia in critically ill patients: a two-center prospective cohort study. *Intensive Care Med Exp*. 2021; 9 (1): 1. DOI: 10.1186/s40635-020-00367-3. PMID: 33491147.
28. *Bosso G., Allegorico E., Pagano A., Porta G., Serra C., Minerva V., Mercurio M., et al.* Lung ultrasound as diagnostic tool for SARS-CoV-2 infection. *Intern Emerg Med*. 2021; 16 (2): 471–476. DOI: 10.1007/s11739-020-02512-y. PMID: 33011929.
29. *Zieleskiewicz L, Markarian T, Lopez A, Taguet C., Mohammedi N., Boucekine M., Baumstarck K., et al.*; AZUREA Network. Comparative study of lung ultrasound and chest computed tomography scan in the assessment of severity of confirmed COVID-19 pneumonia. *Intensive Care Med*. 2020; 46 (9): 1707–1713. DOI: 10.1007/s00134-020-06186-0. PMID: 32728966.
30. *Deng Q., Zhang Y., Wang H., Chen L., Yang Z., Peng Z., Liu Y., et al.* Semiquantitative lung ultrasound scores in the evaluation and follow-up of critically ill patients with COVID-19: a single-center study. *Acad Radiol*. 2020; 27 (10): 1363–1372. DOI: 10.1016/j.acra.2020.07.002. PMID: 32713715.
31. *Rizzetto F., Perillo N., Artioli D., Travaglini F., Cuccia A., Zannoni S., Tombini V.,et al.*; Niguarda COVID-19 Working Group. Correlation between lung ultrasound and chest CT patterns with estimation of pulmonary burden in COVID-19

patients. *Eur J Radiol*. 2021; 138: 109650. DOI: 10.1016/ j.ejrad.2021.109650. PMID: 33743491.

32. *Tung-Chen Y., Martí de Gracia M., Díez-Tascón A., Alonso-González R., Agudo-Fernández S., Parra-Gordo M.L., Ossaba-Vélez S., et al.* Correlation between chest computed tomography and lung ultrasonography in patients with coronavirus disease 2019 (COVID-19). *Ultrasound Med Biol*. 2020; 46 (11): 2918–2926. DOI: 10.1016/j.ultrasmedbio.2020.07.003. PMID: 32771222.

Received 28.01.2023
Accepted 24.11.2023

https://doi.org/10.15360/1813-9779-2023-6-48-53

Endotoxin and Cytokines Removal with Adsorption Device in a Child with Sepsis After Transplantectomy (Case Report)

Alexander A. Eremenko[1,2], Tatyana V. Marchenko[1], Vladimir V. Nikoda[1], Alan K. Zokoev[1], Danila A. Skripalenko[2]*

[1] B. V. Petrovsky Russian Research Center for Surgery, 2 Abrikosov Lane, 119435 Moscow, Russia
[2] I. M. Sechenov First Moscow State Medical University, Ministry of Health of Russia, 8 Trubetskaya Str., Bldg. 2, 119991 Moscow, Russia

For citation: *Alexander A. Eremenko, Tatyana V. Marchenko, Vladimir V. Nikoda, Alan K. Zokoev, Danila A. Skripalenko.* Endotoxin and Cytokines Removal with Adsorption Device in a Child with Sepsis After Transplantectomy (Case Report). *Obshchaya Reanimatologiya = General Reanimatology.* 2023; 19 (6): 48–53. https://doi.org/10.15360/1813-9779-2023-6-48-53 [In Russ. and Engl.]

***Correspondence to:** Danila A. Skripalenko, skripalenko_d_a@student.sechenov.ru

Summary

Sepsis is one of the leading causes of death in kidney transplant recipients.

We present our experience of effective removal of bacterial endotoxins and endogenous inflammatory mediators using a multimodal hemosorbent in sepsis, caused by gram-negative polyresistant *Klebsiella* spp. including *K. pneumoniae.* The device was used in a 15 y.o. patient after treatment failure of graft-bed abscess and removal of kidney transplant.

Results. Two 24-hour sorption procedures on Days 3 and 5 post- transplantectomy in combination with renal replacement therapy resulted in consistent decrease of pro-inflammatory markers concentrations (procalcitonin — 15.1→11.4→7.2 ng/ml; C-reactive protein — 234→199→90 mg/l), preventing therefore further progression of multiple organ dysfunctions.

Conclusion. Inclusion of selective adsorption of cytokines and/or lipopolysaccharides into multimodal intensive therapy in an immunosuppressed pediatric patient with sepsis caused by resistant microorganisms improved treatment outcomes.

Keywords: sepsis; endotoxins; extracorporeal therapy; cytokine sorption; Efferon

Conflict of interest. The authors declare no conflict of interest.

Read the full-text English version at www.reanimatology.com

Introduction

Sepsis in children is a high-risk condition that requires timely diagnosis and treatment. Delayed initiation of treatment is associated with increased mortality [1, 2]. According to Weiss et al, refractory shock is the major cause of death in one-third of children with sepsis who die within the first 72 hours, while multiple organ dysfunction syndrome, respiratory failure, and neurologic complications are the major causes of death after 72 hours [3].

In kidney transplant recipients, sepsis is the main indication for intensive care unit (ICU) admission and a major cause of high in-hospital mortality, which can reach up to 30% [4–6].

Extracorporeal blood purification can be used in the management of patients with sepsis. Devices for the removal of endotoxins and cytokines have great potential, and their use in sepsis caused by Gram-negative pathogens can improve treatment outcomes [7].

Case Report

A 15-year-old patient was admitted to the renal transplant unit with a body temperature of 38°C and discharge from the fistulous tract in the postoperative wound area.

The patient was diagnosed with autosomal recessive polycystic kidney disease at the age of 4 years. Ten months ago, long-term hemodialysis was started due to progression of chronic kidney disease. Three months ago, he underwent right-sided nephrectomy with ABO-incompatible related kidney transplantation with placement of the graft in the retroperitoneal space of the right iliac fossa. In the post-transplant period, the child received immunosuppressive therapy, including tacrolimus 8 mg per day (under control of drug concentration in blood), prednisolone according to the scheme with reduction to 7.5 mg per day, mycophenolate mofetil 500 mg every 12 hours. Prevention of CMV infection (valganciclovir 450 mg per day), Pneumocystis pneumonia and bacterial infection (cefazolin 1 g every 8 hours) was also provided. Graft function was evident immediately, with a decrease in creatinine from the first postoperative day.

In the postoperative period, reconstruction of the arterial anastomosis was performed on day 9 due to the presence of signs of renal artery stenosis of the graft. Six days later, a surgical procedure in-

cluding stopping bleeding and performing prosthetic anastomosis with a xenograft was done. Based on the results of the microbiological examination of the wound discharge (*Klebsiella* spp., including *Klebsiella pneumoniae*, carbapenemase class B (MBL) producing strain), antibacterial therapy was prescribed with meropenem 500 mg every 8 hours, cefotaxime/sulbactam 3 g every 8 hours. Immunosuppressive therapy was continued with solumedrol 100 mg daily, tacrolimus 9 mg daily, while mycophenolate mofetil was suspended. The patient's condition improved, and 51 days after kidney transplantation, with satisfactory graft function (blood creatinine 120–130 μmol/L, GFR 83.7–77.2 mL/min/1.73 m²), the child was discharged from the hospital on immunosuppressive and antihypertensive therapy. The patient was instructed to continue prevention of Pneumocystis pneumonia and CMV infection.

After discharge, the patient developed fever, and ultrasound revealed a fluid collection under the transplanted kidney; the aspirate contained pus.

On readmission to the hospital on day 27 after discharge, the graft function was satisfactory. Computed tomography showed a limited collection of fluid from the L4 level behind the right iliac muscle, pushing it anteriorly and compressing the right common iliac vein, pushing the bladder to the left and extending to the renal graft hilum and the right inguinal region, with a volume of approximately 230 cm³, of non-homogeneous structure with gas bubbles. Microbiological examination of the wound discharge revealed *Klebsiella* spp., including *Klebsiella pneumoniae*, MBL-producing strain. Considering the clinical and laboratory data and the development of infection in a patient on immunosuppressive therapy, antibacterial therapy was prescribed with imipenem/cilastatin 1000/1000 mg every 8 hours, fosfomycin 4 g every 6 hours.

Due to the severity of the disease, persistent subfebrile temperature, increase in the volume of accumulated fluid, compression of iliac blood vessels, increase in inflammatory markers, three days after admission, revision of the retroperitoneal abscess and draining of its cavity were performed.

In the postoperative period, tacrolimus was discontinued, prednisolone dose was reduced, valganciclovir administration was interrupted, leukopoiesis stimulation (filgrastim 300 mcg) and antifungal prophylaxis (fluconazole 600 mg initially, then 300 mg daily) were started. Antimicrobial therapy was adjusted based on the preliminary data from the blood microbiological study (growth of Gram-negative and Gram-positive microorganisms) and included biapenem 600 mg every 12 hours, fosfomycin 4 g every 8 hours.

On the 7th day after the revision and drainage of the retroperitoneal space, the patient had a rise in body temperature to 39.7°C, an increase in proinflammatory markers (C-reactive protein 95.1 mg/L; procalcitonin 0.22 ng/mL). Taking into account: a) the presence of a fluid collection of up to 15 mL (pus) in the graft hilum on CT scan and a high risk of arterial bleeding, b) the polycystic left kidney as a probable source of infection, and c) the ineffectiveness of conservative therapy, transplantectomy and left-sided nephrectomy were performed. Due to sepsis manifestations, a session of renal replacement therapy (RRT) using the Prismaflex RRT device (Baxter, USA) and the oXiris set was started on the first day after surgery. The parameters of the procedure were as follows: blood flow rate 3–5 mL/kg/min (150–180 mL per minute), dialysate flow rate and renal replacement dose 30 mL/kg/hour (1400 mL per hour). Heparin at a dose of 10–18 U/kg/hour was used for anticoagulation during the procedure, and activated clotting time was maintained at 140–160 seconds (reference values 90-120 seconds). Taking into account the results of blood microbiology (*Klebsiella* spp., including *Klebsiella pneumoniae*) and ongoing renal replacement therapy, meropenem 1 g every 12 hours and fosfomycin 2 g every 8 hours were administered. An ultrasound scan revealed right iliac vein thrombosis, so the dose of heparin was increased and the activated clotting time was maintained at approximately 200 seconds.

Over the next three days, the patient's condition did not change significantly: fever up to 38.6°C and tachycardia up to 115 beats/min persisted despite RRT. Laboratory tests showed high levels of proinflammatory markers (procalcitonin increased from 6.58 to 15.13 ng/mL, C-reactive protein increased from 163.6 to 234 mg/L) (see Figure), while endotoxin activity (EAA) was 0.57. Blood pressure was within 120–150/60–90 mmHg without vasopressors, and SpO_2 was 98–99% on air-oxygen mixture (up to 4 L O_2/min).

Considering the lack of treatment effectiveness and negative laboratory changes, Efferon LPS (Efferon, Russia), a device for the adsorption of cytokines and lipopolysaccharide (LPS), was connected to the extracorporeal circuit before the hemofilter. Renal replacement therapy parameters were identical. After 24 h of adsorption, body temperature returned to normal. Based on blood and wound discharge microbiology (*Klebsiella pneumoniae* MDR+ (multidrug resistant), MBL+), the antibiotic therapy was changed to meropenem 2 g every 12 hours, polymyxin B 50 mg every 12 hours, 2, 3-bis (hydroxymethyl) quinoxaline 1, 4-di-N-oxide 300 mg every 8 hours, and Klebsiella polyvalent bacteriophage topical 20 mL every 12 hours.

Emergency surgery was performed on the 4th day after transplantation due to continued bleeding from the site of the removed graft (volume of blood loss was 500 mL). Relaparotomy, revision, lavage and drainage of the abdominal cavity and retroperi-

toneal space were performed. The next day, due to high levels of proinflammatory markers and endotoxin (EAA 0.87), the second session of cytokine and LPS adsorption for 24 hours with Efferon LPS was performed. Antibacterial therapy was again changed to ceftazidime/avibactam 1250 mg every 8 hours, aztreonam 1 g every 8 hours. The patient's condition improved and the levels of inflammatory markers decreased (see Figure).

Later, the patient underwent two surgical procedures for bleeding from the retroperitoneal space on day 8 post-transplantation and from the abdominal cavity on day 13. During the latter surgery, there was a diapedetic hemorrhage from the wound, so renal replacement therapy was continued from day 14 with the use of the oXiris kit and citrate anticoagulation.

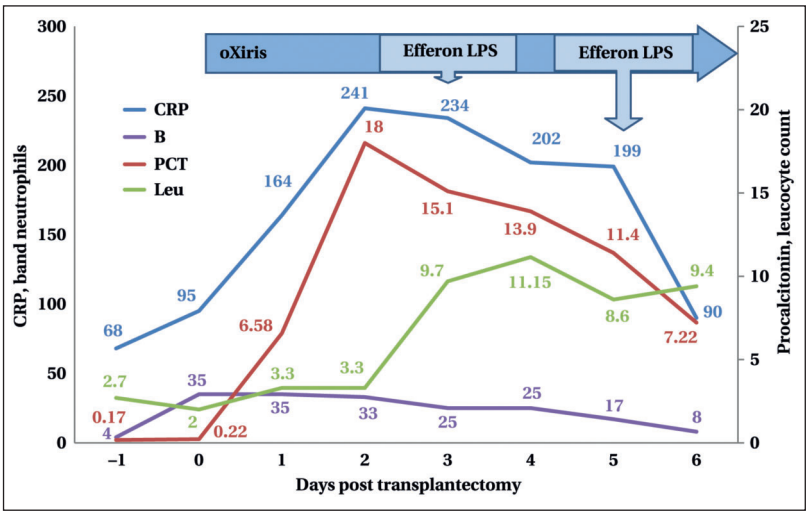

Fig. Changes in laboratory parameters (CRP — C-reactive protein, mg/l; Leu — leukocytes, ×10⁹/l; B — bands, %; PCT — procalcitonin, ng/mL) after transplantectomy.

In total, continuous renal replacement therapy was administered for 21 days. Thereafter, treatment was continued with daily hemodiafiltration procedures with a switch to a long-term regimen of 4 times per week for 4 hours.

Discussion

In 2005, the International Pediatric Sepsis Consensus Conference (IPSCC) proposed age-adjusted definitions of sepsis and its stages in pediatrics, which relied on the presence of systemic inflammatory response syndrome (SIRS) as the main criterion. However, because SIRS is not specific for sepsis, the IPSCC criteria for diagnosing sepsis have low specificity and sensitivity. As a result, the proposed definitions of sepsis and septic shock for adult patients (Sepsis-3) have been adapted for pediatric use.

Sepsis is the response of the body to an infection. It can be uncontrolled and «exaggerated» with severe clinical manifestations or mild due to immunosuppression [8]. Piskin et al. showed that in the first two months after kidney transplantation, when immunosuppression was most intense, infection was the only primary cause of mortality [9].

Gram-negative bacteremia is a common complication of renal transplantation [10]. LPS is the main mediator of sepsis under these conditions. LPS itself is not considered toxic, and its endotoxic effects are mediated by activation of the immune system. Sensitivity to LPS depends primarily on factors that influence the susceptibility of the body rather than the actual mechanisms of action of LPS [11]. It triggers the release of pro-inflammatory cytokines, including tumor necrosis factor-alpha and interleukins (IL), by the cells of the body. The imbalance between pro- and anti-inflammatory mediators serves as a factor in the development of sepsis [12]. To suppress redundant systemic effects in sepsis, it is necessary, among other things, to eliminate cytokines below an individual critical threshold. Cytokines are considered as prime targets for modulation to improve the condition of patients with severe inflammation, sepsis, and septic shock [13].

Currently, there are three methods of treatment for end-stage chronic kidney disease, including in children, which are peritoneal dialysis, hemodialysis and kidney transplantation.

According to the Russian Register of Renal Replacement Therapy for 2019, 81 children received hemodialysis, 130 peritoneal dialysis, and 434 children had a functioning kidney transplant [14]. Kidney transplantation is the optimal treatment for children with stage 5 chronic kidney disease, leading to significant improvements in survival, duration and quality of life compared to dialysis [15]. However, continuous immunosuppression makes patients more susceptible to viral and bacterial infections [16, 17].

Infectious complications after kidney transplantation may be associated with pre-transplant infection of the recipient, infection of the donor organ, presence of hospital (nosocomial) or community-acquired infection [18]. In addition, the clinical presentation of the infectious process may be altered in patients receiving immunosuppressive therapy, leading to diagnostic difficulties. And once the infection has developed, the decline in the body's immune response is critical to the outcome of the disease. Infectious and cardiovascular complications are the main causes of death in kidney transplant recipients [19]. The most dangerous period for the development of infectious and inflammatory complications is the first 1–2 months after transplantation [20].

Urinary tract infection (UTI) is a major cause of complications, including sepsis, in kidney recipients [21–23]. Typically, UTIs are caused by ascending Gram-negative bacteria [24]. Treatment of infections caused by multidrug-resistant ESKAPE (*Enterococcus faecium*, *Staphylococcus aureus*, *Klebsiella pneumoniae*, *Acinetobacter baumannii*, *Pseudomonas aeruginosa*, and *Enterobacter species*) pathogens can be especially challenging [25].

The emergence of multidrug-resistant bacteria has become a significant challenge in disease management, leading to increased mortality rates due to ineffective treatment. ESKAPE pathogens, through genetic mutation and acquisition of mobile genetic elements, have developed resistance mechanisms to a wide range of antibiotics including oxazolidinones, lipopeptides, macrolides, fluoroquinolones, tetracyclines, beta-lactams, combinations of beta-lactams and beta-lactamase inhibitors, as well as «last resort» antibiotics such as carbapenems, glycopeptides, and polymyxins. Infections caused by carbapenem-resistant Enterobacteriaceae have particularly high mortality rates, often surpassing 40% globally. Among these infections, carbapenem-resistant strains of *K. pneumoniae* (CRKP) are associated with the most severe cases [26].

After kidney transplantation, *K. pneumoniae* is found in blood cultures in approximately one-third of cases (as in this observation), and in more than half of cases, it is resistant to most antibacterial drugs [20]. The progression of infection to sepsis can be rapid and unpredictable, and antimicrobial therapy is not always effective because of the resistance of the recipient's microflora caused by multiple previous courses of antibiotics [20]. Septic complications are the major cause of mortality after parenchymal organ transplantation. In immunosuppressed patients, sepsis is associated with a 50% mortality [27].

Infectious complications such as acute graft pyelonephritis and sepsis are the most common indications for graft removal in the early postoperative period. Kidney recipients who develop Gram-negative bacteremia after transplantation have a higher risk of allograft loss and death [10].

In addition to appropriate antibiotic therapy and source control of sepsis in surgical cases, techniques for removing cytokines and/or lipopolysaccharides show great promise in managing infectious complications. Renal replacement therapy alone may not be sufficient.

Currently available devices for selective adsorption of cytokines (CytoSorb, CytoSorbents Corporation, USA; HA330, Jafron Biomedical Co., China; Efferon CT, «Efferon», Russia) and endotoxins (Alteco LPS Adsorber, Alteco Medical AB, Sweden; Toraymyxin, Toray Medical Co, Ltd, Japan; Toxipak, NPF «POCARD», Russia; Efferon LPS Adsorption Device «Efferon», Russia) for adsorption of LPS and excess of endogenous inflammatory mediators, can be used alone or in combination with renal replacement therapy. Often more than one session is required, and the duration of such treatment depends on the type of adsorption cartridge used [7, 28, 29].

The results of the use of such devices for the treatment of bacterial sepsis are currently controversial. The evidence of their effectiveness is insufficient. According to some authors, the results of treatment depend on the initial concentration of inflammatory mediators and the stage of the process at the beginning of adsorption. Therefore, the use of such methods should be personalized [28].

Our observation demonstrates that the use of multimodal hemosorbent for removal of bacterial endotoxins and endogenous inflammatory mediators allows to reduce the excessive inflammatory response of the organism against the infection and to prevent further progression of multiorgan dysfunction in Gram-negative sepsis caused by multidrug-resistant pathogens.

Conclusion

Inclusion of selective adsorption of cytokines and/or lipopolysaccharides into the intensive treatment of an immunosuppressed pediatric patient with sepsis caused by resistant microorganisms improved the treatment outcome.

References

1. *Linares L., Cofán F., Cervera C., Ricart M.J., Oppenheimer F., Campistol J.M., Moreno A.* Infection-related mortality in a large cohort of renal transplant recipients. *Transplant Proc.* 2007; 39 (7): 2225–7. DOI: 10.1016/j.transproceed.2007.07.047. PMID: 17889145.
2. Kissoon *N., Reinhart K., Daniels R., Machado M.F.R., Schachter R.D., Finfer S.* Sepsis in children: global implications of the World Health Assembly Resolution on sepsis. *Pediatr Crit Care Med*. 2017; 18 (12): e625–e627. DOI: 10.1097/PCC.0000000 000001340. PMID: 28914721.
3. *Weiss S.L., Balamuth F., Hensley J., Fitzgerald J.C., Bush J., Nadkarni V.M., Thomas N.J., et al.* The epidemiology of hospital death following pediatric severe sepsis: when, why, and how children with sepsis die. *Pediatr Crit Care Med.* 2017; 18 (9): 823–830. DOI: 10.1097/PCC.0000000000001222. PMID: 28549024.
4. *Freitas F.G.R., Lombardi F., Pacheco E.S., Sandes-Freitas T.V., Viana L.A., Junior H.T.-S., Medina-Pestana J.O., et al.* Clinical features of kidney transplant recipients admitted to the intensive care unit. *Prog Transplant.* 2018; 28 (1): 56–62. DOI: 10.1177/1526924817746685. PMID: 29258377.
5. *Okidi O.O., Van Dellen D., Sobajo C., Summers A., Greer J.R., Augustine T.* Kidney transplant recipients requiring critical care admission within one year of transplant. *Exp Clin Transplant.* 2017; 15 (1): 40–46. DOI: 10.6002/ect.2015.0356. PMID: 27915963.
6. *Canet E., Zafrani L,, Azoulay É.* The critically ill kidney transplant recipient: a narrative review. *Chest.* 2016; 149 (6): 1546–55. DOI: 10.1016/j.chest.2016.01.002. PMID: 26836919.
7. *Rey S., Kulabukhov V.M., Popov A., Nikitina O., Berdnikov G., Magomedov M., Kim T., et al.* Hemoperfusion using the LPS-selective mesoporous polymeric adsorbent in septic shock: a multicenter randomized clinical trial. *Shock.* 2023; 59 (6): 846–854. DOI: 10.1097/SHK.0000000000002121. PMID: 37018802.
8. *Garcia P.C.R., Tonial C.T., Piva J.P.* Septic shock in pediatrics: the state-of-the-art. *J Pediatr (Rio J).* 2020; 96 Suppl 1(Suppl 1): 87–98. DOI: 10.1016/j.jped.2019.10.007. PMID: 31843507.
9. *Piskin T., Simsek A., Murat-Dogan S., Demirbas B.T., Unal B., Yildirim I.O., Toplu S.A., et al.* Mortality after kidney transplantation: 10-year outcomes. *Cir Cir.* 2022; 90 (2): 172–179. DOI: 10.24875/CIRU.21000300. PMID: 35349567.
10. *Al-Hasan M.N., Razonable R.R., Kremers W.K., Baddour L.M.* Impact of gram-negative bloodstream infection on long-term allograft survival after kidney transplantation. *Transplantation.* 2011; 91 (11): 1206–10. DOI: 10.1097/TP.0b013e3182180535. PMID: 21494179.
11. *Page M.J., Kell D.B., Pretorius E.* The role of lipopolysaccharide-induced cell signaling in chronic inflammation. *Chronic Stress (Thousand Oaks).* 2022; 6: 24705470221076390. DOI: 10.1177/24705470221076390. PMID: 35155966.
12. *Gabarin R.S., Li M., Zimmel P.A., Marshall J.C., Li Y., Zhang H.* Intracellular and extracellular lipopolysaccharide signaling in sepsis: avenues for novel therapeutic strategies. *J Innate Immun.* 2021; 13 (6): 323–332. DOI: 10.1159/000515740. PMID: 34004605.
13. *Harm S., Gabor F., Hartmann J.* Characterization of adsorbents for cytokine removal from blood in an in vitro model. *J Immunol Res.* 2015; 2015: 484736. DOI: 10.1155/2015/484736. PMID: 26770992.
14. *Молчанова Е.А.* Заместительная почечная терапия хронической болезни почек 5 стадии у детей в Российской Федерации в 2015–2019 гг. Отчёт по данным Общероссийского Регистра заместительной почечной терапии Российского диализного общества. *Нефрология и диализ.* 2022. 24 (4): 566–576. [*Molchanova E.A.* Renal replacement therapy for pediatric patients with stage 5 chronic kidney disease in Russian Federation in 2015–2019. Russian National Kidney Replacement Therapy Registry Report of Russian Public Organization of Nephrologists «Russian Dialysis Society». *Nephrology and Dialysis/Nefrologiya i Dializ.* 2022; 24 (4): 566–576. (in Russ.)]. DOI: 10.28996/2618-9801-2022-4-566- 576.
15. *Oomen L., de Wall L.L., Cornelissen E.A.M., Feitz W.F.J., Bootsma-Robroeks C.M.H.H.T.* Prognostic factors on graft function in pediatric kidney recipients. *Transplant Proc.* 2021; 53 (3): 889–896. DOI: 10.1016/j.transproceed.2020.10.017. PMID: 33257001.
16. *Fishman J.A.* Infection in organ transplantation. *Am. J. Transplant.* 2017; 17 (4): 856–879. DOI: 10.1111/ajt.14208. PMID: 28117944
17. *Mella A., Mariano F., Dolla C., Gallo E., Manzione A.M., Di Vico M.C., Cavallo R., et al.* Bacterial and viral infection and sepsis in kidney transplanted patients. *Biomedicines.* 2022; 10 (3): 701. DOI: 10.3390/biomedicines10030701. PMID: 35327510.
18. *Волынчик Е.П., Большаков Л.В., Балакирев Э.М., Богомолова Н.С.* Профилактика и лечение инфекционных осложнений, вызванных нозокомиальной флорой, после пересадки родственных аллогенных почек. *Трансплантология.* 2011; (2–3): 63–68. [*Volynchik E.P., Bolshakov L.V., Balakirev E.M.,*

Bogomolova N.S. The prophylaxis and treatment of infectious complications caused by nosocomial flora after kidney transplantation from living related donor. *Transplantology/ Transplantologiya*. 2011; (2–3): 63–68. (in Russ.)]. DOI: 10.23873/2074-0506-2011-0-2-3-63-68

19. *Султанов П.К., Хаджибаев Ф.А., Эргашев Д.Н., Исматов А.А.* Анализ осложнений после трансплантации почки. *Вестник экстренной медицины*. 2021; 1 (14): 55–64. [*Sultanov P.K., Khadjibaev F.A., Ergashev D.N., Ismatov A.A.* Analysis of complications after kidney transplantation. *Bulletin of Emergency Medicine/ Vestnik Ekstrennoy Meditciny*. 2021; 1 (14): 55–64. (in Russ.)]. https: //cyberleninka.ru/article/n/analiz-oslozhneniy-posle-transplantatsii-pochki.
20. *Барканова О.Н., Перлин Д.В., Шепелева Ю. Б., Реброва Е.В., Ильченко О.В.* Инфекционные осложнения раннего послеоперационного периода у пациентов после трансплантации почки. *Вестник ВолГМУ*. 2016; 2: 58. [*Baranova O.N., Perlin D.V., Shepeleva Y. B., Rebrova E.V., Ilchenko O.V.* Infectious complications of early postoperative period in patients after kidney transplantation. *Bulletin of VolGMU/Vestnik VolGMU*. 2016; 2: 58. (in Russ.)]. https://cyberleninka.ru/article/n/infektsionnye-oslozhneniya-rannego-posleoperatsionnogo-perioda-u-patsientov-posle-transplantatsii-pochki.
21. *Lee J.R., Bang H., Dadhania D., Hartono C., Aull M.J., Satlin M., August P., et al.* Independent risk factors for urinary tract infection and for subsequent bacteremia or acute cellular rejection: a single-center report of 1166 kidney allograft recipients. *Transplantation*. 2013; 96 (8): 732–738. DOI: 10.1097/TP.0b013e3182a04997. PMID: 23917724.
22. *Fiorentino M., Pesce F., Schena A., Simone S., Castellano G., Gesualdo L.* Updates on urinary tract infections in kidney transplantation. *J. Nephrol*. 2019; 32 (5): 751–761. DOI: 10.1007/s40620-019-00585-3. PMID: 30689126.
23. *Cervera C., Fernández-Ruiz M., Valledor A. Linares* L., *Antón* A., *Marcos* M.A., *Sanclemente* G. et al. Epidemiology and risk factors for late infection in solid organ transplant recipients. *Transpl Infect Dis*. 2011; 13 (6): 598–607. DOI: 10.1111/j.1399-3062.2011.00646.x PMID: 21535336.
24. *Alangaden G.J., Thyagarajan R., Gruber S.A., Morawski K., Garnick J., El-Amm J.M., West M.S., et al.* Infectious complications after kidney transplantation: current epidemiology and associated risk factors. *Clin.Transplant*. 2006; 20 (4): 401–409. DOI: 10.1111/j.1399-0012.2006.00519.x. PMID: 16842513.
25. *Mella A., Mariano F., Dolla C., Gallo E., Manzione A.M., Di Vico M.C., Cavallo R., et al.* Bacterial and viral infection and sepsis in kidney transplanted patients. *Biomedicines*. 2022; 10 (3): 701. DOI: 10.3390/biomedicines10030701. PMID: 35327510.
26. *De Oliveira D.M.P., Forde B.M., Kidd T.J., Harris P.N.A., Schembri M.A., Beatson S.A., Paterson D.L., et al.* Antimicrobial resistance in ESKAPE pathogens. *Clin Microbiol Rev*. 2020 May 13; 33 (3): e00181-19. DOI: 10.1128/CMR.00181-19. PMID: 32404435.
27. *Candel F.J., Grima E., Matesanz M., Cervera C., Soto G., Almela M., Martínez J.A., et al.* Bacteremia and septic shock after solid-organ transplantation. *Transplant Proc*. 2005; 37 (9): 4097–9. DOI: 10.1016/j.transproceed.2005.09.181. PMID: 16386636.
28. *Ankawi G., Neri M., Zhang J., Breglia A., Ricci Z., Ronco C.* Extracorporeal techniques for the treatment of critically ill patients with sepsis beyond conventional blood purification therapy: the promises and the pitfalls. *Crit Care*. 2018; 22 (1): 262. DOI: 10.1186/s13054-018-2181-z. PMID: 30360755.
29. *Ярустовский М.Б., Шукевич Д.Л., Ушакова Н.Д., Соколов А.А., Рей С.И.* Возможности и показания к применению методов экстракорпоральной гемокоррекции в комплексном лечении пациентов с новой коронавирусной инфекцией. *Анестезиология и реаниматология*. 2020; (5): 47–55. [*Yarustovsky M.B., Shukevich D.L., Ushakova N.D., Sokolov A.A., Rey S.I.* Blood purification methods in complex treatment of patients with a new coronavirus infection. Anesthesiology and Reanimatology/ *Anesteziologiya i Reanimatologiya*. 2020; (5): 47–55. (in Russ.)]. DOI: 10.17116/anaesthesiology202005147.

Received 15.06.2023
Accepted 26.09.2023

https://doi.org/10.15360/1813-9779-2023-6-54-61

Influence of Stress Resistance on Myocardial Expression of the Pro-Autophagic Protein Beclin-1 After Cardiac Contusion in Experimental Setting

Evgenia I. Klyuchnikova*, Olga V. Korpacheva, Sergey I. Mozgovoy, Alexander N. Zolotov, Alexey V. Kononov

Omsk State Medical University, Ministry of Health of Russia,
12 Lenin Str., 644099 Omsk, Russia

For citation: *Evgenia I. Klyuchnikova, Olga V. Korpacheva, Sergey I. Mozgovoy, Alexander N. Zolotov, Alexey V. Kononov.* Influence of Stress resistance on Myocardial Expression of the Pro-Autophagic Protein Beclin-1 After Cardiac Contusion in Experimental Setting. *Obshchaya Reanimatologiya = General Reanimatology.* 2023; 19 (6): 54–61. https://doi.org/10.15360/1813-9779-2023-6-54-61 [In Russ. and Engl.]

***Correspondence to:** Evgenia I. Klyuchnikova, kei_omsk@mail.ru

Summary

Objective. Evaluation of myocardial expression of the pro-autophagic protein Beclin-1 after cardiac contusion in experimental animals with different stress resistance.

Materials and methods. The study included 68 white mongrel male rats weighing 250–300 g. After ranking for extreme variants of stress resistance, moderately stress-resistant rats (*N*=36) were excluded from the study. The remaining animals were split into the control (*N*=16) and study (*N*=16) groups, each group composed of 8 high stress resistant and 8 low stress resistant rats. In the study group, 24 hours after inflicted cardiac contusion, 5×5 mm myocardial tissue specimens were sampled from the intraventricular septum, anterior walls of the left and right ventricles, histological sections were made, and a reaction with primary polyclonal Anti-Beclin-1 antibodies was performed. Beclin-1 expression was evaluated under the microscope.

Results. Immunohistochemical evaluation revealed a statistically significant increase in Beclin-1 protein expression (*P*=0.0002) in the cytoplasm of cardiomyocytes in the study group vs the control group, regardless of animals' baseline stress resistance. However, expression of Beclin-1 protein in the myocardium of highly stress-resistant rats (*Me*=4.3; *LQ*=4.0; *HQ*=4.3) was significantly higher versus low-resistant animals (*Me*=3.6; *LQ*=3.3; *HQ*=3.6) (*P*=0.0009).

Conclusion. Increased expression of Beclin-1 protein in the post-traumatic period of experimental cardiac contusion indicates autophagic flux activation. Intensity of autophagy varied depending on the animal's stress resistance.

Keywords: cardiac contusion, autophagy, Beclin-1, stress resistance

Conflict of interest. The authors declare no conflict of interest.

Read the full-text English version at www.reanimatology.com

Introduction

The main pathogenetic factors of the post-traumatic period of cardiac contusion are circulatory hypoxia and disruption of energy-dependent processes [1, 2], together with mechanical damage leading to accumulation of damaged organelles, unfolded proteins, lactate, Ca^{2+} ions, as well as lack of substrate to maintain the necessary level of homeostasis and initiate reparative processes [3–5]. In models of myocardial ischemic injury, these factors are described as triggers capable of increasing the intensity of autophagy, a type of programmed cell death, which involves the degradation of damaged organelles which are further used by the cell to restore metabolism and form new fully functional structures [6]. In addition, the stress response related to the general adaptation syndrome plays an important role in the pathogenesis of blunt cardiac trauma. Previous studies have identified patterns of systemic and tissue hormonal and metabolic shifts in the post-traumatic period of experimental cardiac contusion that are characteristic of the stress response but vary in severity in animals with different levels of stress resistance [7]. Another study [8] demonstrated the dependence of hematopoietic organ functions on the activity of the sympathetic and hypothalamic-pituitary-adrenal systems in dogs with different stress sensitivity.

Based on this assumption, it is hypothesized that autophagy as a stress-associated response of myocardial tissue may occur during the post-traumatic period of cardiac contusion and its severity may vary depending on the level of stress resistance in the organism.

Aim: To evaluate the expression of the autophagy protein Beclin-1 in myocardium after experimental cardiac contusion, taking into account different levels of stress resistance.

Materials and Methods

Sixty-eight male white albino rats, weighing 250–300 g, were used in the study in accordance

with the rules for conducting research and animal care (Order of the Ministry of Health of the Russian Federation dated 01.04.2016 No. 199n «On approval of the rules of good laboratory practice»), with free access to combined food and water. The study was approved by the local ethics committee of Omsk State Medical University of the Ministry of Health of Russia. Zoletil 100 (tiletamine, zolazepam) at a dose of 30 mg/kg intraperitoneally was used as an anesthetic for all invasive stages of the experiment.

To create control (C) and experimental (E) groups, we performed an assessment of the animals' stress resistance using a modified ranking method that included open field and Porsolt forced swim tests [9]. Previous studies evaluating the concentration of corticosterone, glucose, triglycerides, lactate in blood plasma, as well as the levels of restored glutathione and total antioxidant capacity in myocardium, indicated that the modified ranking method for rat stress resistance allows the selection of subjects with the most pronounced differences in systemic and tissue stress response markers [7].

Animals with average stress resistance (*N*=36) were excluded from the study because extreme variants of stress resistance were used as selection criteria.

In each group, animals with low (L) and high (H) stress resistance were included. Thus, two subgroups of the control group (CH and CL) and two subgroups of the experimental group (EH and EL) were formed, with 8 animals in each subgroup.

Cardiac contusion was simulated in the experimental group using an original device that mimics the impact of the frontal surface of the chest against the steering column in a collision of a moving car with an obstacle [10].

Rat heart was harvested 24 hours after the trauma simulation and heart sections were prepared. To identify the damaged areas, the sections were stained with a solution of nitroblue tetrazolium and then placed in a 10% formalin solution for 30 minutes to enhance the contrast of the staining. The damaged myocardial areas were gray-white in color, whereas the undamaged myocardium was blue-black (Fig. 1). Myocardial fragments measuring 5×5 mm were harvested from the areas of greatest trauma, including the interventricular septum and the anterior walls of the left and right ventricles. The specimens were processed for microscopy using standard techniques and embedded in paraffin. Histologic sections of 5 micrometers thickness were prepared using an Epredia HM 340E microtome (Epredia, UK) and placed on adhesive-coated slides. The resulting samples were deparaffinized with xylene and treated with descending concentrations of alcohol.

To evaluate the expression of the autophagy protein Beclin-1, a reaction was performed using primary rabbit polyclonal anti-Beclin-1 antibody

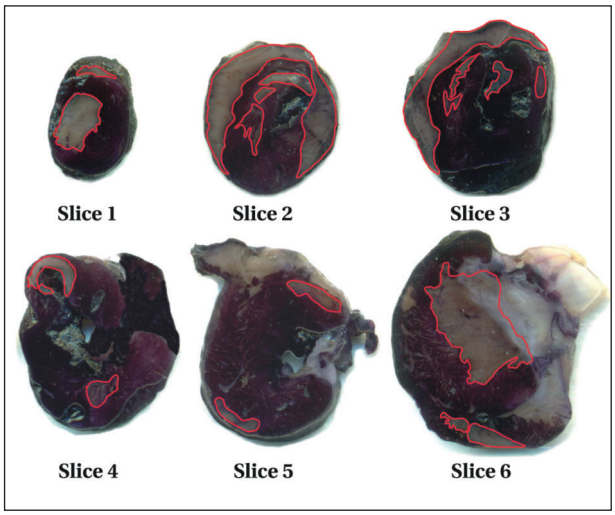

Fig. 1. Macroscopic visualization of myocardial injury foci with nitroblue tetrazolium solution.
Note. The areas of injury are outlined with a red line.

(HUABIO, China), No. R1509-1, diluted 1:100. The results of the immunohistochemical study were visualized using the «Universal Two-Step Detection System PrimeVision»: Mouse/Rabbit IgG Antibodies — HRP/DAB» kit (PrimeBioMed, Russia). Slides were counterstained with hematoxylin. The immunohistochemical reaction was considered positive when brown staining appeared in the cytoplasm of cardiomyocytes. Light microscopy was performed with an Axioskop 40 microscope (Zeiss, Germany) at 400× magnification in 10 fields of view for each slide. Images of each field of view were captured using an Axiocam 503 color camera (Zeiss, Germany) and ZenBlue graphics software for further evaluation of immunohistochemical study results.

Myocardial image analysis was performed using a semi-quantitative method. The scoring system considered two parameters: the intensity of immunohistochemical staining on a four-point scale (0, no staining; 1, weak staining intensity; 2, moderate staining intensity; 3, strong staining), and the staining area expressed in points corresponding to the percentage of stained cardiomyocytes among all cardiomyocytes in the field of view (0–20% — 1 point, 20–40% — 2 points, 40–60% — 3 points, 60–80% — 4 points, 80–100% — 5 points). The final result was the sum of the intensity and area points for each individual field of view, followed by calculation of the arithmetic mean for all 10 fields of view and calculation of the expression index for each animal. The values of the indicators obtained from animals in different groups and subgroups were then compared.

Cardiac injury modeling and sample preparation were performed in the laboratory of the Department of Pathophysiology, and immunohistochemical analysis was performed in the laboratory

of the Department of Pathological Anatomy of Omsk State Medical University.

Normality of the distribution of quantitative variables was tested using the Shapiro–Wilk test. Data were analyzed using descriptive statistics and sample comparisons (Mann–Whitney *U* test). A significance level of 0.05 was used. The data were processed using IBM SPSS Statistics 23 software. The results are presented as median *(Me)* and interquartile range *(UQ–LQ)*.

Results

Macroscopic changes in the myocardium after staining with nitroblue tetrazolium solution consisted of gray-white staining in the damaged areas and blue-black staining in the undamaged areas. Microscopic examination of the myocardial injury zone after experimental cardiac contusion revealed edema and widening of spaces between cardiomyocytes, irregular structure of intercalated discs, focal loss of cross-striations with the appearance of hyper-eosinophilic areas, wave-like deformation of cardiomyocytes, and the beginning of fragmentation of single cardiomyocytes.

Immunohistochemical analysis revealed a significant increase (*P*=0.0002) in the expression of the autophagy protein Beclin-1 in the cytoplasm of cardiomyocytes in the experimental group compared to that in the control group (Fig. 2). A significantly higher level (*P*=0.0009) of Beclin-1 expression (*Me*=4.3; *LQ*=4.0; *UQ*=4.3) was observed in the myocardium of stress-resistant traumatized rats (subgroup EH) than in stress-sensitive rats from subgroup EL (*Me*=3.6; *LQ*=3.3; *UQ*=3.6). No differences were observed between the subgroups in the control group (*Me*=3.0; *LQ*=3.0; *UQ*=3.0).

Qualitative assessment of Beclin-1 expression showed that in the control group, positive reactions were either absent or detected in small amounts as irregular inclusions of low-intensity brown color in the cytoplasm of cardiomyocytes. No differences were observed between stress-resistant and stress-sensitive animals in the control group (CH and CL subgroups) (Fig. 3, *a*, *b*).

In high stress resistance rats subjected to blunt cardiac injury, we observed uneven diffuse moderate or high intensity staining of the cytoplasm (Fig. 3, *c*). In the subgroup of low stress resistant traumatized rats (EL), single foci of cardiomyocytes with moderate or low intensity cytoplasmic staining (Fig. 3, *d*) were found. In traumatized animals, regardless of stress resistance (subgroups EH and EL), there was a tendency for increased staining intensity and number of positively stained cardiomyocytes towards the epicardium in the areas of traumatic injury.

Discussion

Beclin-1 is a major subunit of the class III phosphatidylinositol 3-kinase complex (PI3K class III

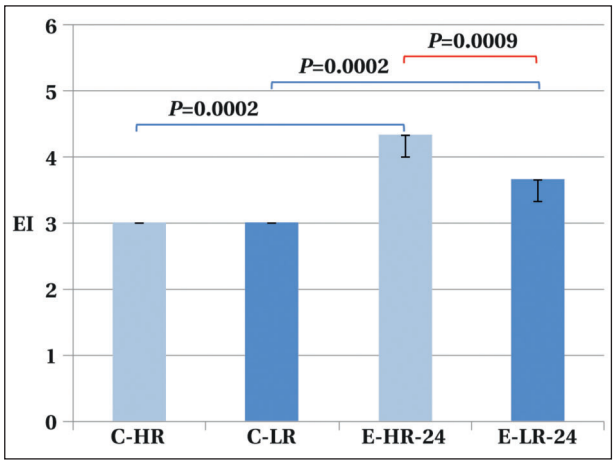

Fig. 2. Expression of the autophagy protein Beclin-1 in the cytoplasm of cardiomyocytes in the area of cardiac injury 24 hours after cardiac contusion modeling.
Note. EI (expression index) is the index of expression in absolute units, which represents the result of dividing the sum of staining intensity scores and staining area scores by the number of fields of view; CH — control group, subgroup with high stress resistance; CL — control group, subgroup with low stress resistance; EH — experimental group, subgroup with high stress resistance; EL — experimental group, subgroup with low stress resistance.

C1), which triggers autophagy by producing phosphatidylinositol 3-phosphate (PtdIns3P) and recruiting the DFCP1 and WIPI genes, which are responsible for the formation of the insulating membrane and its separation from the endoplasmic reticulum (Fig. 4). In addition, Beclin-1 is a member of PI3K class III C2, whose main effects are realized at the stage of autophagosome and lysosome fusion to ensure the degradation of intracellular substrates [12–14]. The observed increase in Beclin-1 protein expression in animals of the experimental group compared to the control group indicates the activation of autophagic flux in the post-traumatic period of experimental cardiac contusion.

Autophagy activation after blunt cardiac injury is associated with oxidative stress in cardiomyocytes, organelle damage, accumulation of reactive oxygen species (ROS) and Ca^{2+} ions, inadequate synthesis of adenosine triphosphate (ATP) and, as a consequence, increasing energy deficit [15–17]. Mitochondrial stress leads to increased production of ROS in the respiratory chain. ROS are the primary triggers of autophagic flux and can directly inactivate the mTOR complex (Fig. 4), thereby initiating autophagy processes [18, 19]. The decrease in the levels of reduced glutathione and total antioxidant capacity in traumatized rats with low stress resistance (EL subgroup) compared to highly resistant animals (EH subgroup) confirms a more intense oxidative stress and subsequent accumulation of ROS in cardiomyocytes. According to this logic, the intensity of autophagy in the damaged myocardium should also be significantly greater in the case of higher ROS in the low stress resistant animals. However,

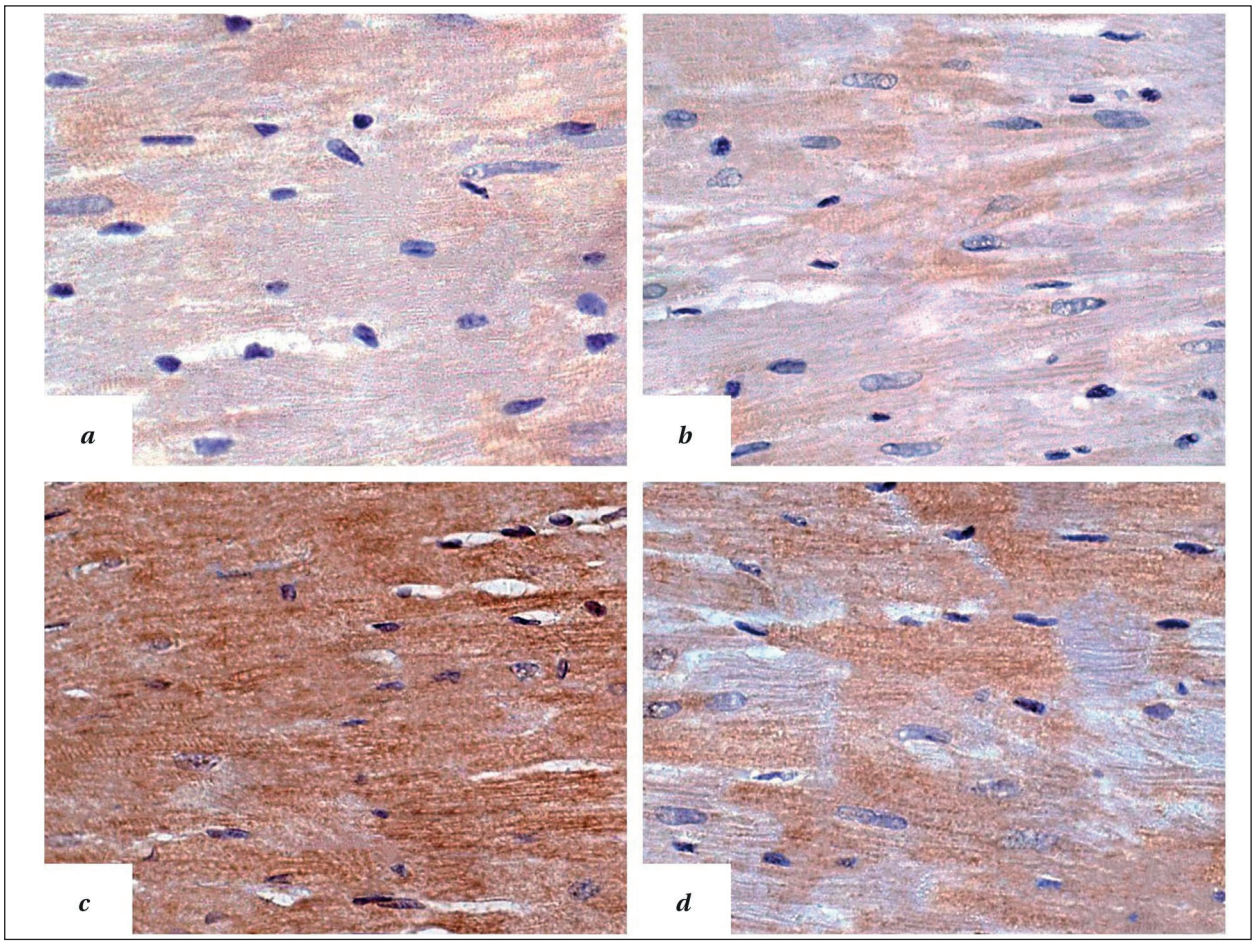

Fig. 3. Beclin-1 protein expression in rat left ventricular cardiomyocytes. Longitudinal section of the myocardium.
Note. Immunohistochemical staining, ×400. *a* — control group, subgroup with high stress resistance (CH); *b* — control group, subgroup with low stress resistance (CL); *a, b* — weak cytoplasmic expression in single cardiomyocytes; *c* — experimental group, subgroup with high stress resistance (EH); cytoplasmic expression of high and moderate diffuse intensity; *d* — experimental group, subgroup with low stress resistance (EL); single cardiomyocyte foci with cytoplasmic expression of moderate intensity.

the immunohistochemical data reveal that the expression of Beclin-1 in low stress resistant animals from the experimental group was less pronounced than in rats with high stress resistance.

This may be explained by the fact that the consequences of autophagy may differ significantly under different conditions (varying models and severity of injury). For example, in relatively mild trauma, autophagy plays an exclusively protective and adaptive role [20], whereas in more severe trauma, hyperactivation of the autophagic flux or its incompleteness, in particular excessive production and accumulation of autophagosomes without their further fusion with lysosomes, can lead to cell death [21, 22]. Conversely, moderate levels of ROS in the cell cause an increase in autophagy, which promotes cell repair and survival (Fig. 4). However, accumulation of ROS above a certain level can lead to increased phosphorylation of the proapoptotic protein Bcl-2 [23], as well as permanent activation of the JNK pathway, which mediates cell death through mitochondrial pathways, enhancing apoptosis and inhibiting autophagy [16]. Probably, due to the excessive concentration of oxygen metabolites in cardiomyocytes and the low initial stress resistance of the animals, causing an excessive level of stress-related system tension, the traumatic impact first triggered autophagy and then, due to its inefficiency, switched the cell death program to the apoptosis pathway.

Damage to the mitochondria also leads to a decrease in ATP synthesis and a disturbance in the cellular energy balance. Adenosine monophosphate-activated protein kinase (AMPK) acts as a sensor that monitors the ATP/AMP ratio and is able to induce autophagy by inactivating the mTOR complex in response to insufficient ATP levels in the cell (Fig. 4). As an adaptive mechanism, autophagy provides the cell with energy by degrading damaged organelles and abnormal proteins. However, when the equilibrium achieved by the activation of this backup mechanism is disturbed, autophagy is inhibited and apoptotic cell death is triggered with the participation of Bax/Bak proteins (members of the Bcl-2 family necessary for the permeabilization of the outer mitochondrial membrane) or by direct activation of

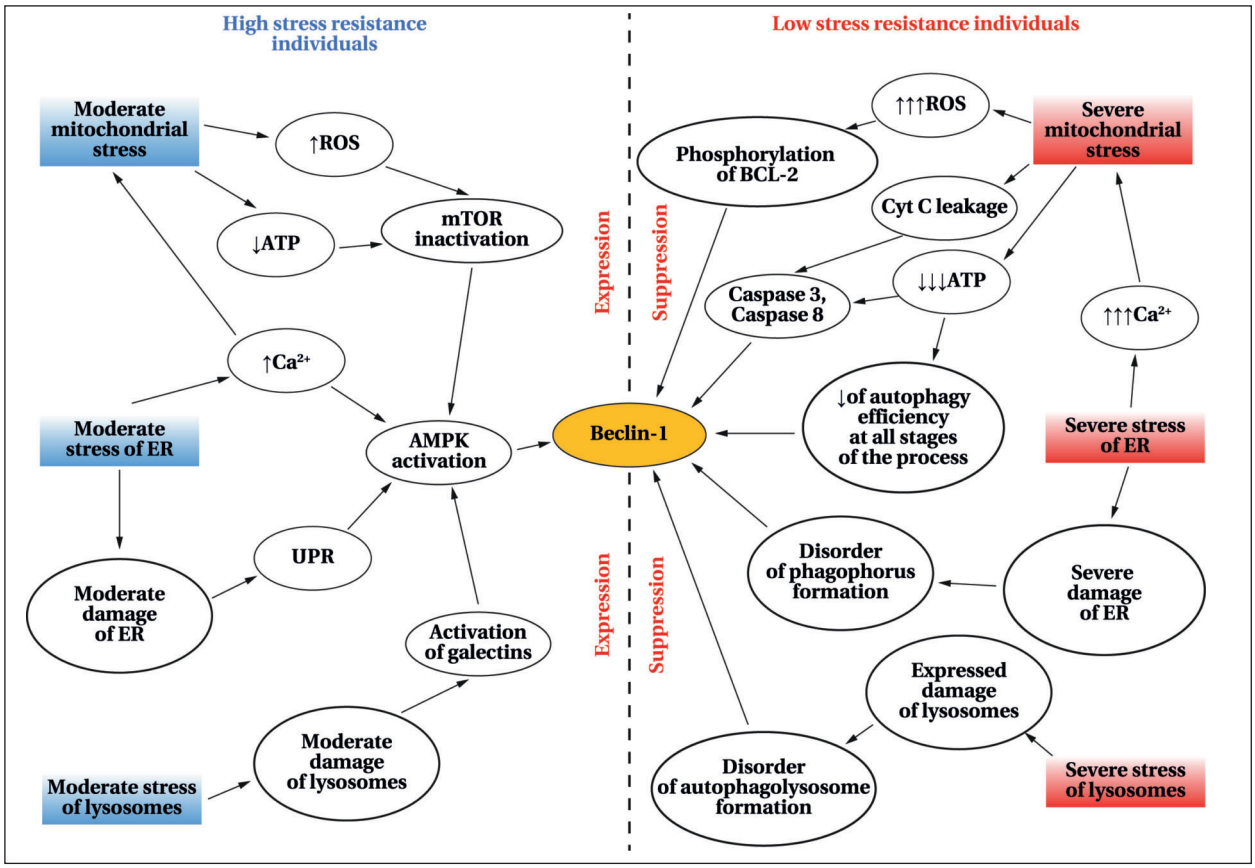

Fig. 4. Expression of the autophagy protein Beclin-1 in the myocardial injury zone after heart contusion modeling under different stress resistance levels. Authors' illustration.

Note. ER — endoplasmic reticulum; ROS — reactive oxygen species; ATP — adenosine triphosphate; AMPK — adenosine monophosphate-activated protein kinase; UPR — unfolded protein response; cyt C — cytochrome C; mTOR — mammalian target of rapamycin.

caspases due to the inability to compensate for the cellular energy deficit. In addition, the autophagy process itself consumes a large amount of ATP at all stages, from initiation to autophagolysosome formation, so a significant energy deficit can directly affect any stage of autophagy [24].

The increase in blood lactate concentration after experimental cardiac injury [7] reflects the accumulation of products of anaerobic glycolysis and indirectly indicates the development of cellular energy depletion. Higher lactate levels in traumatized animals with low stress resistance suggest that the ATP content in their cardiomyocytes was also significantly lower than in those with high stress resistance. Under these conditions, the initiation of autophagy was probably impossible or the progression of autophagic reactions was halted at some stage.

The stress induced by blunt cardiac trauma on cardiomyocytes leads to the accumulation of misfolded proteins and the release of Ca^{2+} ions from the endoplasmic reticulum (ER), the primary storage site of intracellular calcium. Both factors can trigger the process of autophagy. In the first case, initiation occurs via the unfolded protein response (UPR) and activation of ER transmembrane proteins that indirectly affect the AMPK and mTOR complexes (Fig. 4). However, in situations of significant structural damage to the ER, the process of autophagy can be disrupted or halted at the stage of phagophore formation [25].

In turn, an increase in the concentration of Ca^{2+} ions in the cytoplasm leads to the activation of the AMPK complex by calcium/calmodulin-dependent protein kinase (CaMKK), resulting in the inhibition of mTOR and the initiation of autophagic processes [17]. However, due to the significant accumulation of calcium in the cell, there is a corresponding increase in the unidirectional transport of Ca^{2+} across the mitochondrial membrane, which, like the endoplasmic reticulum, serves as a storage site. The increased calcium content in the mitochondria leads to a significant activation of the electron transport chain to generate more ATP, but these processes are accompanied by leakage of free electrons, resulting in the formation of reactive oxygen species (Fig. 4). In addition, excessive calcium uptake by mitochondria can cause their dysfunction and leakage of cytochrome C, which contributes to the activation of the caspase cascade and the implementation of the programmed cell death pathway [25].

When lysosomes are damaged, Ca^{2+} ions may also leak out, as calcium is used in the regulation of

autophagy to facilitate the fusion of autophagosomal and lysosomal membranes. However, Ca^{2+} release from lysosomes also contributes to elevated cytoplasmic calcium levels, which can trigger autophagic repair and overload the mitochondrial respiratory chain, leading to apoptosis [25]. In addition, structural defects of lysosomes cause activation of proteins of the galectin family, which are sensors of lysosomal damage and regulate the processes of autophagy aimed at repairing lysosomes directly (Fig. 4). However, when they are severely damaged or lysophagy is ineffective, structurally and functionally defective lysosomes inhibit autophagy at the fusion and degradation stages, leading to the accumulation of autophagosomes in the cell and autophagic cell death, called «autosis». In addition, significant damage to the lysosomal membrane can lead to the release of cathepsins into the cytoplasm and cell death [26].

In addition, the expression of Beclin-1 can be influenced by various apoptotic factors, such as Bcl-2, caspase-3, caspase-8, which are activated by excessive damage to cardiomyocyte organelles, accumulation of reactive oxygen species, Ca^{2+}, and severe ATP deficiency (Fig. 4). The pro-apoptotic protein Bcl-2 can inhibit autophagy by binding to Beclin-1 in the BH3 domain, leading to the dissociation of Beclin-1 and Vps-34 and the release of Beclin-1 from the active complexes PI3K class IIIC1 and PI3K class IIIC2 [13]. During the initiation of apoptotic processes, activated caspase-3 and caspase-8 can cleave the Beclin-1 protein into fragments that lack autophagic activity [13, 27, 28]. Furthermore, the cleavage products of Beclin-1 can bind to the mitochondrial membrane, leading to the release of pro-apoptotic factors that accelerate the apoptotic process. Other autophagic factors such as Vps-34, Atg5, LC3-II, AMBRA can also be targeted by apoptotic proteases, resulting in the inhibition of autophagy [29].

Thus, upregulation of the autophagy protein Beclin-1 in the posttraumatic period of experimental cardiac contusion in highly stress-resistant rats (subgroup EH) compared with low-resistant animals (subgroup EL) may be associated with optimal implementation of the stress-related response cascade and a lower degree of structural damage to cardiomyocytes. The protective effect of autophagy by eliminating defective cellular structures may only exist up to a certain degree of cardiomyocyte damage, which was observed in highly stress-resistant rats. Exceeding this degree of damage can lead to inhibition of autophagy, as seen in animals with low stress resistance, and the initiation of apoptotic processes. The mortality rate, which was 0% in highly stress-resistant animals (OV subgroup) and 25% in low stress-resistant animals (OH subgroup), can be considered as a parameter indirectly representing the severity of cardiomyocyte damage in experimental cardiac contusion and the resulting hemodynamically significant decrease in myocardial contractility.

Conclusion

In the post-traumatic period of experimental cardiac contusion, factors that activate autophagy appear at the site of a myocardial injury, as evidenced by increased expression of the autophagy protein Beclin-1. The extent of autophagy varies depending on the stress resistance of the organism, with significantly higher protein expression levels observed in highly stress-resistant animals compared to those with lower stress resistance.

References

1. *Новоселов В.П., Савченко С.В., Кошляк Д.А., Воронковская М.В., Степанищев И.В.* Оценка ультраструктурных изменений сократительного аппарата кардиомиоцитов после ушиба сердца. *Судебно-медицинская экспертиза.* 2010; 53 (2): 13–15. [*Novoselov V.P., Savchenko S.V., Koshliak D.A., Voronkovskaia M.V., Stepanishchev I.V.* Assessment of ultrastructural changes in the contractile apparatus of cardiomyocytes after heart contusion. *Sud Med Ekspert.* 2010; 53 (2): 13–15. (In Russ.)]. PMID: 20560503.
2. *Приймак А.Б., Корпачева О.В., Золотов А.Н.* Нерешенные вопросы патогенеза ушиба сердца. *Вестник СурГУ. Медицина.* 2020; 44 (2): 66–72. [*Priymak A.B., Korpacheva O.V., Zolotov A.N.* Unresolved issues of pathogenesis of myocardial contusion. *Vestnik SurGU. Medicina.* 2020; 44 (2): 66–72. (In Russ.)]. DOI: 10.34822/2304-9448-2020-2-66-72.
3. *Guan D.-W., Zhang X.-G., Zhao R., Lu B., Han Y., Hou Z.-H., Jia J.T.* Diverse morphological lesions and serious arrhythmias with hemodynamic insults occur in the early myocardial contusion due to blunt impact in dogs. *Forensic Sci Int.* 2007; 166 (1): 49–57. DOI: 10.1016/j.forsciint.2006.03.028. PMID: 16697542.
4. *Новоселов В.П., Савченко С.В., Кошляк Д.А., Воронковская М.В.* Гистохимическое исследование структуры миокарда при ушибе сердца. *Морфология.* 2009; 136 (6): 53–56. [*Novoselov V.P., Savchenko S.V., Koshliak D.A., Voronkovskaia M.V.* Histochemical study of the myocardium structure in the heart contusion. *Morfologiia.* 2009; 136 (6): 53–56. (In Russ.)]. PMID: 20358774.
5. *Acýpayam A., Eser N., Yaylalý A., Karacaoðlu Ý.C., Yoldas A., Tolun F.I., Aksu E.* Effects of amifostine against blunt chest trauma-induced cardiac injury in rats. *Ulus Travma Acil Cerrahi Derg.* 2023; 29 (3): 266–276. DOI: 10.14744/tjtes.2023.84308. PMID: 36880625.
6. *Благонравов М.Л., Коршунова А.Ю., Азова М.М., Бондарь С.А., Фролов В.А.* Аутофагия кардиомиоцитов и морфологические изменения миокарда левого желудочка при острой очаговой ишемии. *Бюллетень экспериментальной биологии и медицины.* 2016; 160 (3): 398–400. [*Blagonravov M.L., Korshunova A.Y., Azova M.M., Bondar' S.A., Frolov V.A.* Cardiomyocyte autophagia and morphological alterations in the left ventricular myocardium during acute focal ischemia. *Bull Exp Biol Med.* 2016; 160 (3): 398–400. (In Russ.)]. DOI: 10.1007/S10517-016-3180-1. PMID: 26742735.
7. *Приймак А.Б., Корпачева О.В., Золотов А.Н., Новиков Д.Г.* Стратегии адаптации при ушибе сердца у крыс с различной стрессоустойчивостью. *Вестник СурГУ. Медицина.* 2021; 50 (4): 110–116. [*Priymak A.B., Korpacheva O.V., Zolotov A.N., Novikov D.G.* Strategies for adaptation in rats with various stress resistance after myocardial contusion. *Vestnik SurGU. Medicina.* 2021; 50 (4): 110–116. (In Russ.)]. DOI: 10.34822/2304-9448-2021-4-110-116.
8. *Кузнецов А.И., Васильева Т.А.* Влияние тонуса симпатоадреналовой и гипоталамо-гипофизарно-надпочечниковой системы на функцию кроветворных органов у собак с разной стрессовой чувствительностью. *Известия ОГАУ.* 2019; 79 (5): 185–188. [*Kuznetsov A.I., Vasilyeva T.A.* Influence of the tonus of sympatho-adrenal and hypothalamic-pituitary-adrenal system on the function of hepatogenic organs in dogs with different stress sensibility. *Izvestia Orenburg State Agrarian University.* 2019; 79 (5): 185–188. (In Russ.)].
9. *Приймак А.Б., Корпачева О.В., Золотов А.Н., Ключникова Е.И.* Методика ранжирования крыс по стрессоустойчивости и определение объема выборки при экспериментальном ушибе сердца. *Современные проблемы науки и образования.* 2022; 4: 120. [*Priymak A.B., Korpacheva O.V., Zolotov A.N., Klyuchnikova E.I.* The method of ranking rats by stress resistance and sample size determination in experimental heart contusion. *Current Problems of Science and Education/Sovremenniye Problemy Nauki i Obrazovaniya.* 2022; 4: 120. (In Russ.)]. DOI: 10.17513/spno.31965.
10. Патент № 374227 Российская Федерация, МПК G09D9/00 (2000.01). Способ моделирования ушиба сердца у мелких лабораторных животных (полезная модель): №2003133897/20 (036729); заявл. 24.11.2003; опубл. 20.04.2004. *Долгих В.Т., Корпачева О.В., Ершов А.В.*; заявитель Омская государственная медицинская академия; 3 с. [Patent № 374227 Russian Federation, MPK G09D9/00 (2000.01). Mechanism for myocardial contusion simulation in small laboratory animals (useful model): № 2003133897/20 (036729); claim 24.11.03; published 20.04.04. *Dolgikh V.T., Korpacheva O.V., Ershov A.V.*; applicant and assignee Omsk State Medical Academy; 3 p.].
11. Патент № 2799815 C1 Российская Федерация, МПК G01N 33/50, G01N 1/30, A61B 5/00. Способ макроскопической паноптической визуализации очагов повреждения и расчета объема поврежденного миокарда при моделировании ушиба сердца (полезная модель): №2023111413; заявл. 03.05.23; опубл. 12.07.23. *Ключникова Е.И., Золотов А.Н., Корпачева О.В, Мозговой С.И., Храмых Т.П., Ермолаев П.А.*; заявитель Федеральное государственное бюджетное образовательное

учреждение высшего образования «Омский государственный медицинский университет» Министерства здравоохранения Российской Федерации, 13 с. [Patent № 2799815 C1 Russian Federation, МРК G01N 33/50, G01N 1/30, A61B 5/0. Method of macroscopic panoptic visualization of lesions and calculation of the volume of damaged myocardium when modeling a heart contusion (useful model): № 2023111413; claim 03.05.23; published 12.07.23. *Klyuchnikova E.I., Zolotov A.N., Korpacheva O.V., Mozgovoi S.I., Khramykh T.P., Ermolaev P.A.;* applicant and assignee Omsk State Medical University; 13 p].

12. *He C., Levine B.* The Beclin 1 interactome. *Curr Opin Cell Biol.* 2010; 22 (2): 140–149. DOI: 10.1016/j.ceb.2010.01.001. PMID: 20097051.
13. *Maejima Y., Isobe M., Sadoshima J.* Regulation of autophagy by Beclin 1 in the heart. *J Mol Cell Cardiol.* 2016; 95: 19–25. DOI: 10.1016/j.yjmcc.2015.10.032. PMID: 26546165.
14. *Tran S., Fairlie W.D., Lee E.F.* BECLIN1: protein structure, function and regulation. *Cells.* 2021; 10 (6): 1522. DOI: 10.3390/cells10061522. PMID: 34204202.
15. *Guo Q.Q., Wang S.-S., Zhang S.-S., Xu H.-D., Li X.-M., Guan Y., Yi F., et al.* ATM-CHK2-Beclin 1 axis promotes autophagy to maintain ROS homeostasis under oxidative stress. *EMBO J.* 2020; 39 (10): e103111. DOI: 10.15252/embj.2019103111. PMID: 32187724.
16. *Gao Q.* Oxidative stress and autophagy. In: *Qin Z.-H. (eds.).* Autophagy: biology and diseases. Advances in experimental medicine and biology. Springer, Singapore; 2019; 1206: 179–198. DOI: 10.1007/978-981-15-0602-4_9. ISBN: 978-981-15-0601-7.
17. *Saikia R., Joseph J.* AMPK: a key regulator of energy stress and calcium-induced autophagy. *J Mol Med (Berl).* 2021; 99 (11): 1539–1551. DOI: 10.1007/s00109-021-02125-8. PMID: 34398293.
18. *Filomeni G., De Zio D., Cecconi F.* Oxidative stress and autophagy: the clash between damage and metabolic needs. *Cell Death Differ.* 2015; 22 (3): 377–388. DOI: 10.1038/cdd.2014.150. PMCID: PMC4326572.
19. *Wang Y., Zhang H.* Regulation of autophagy by mTOR signaling pathway. In: *Qin Z.-H. (eds.).* Autophagy: biology and diseases. Advances in experimental medicine and biology. Springer, Singapore; 2019; 1206: 67–83. DOI: 10.1007/978-981-15-0602-4_3. ISBN: 978-981-15-0601-7.
20. *Viscomi M.T., D'Amelio M., Cavallucci V., Latini L., Bisicchia E., Nazio F., Fanelli F., et al.* Stimulation of autophagy by rapamycin protects neurons from remote degeneration after acute focal brain damage. *Autophagy.* 2012; 8 (2): 222–235. DOI: 10.4161/auto.8.2.18599. PMID: 22248716
21. *Sakai K., Fukuda T., Iwadate K.* Immunohistochemical analysis of the ubiquitin proteasome system and autophagy lysosome system induced after traumatic intracranial injury: association with time between the injury and death. *Am J Forensic Med Pathol.* 2014; 35 (1): 38–44. DOI: 10.1097/PAF. 0000000000000067. PMID: 24317096.
22. *He M., Ding Y., Chu C., Tang J., Xiao Q., Luo Z.G.* Autophagy induction stabilizes microtubules and promotes axon regeneration after spinal cord injury. *Proc Natl Acad Sci U S A.* 2016; 113 (40): 11324–11329. DOI: 10.1073/pnas.1611282113. PMID: 27638205.
23. *Chen Y., Zhang W., Guo X., Ren J., Gao A.* The crosstalk between autophagy and apoptosis was mediated by phosphorylation of Bcl-2 and beclin1 in benzene-induced hematotoxicity. *Cell Death Dis.* 2019; 10 (10): 772. DOI: 10.1038/s41419-019-2004-4. PMID: 31601785.
24. *Yang J., Zhou R., Ma Z.* Autophagy and energy metabolism. In: *Qin Z.-H. (eds.).* Autophagy: biology and diseases. Advances in experimental medicine and biology. Springer, Singapore; 2019; 1206: 329-357. DOI: 10.1007/978-981-15-0602-4_16. ISBN: 978-981-15-0601-7.
25. *Hu Y.-X., Han X.-S., Jing Q.* Ca (2+) Ion and Autophagy. In: *Qin Z.-H. (eds.).* Autophagy: biology and diseases. Advances in experimental medicine and biology. Springer, Singapore; 2019; 1206: 151-166. DOI: 10.1007/978-981-15-0602-4_7. ISBN: 978-981-15-0601-7.
26. *Ballabio A., Bonifacino J.S.* Lysosomes as dynamic regulators of cell and organismal homeostasis. *Nat Rev Mol Cell Biol.* 2020; 21 (2): 101–118. DOI: 10.1038/s41580-019-0185-4. PMID: 31768005.
27. *Zhu Y., Zhao L., Liu L., Gao P., Tian W., Wang X., Jin H., et al.* Beclin 1 cleavage by caspase-3 inactivates autophagy and promotes apoptosis. *Protein Cell.* 2010; 5 (1): 468–477. DOI: 10.1007/s13238-010-0048-4. PMID: 21203962.
28. *Cho D.-H., Jo Y.K., Hwang J.J., Lee Y.M., Roh S.A., Kim J.C.* Caspase-mediated cleavage of ATG6/Beclin-1 links apoptosis to autophagy in HeLa cells. *Cancer Lett.* 2009; 274 (1): 95–100. DOI: 10.1016/j.canlet.2008.09.004. PMID: 18842334.
29. *Pagliarini V., Wirawan E., Romagnoli A., Ciccosanti F., Lisi G., Lippens S., Cecconi F., et al.* Proteolysis of Ambra1 during apoptosis has a role in the inhibition of the autophagic prosurvival response. *Cell Death Differ.* 2012; 19 (9): 1495–1504. DOI: 10.1038/cdd.2012.27. PMID: 22441670.

Received 01.06.2023
Accepted 21.09.2023

https://doi.org/10.15360/1813-9779-2023-6-62-70

Comprehensive Cardiopulmonary Resuscitation Training for Foreign Medical Students

Rocha Ferreira Samantha[1], Svetlana A. Perepelitsa[2]*, Shraddha A. Narode[3], Karina Yu. Koreshkova[2], Aditi M. Harer[3], Komal S. Borate[3], Nirzara R. Tuklia[3]

Country: [1] Brazil; [2] Russia; [3] India
Immanuel Kant Baltic Federal University,
14A Nevskiy Str., 236041 Kaliningrad, Russia

For citation: *Rocha Ferreira Samantha, Svetlana A. Perepelitsa, Shraddha A. Narode, Karina Yu. Koreshkova, Aditi M. Harer, Komal S. Borate, Nirzara R. Tuklia.* Comprehensive Cardiopulmonary Resuscitation Training for Foreign Medical Students. *Obshchaya Reanimatologiya = General Reanimatology.* 2023; 19 (6): 62–70. https://doi.org/10.15360/1813-9779-2023-6-62-70 [In Russ. and Engl.]

***Correspondence to:** Svetlana A. Perepelitsa, sveta_perepeliza@mail.ru

Summary

The purpose of this study was to assess acquired knowledge and practical skills in foreign medical students (FMS) after theoretical and practical training in cardiopulmonary resuscitation.

Material and methods. We conducted a prospective randomized trial «Simulation-based CPR training among international medical students: perspectives for medical education» involving students undergoing training in the 31.05.01 specialty — General Medicine in English. Sealed envelope randomization was used to assign the participants (*N*=71) to 3 groups. European Resuscitation Council (ECR) educational Guidelines for Resuscitation was studied by students of all 3 groups. Group 1 (*N*=21) students did not receive additional training materials and practices. Group 2 (*N*=25) students were additionally provided a link to a video lesson on CPR on the ECR YouTube channel. Students from Group 3 (*N*=25) were additionally involved in developing 3 mind maps: on the anatomy and physiology of the heart and CPR algorithm. All participants underwent theoretical training at the 1st stage, and «Basic Cardiopulmonary Resuscitation and Automated External Defibrillation (AED)» simulation training at the second stage. At the end of the course, students' practical skills in performing continuous chest compressions were examined.

Results. Most examinees passed the ECR platform test on the first or second attempt. The participants of the simulation course demonstrated high learning efficiency: there were no statistically significant differences between the groups in the number and average frequency of compressions performed. Almost all participants correctly performed hand placement in the center of the chest for chest compression. Decompression phase efficiency reached 71–77% (*P*=0.811) in all groups. Most examinees performed chest compressions to the required depth and with the recommended frequency (*P*=0.62).

Conclusion. The educational project initiated by foreign students yielded positive results: acquired knowledge of CPR algorithm, gained essential techniques of performing chest compressions and giving rescue breaths, retained skills in using an automated external defibrillator, as well as teamwork skills.

Keywords: simulation training; cardiac arrest; training; chest compression; decompression; mind map.

Conflict of interest. The authors declare no conflict of interest.

Read the full-text English version at www.reanimatology.com

Introduction

Modern medical education is currently undergoing significant transformations aimed at improving the quality of students' education. The main objective of education is to train doctors who possess specific competencies and are capable and prepared for independent professional practice [1–4]. The rapidly evolving nature of the medical profession is driven by advancements in medical technologies, necessitating the re-engineering of the educational process [5–8], and the development and implementation of modern pedagogical technologies, including «hybrid» learning. The integration of educational engineering into pedagogical practice enables students to construct their individualized learning trajectory and utilize not only traditional teaching methods, but also electronic, simulation, and imitation training. Ultimately, this approach will contribute to the development of essential universal, general professional, and specialized competencies [1, 9, 10].

Currently, medical education is increasingly adopting a «hybrid» learning model that consists of four distinct components:

1. Theoretical component, which encompasses lectures (face-to-face or online), seminars, and practical sessions. Various technologies, such as mind maps, medical animations, and knowledge trees, are used to facilitate the acquisition of theoretical knowledge by the students.

2. Online learning, which involves the use of educational platforms that offer a wide range of learning resources and assessment tools. The main advantage of this approach is its flexibility, allowing

students to access information at any time and review materials repeatedly, as well as to have a level and final assessment. Additionally, students can independently tailor their learning trajectory on these platforms, which significantly enhances their motivation [11, 12]. An example of such a resource is the European Resuscitation Council (ERC) platform, specifically designed for teaching cardiopulmonary resuscitation (CPR).

3. Simulation training (ST), which is a rapidly evolving method of teaching practical clinical skills in simulated settings. Various clinical situations are modeled, providing an opportunity to systematically develop practical clinical skills without involving real patients [13, 14]. Various types of mannequins and simulators, from simple models to highly realistic computerized robots, are used for training. The advantage of this training is the ability to make mistakes without harming a real patient, to repeat the necessary algorithms based on clinical guidelines and standards of medical care, and to participate in the realization of sophisticated scenarios such as cardiac arrest or rare clinical cases, etc. Simulation training is integrated into the curriculum in a way that promotes the development of necessary practical skills and enables the successful application of acquired skills in clinical practice [1, 13, 14].

4. Clinical practical sessions, in which students apply the knowledge and experience gained in the previous stages.

Training students and physicians to perform effective cardiopulmonary resuscitation is a priority worldwide [14–17]. However, there are several issues that need to be addressed. These include fear of training, lack of dedicated teaching hours for CPR within the curriculum, large student groups that make it difficult to provide quality training during scheduled class time, missing pedagogical experience, and a lack of unified teaching doctrine for this subject. As a result, alternative learning opportunities arise, where students initiate their training on the topic of interest. The problem of cardiac mortality is a global issue, which is why international students studying in Russian medical universities seek high-quality education that includes both theoretical and practical training, including CPR training.

Publications focusing on the training of cardiopulmonary resuscitation (CPR) only reflect the results of simulation training and the evaluation of compression performance (depth, rate) and decompression quality. The theoretical preparation that precedes practical sessions is rarely discussed.

This study aims to examine the effectiveness of theoretical preparation and acquisition of practical skills during CPR training for international medical students.

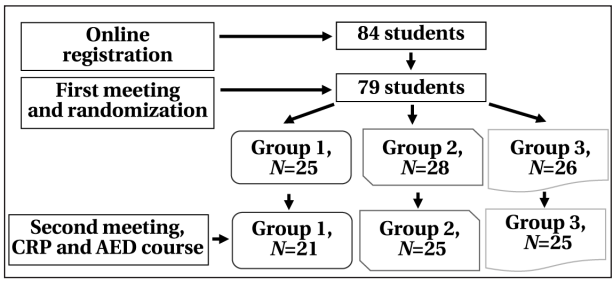

Fig. 1. The design of the prospective randomized trial.

Materials and Methods

We conducted a prospective randomized study on «Simulation-based CPR training among international medical students: perspectives for medical education.» The study included 71 international students learning general medicine (code within the Russian education system 31.05.01) in English. The participants were predominantly from India (68; 95.8%), with a smaller number from Brazil (2; 2.8%) and Ecuador (1; 1.4%). The study was approved by the Independent Ethics Committee of the Clinical Research Center of Immanuel Kant Baltic Federal University (Protocol of the IEC Meeting No. 39 dated April 26, 2023).

The prospective, randomized study design is shown in Figure 1. Participation was voluntary. Invitations and registration links to participate in the study were sent to all international students enrolled in years 2–5 of the specialty program. A total of 84 students registered and were invited to the first meeting. Of these, 79 students attended the meeting where the project was presented and all participants and organizers signed the informed consent form. The participants were then randomized into three groups using the envelope method.

Group 1 consisted of 25 students who studied the Instructor's Guide on the ERC platform.

Group 2 included 28 students who were provided with a link to a video lesson on CPR on the ERC YouTube channel in addition to the materials from the instructional manual on the ERC platform.

Group 3 comprised 26 students who studied the Instructor's Guide on the ERC platform and worked to create three mind maps on cardiac anatomy and physiology and the CPR algorithm.

The training was planned as part of the European Resuscitation Council (ERC) provider course, for which all participants were also registered on the platform.

The students in the study had no theoretical knowledge or practical skills in CPR. They were trained for the first time on this topic.

The activity was carried out in two phases: distance learning (theoretical training) and face-to-face training (simulation practice). The theoretical training differed between groups. Basic training for all groups

included studying the European Resuscitation Council materials «Basic Life Support and Automatic External Defibrillation», an online testing on the ERC platform. The subsequent theoretical training depended on the group to which the participant was randomly assigned. Students were given 5 days to study all the material and complete the assignments.

The mandatory requirement for all participants was to pass the online test on the ERC platform. Everyone was required to complete the test one day prior to the start of the CPR provider course. Performance on the ERC platform was graded on a pass/fail basis with a passing score of ⩾80%. In the event of a failed attempt, participants were given the opportunity to retake the test up to 5 times until they achieved a passing score. The following indicators were used to evaluate test performance: number of attempts, maximum total score, and time taken to complete the test.

The second meeting of the project was a practical stage, which consisted of simulation training on «Basic life support and automated external defibrillation». This training was conducted at the Regional Resource Center for Simulation Education and Accreditation in Medicine, under the Department of surgical disciplines at the Institute of Medicine and Life Sciences of Immanuel Kant Baltic Federal University.

A total of 71 students participated in the practical session, divided into the following groups:

- Group 1: 21 students, including 11 males (52.4%) and 10 females (47.6%).
- Group 2: 25 students, including 8 males (32%) and 17 females (68%).
- Group 3: 25 students, including 10 males (40%) and 15 females (60%).

The Braydenpro manikin (Innosian Inc., Korea) was used for training. This manikin is designed to teach basic cardiopulmonary resuscitation and provides visual light control feedback on the effectiveness of chest compressions, as well as independent assessment of the quality of chest compressions, including correct hand placement, compression rate and depth, and decompression effectiveness. In addition, the AED Trainer XFT-120C+ (Shenzhen XFT Medical Limited, China) was used for defibrillation training.

At the end of the course, the practical skill of performing continuous chest compressions was evaluated. During the examination, male participants performed 120 continuous compressions, while female participants performed 90 compressions. Criteria for the effectiveness of CPR included proper hand placement in the middle of the chest, compression rate of 100–120 per minute, compression depth of 5–6 cm, and complete decompression.

After completing the training, an online survey was conducted to assess participant satisfaction. The students answered the following questions:

1. Was the theoretical preparation important for you?
2. Was the online course on the ERC platform helpful during the training process?
3. How was the overall atmosphere during the course?
4. Did you acquire the necessary theoretical knowledge that contributed to effective simulation training?
5. Did you acquire the necessary practical skills to conduct CPR and use AED?
6. Did you feel a constant connection with the course organizers and instructors?

All stages of the training were conducted in English.

Statistical analysis. Statistical analysis of the collected data was performed using Jamovi version 2.3.21 software package for Windows. The normality of the distribution of variables was assessed using the Kolmogorov–Smirnov test with Lilliefors correction. For data with a normal distribution, the mean *(M)* and standard deviation *(SD)* were calculated. For quantitative variables with non-normal distribution, the median *(Me)* and interquartile range *(Q1; Q3)* were determined. Qualitative variables were analyzed by calculating the percentage of each value. Categorical variables were compared using the Pearson chi-squared test, and an unpaired *t*-test was used to determine group differences in continuous variables. One-way analysis of variance (ANOVA) was used to compare groups. A two-tailed *P*-value was not used. Differences between groups were considered significant at $P<0.05$.

Results

All criteria for inclusion in the study were met by 71 international students, including 42 (59.2%) females and 29 (40.8%) males. Each group consisted of students studying in the 2nd to 5th year. The distribution of participants by year is shown in Fig. 2. In all groups, the maximum number of participants were studying in the 4th year, with the proportion of 5th year students being 2.3 times lower. Almost

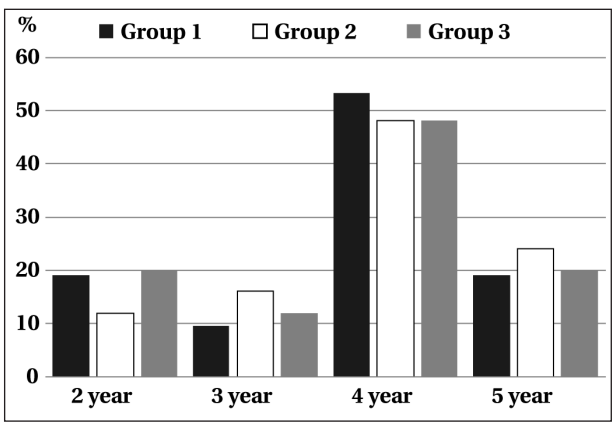

Fig. 2. Categorization of participants based on their academic year of study.

30% of participants were studying in the 2nd and 3rd years.

The level test on the ERC platform (Fig. 3) showed that the majority of students in all groups passed the test on their 1st or 2nd attempt. In the 3rd group, 4 students (16%) made 4 attempts, while in the 1st and 2nd groups, 5 students made more than 5 attempts.

The time taken to complete the test varied significantly among the groups. In the 1st group, the range was from 16 to 305 minutes, with a median time of 49.5 [30; 79] minutes. In the 2nd group, the time ranged from 10 to 161 minutes, with a median time of 49 [24; 87] minutes. In the 3rd group, students spent between 10 and 182 minutes on the test, with a median time of 61 [28; 83] minutes. No significant differences were found between the groups (P=0.996).

During the practical session on basic life support and automated external defibrillation, students learned the management algorithm for cardiac arrest and the rules of effective and safe use of AED. Attention was paid to the correct placement of hands, compression depth and rate, and complete decompression when performing chest compressions. The main results of the assessment of compression accuracy are presented in Fig. 4.

No significant differences were found between the groups in terms of the number of compressions performed and their average rate. The mean overall score was practically the same (P=0.673).

Central hand placement was performed by almost all students. The efficiency of decompressions in the groups was 71–77% (Fig. 5). There were no significant differences in these parameters between the groups (P=0.811).

Figure 5 shows the results of compression depth performance. In group 1, 13 (62%) students performed 90–100% of compressions to the depth of 5–6 cm, 5 (23.8%) students performed 70–89% of compressions to the required depth and 3 (14.3%) students performed less than 69% of quality compressions, the rest performed compressions to a depth of less than 5 cm. In group 2, 15 (60%) students performed 90–100% compressions to the required depth, 6 (24%) had effective 70–89% compressions and 4 (16%) students performed less than 69% quality compressions. In group 3, 13 (52%) students performed 90–100% compressions to the required depth, 8 (32%) had effective 70–89% compressions and 4 (16%) students performed less than 69% quality compressions (Fig. 6, *a*). No significant differences were found between the groups in terms of quality of compression depth (P=0.62).

Optimal blood circulation is achieved not only by the depth of compressions but also by their rate. Fig. 6, *b* illustrates the performance of chest compression rate in the groups.

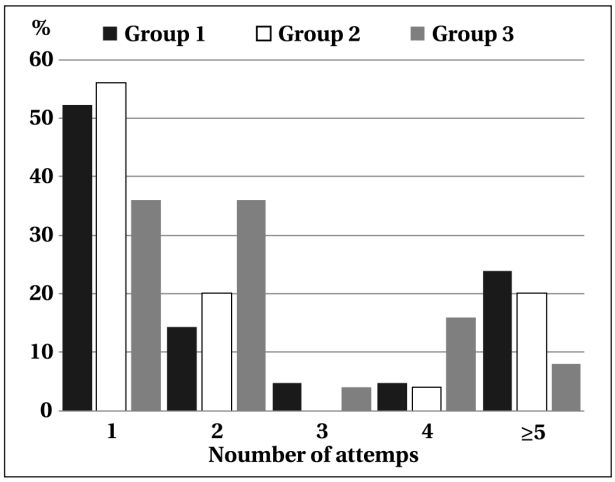

Fig. 3. Number of attempts at passing the test on the ERC platform.

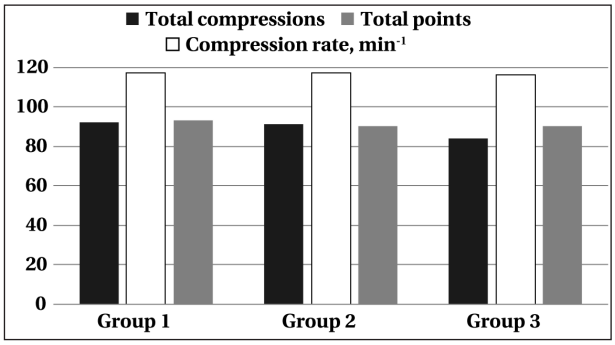

Fig. 4. Main training results.

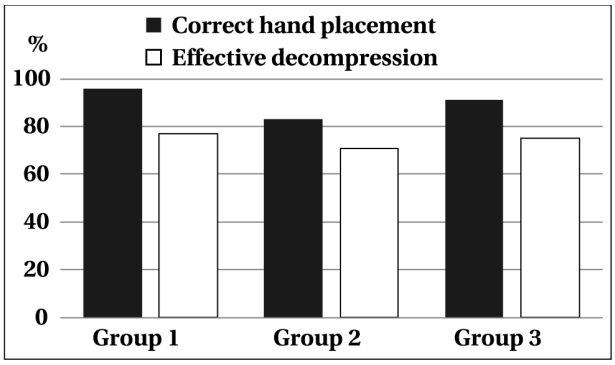

Fig. 5. Assessment of hand placement and decompression in the study groups.

In group 1, 13 (62%) students performed 70–100% of compressions with a rate of 100–120 min^{-1}, while 8 (38%) students performed 50% of compressions with a rate greater than 120 min^{-1}. In group 2, 11 (44%) students performed 70–100% of compressions at a rate of 100–120 min^{-1}, 11 (44%) students performed 50% of compressions at a rate greater than 120 min^{-1}, and 3 (12%) students performed 50% of compressions at a rate less than 100 min^{-1}. In group 3, 13 (52%) students performed 70–100% of compressions at a rate of 100–120 min^{-1}, 9 (36%) students performed 50% of compressions at a rate greater than 120 min^{-1}, and 3 (12%) students per-

formed 50% of compressions at a rate less than 100 min^{-1}. There were no significant differences in the rate of compressions between the groups (P=0.652).

Students who performed CPR at a rate of more than 120 compressions per minute had lower compression depths and a lower percentage of complete decompressions. The survey revealed that theoretical preparation prior to the provider course was important for 20 (95.2%) students in the first group, 25 (100%) participants in the second group, and 23 (92%) in the third group. Participants in all groups noted that the theoretical course on the ERC platform was helpful during the learning process. Participants in all groups also reported that they acquired the necessary practical skills to perform CPR and use AEDs, and found the course convenient and conducive to material assimilation. 17 (80.9%) students in the first group, 20 (80%) in the second group, and 25 (100%) in the third group felt a strong connection to the instructor and course organizers. To better understand the role of alternative materials/methods in theoretical training, students in the second and third groups were asked additional questions. When asked, «Do you think the videos helped you learn and improved your knowledge?» 100% of the students in the second group answered «yes». When students in the third group were asked, «Do you believe that the mind maps facilitated your learning process?» 87.5% of the students answered «yes» and 12.5% answered «more yes than no». None of the students had difficulty creating mind maps on the topic being studied.

A sample mind map is shown in Fig. 7. The map systematizes and presents detailed information about cardiac physiology. It is notable for its in-depth exploration of the topic and emphasis on key points, such as the detailed structure of the heart, direction of blood flow, characteristics of systole, diastole, and others. The author of the mind map used his own images and notes.

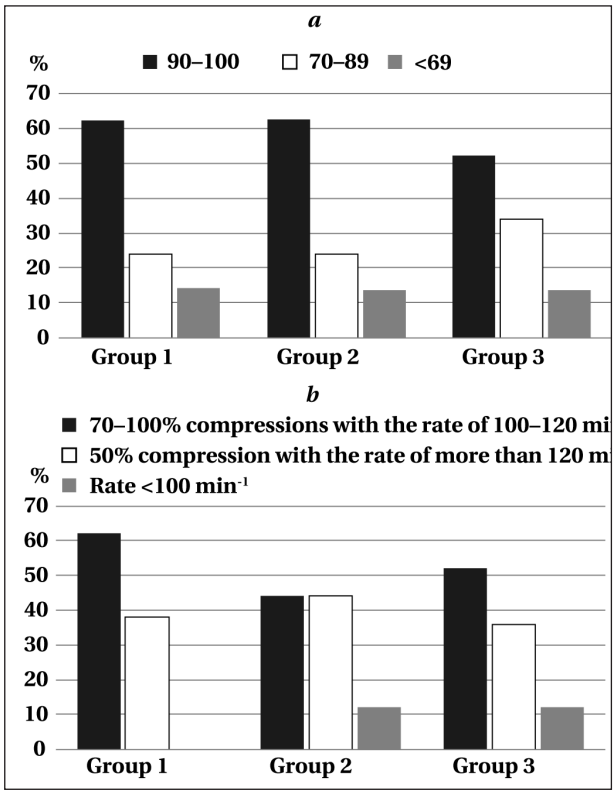

Fig. 6. Student performance in chest compression depth *(a)* and chest compression rate *(b)*.

Discussion

Training in cardiopulmonary resuscitation for sudden cardiac arrest is expanding beyond the «Anesthesiology, resuscitation and intensive care» subject, which is only taught in the 6th year of the internal medicine curriculum. This training is becoming increasingly important for international students in years 2–5, as the high mortality rate from cardiac causes is often due not only to high morbidity [18, 19], but also to reduced availability of quality medical care. Not all medical professionals know how to perform CPR when cardiac arrest occurs right in front of them, which increases the relevance of training medical professionals, including future physicians [11, 12, 20].

Training international students to perform high-quality CPR is a priority in higher medical education. Therefore, many authors emphasize the need for prospective research among students in higher medical institutions focusing on CPR skills training [20–22].

An integrated approach to CPR training should include two components, i.e., theoretical preparation and practical training in a simulation center. Theoretical preparation prior to hands-on training plays a critical role because it requires a thorough understanding of both the CPR algorithm and cardiovascular anatomy and physiology. This enables the physician performing CPR to gain a better understanding of the mechanisms of cardiac arrest, assess the effectiveness of resuscitation, and develop a treatment plan for the patient.

For theoretical preparation, educational materials, video resources, and concept maps can be used to enhance learning effectiveness [16, 17, 23–25].

The European Resuscitation Council (ERC) has developed and continuously updates guidelines for cardiopulmonary resuscitation (CPR) [23], which have been successfully integrated into the training process for specialists in many countries, including the Russian Federation. The ERC manual serves as the basis for learning the CPR algorithm and covers key principles such as the importance of proper hand placement, compression and decompression depth and rate. Prior to simulation training, theo-

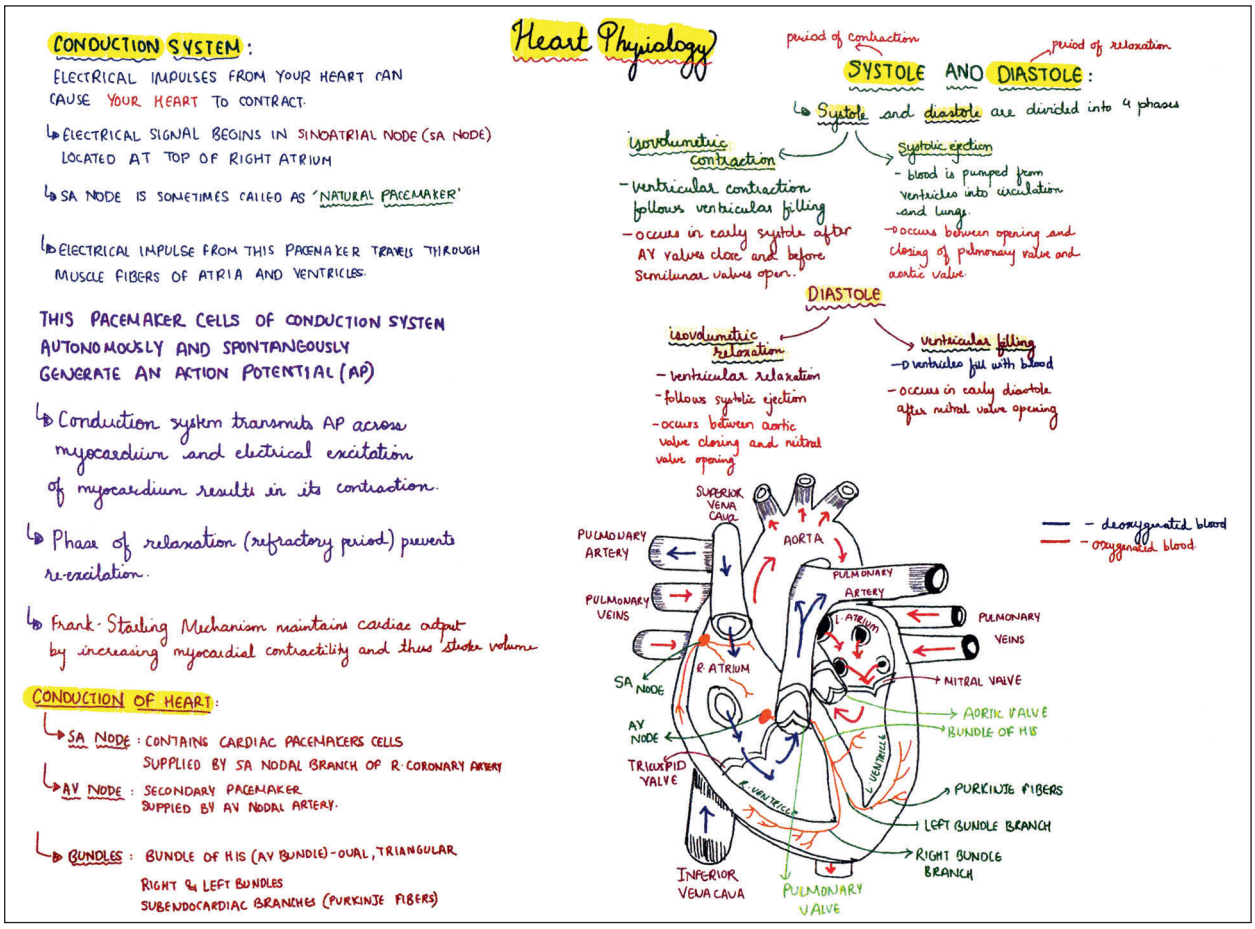

Fig. 7. Example of a mind map on cardiac physiology.

retical knowledge is assessed through an online platform. Tests conducted on the ERC platform showed that students who participated in the training had a good level of theoretical preparation, as the majority of participants passed the test on their first or second attempt. Although it was recommended not to take more than 5 attempts at the test, some students took the test repeatedly until they obtained a positive result, indicating their high motivation to learn. The time taken to complete the test varied widely, demonstrating the students' interest in this method of knowledge assessment.

The ERC manual served as the basic educational resource for all students. The video resources and mind maps provided a supplementary tool for two groups of participants, allowing for detailed and repeated viewing of all phases of resuscitation, key moments of performance, and technical accuracy. The use of mind maps helped students organize their knowledge of cardiovascular anatomy and physiology. The research results showed that theoretical preparation prior to practical sessions, regardless of its form, was effective. Students in all groups noted the usefulness of the theoretical course. Moreover, the students had a positive attitude toward watching the video and creating mind maps, despite the additional time required compared to the first group of students. All participants agreed that the training improved their knowledge and helped them master the CPR algorithm. The simulation training was the culmination of the training because it allowed for the development of technical skills necessary for practical medical activities [20–22]. During the simulation, participants learned to perform chest compressions at a specific depth and rate as well as to deliver decompressions. Some participants encountered a problem with a high compression rate, resulting in reduced depth. By analyzing their results, they understood that the quality of CPR decreases significantly in such cases. Collaboration between the instructor and students helped to improve the results. It is important to note that the training environment was friendly, and the organizers and instructors fostered a feeling of strong connection between students and teachers. The project participants rated all the proposed teaching methods positively.

The study limitation includes the lack of a priori sample calculation.

Conclusion

The educational project initiated by the international students has shown promising results, re-

gardless of the theoretical background of the students. These results include the mastery of the cardiopulmonary resuscitation algorithm, the development of technical skills in chest compressions and ventilations, the competence in the use of an automated external defibrillator, and the promotion of teamwork skills. Several resources were used to prepare for the hands-on sessions, including a teaching manual, video resources, and mind maps.

The integrated approach to student education plays an important role in developing essential theoretical knowledge and practical skills.

References

1. *Звонников В.И., Свистунов А.А., Семенова Т.В.* Оценка профессиональной готовности специалистов в системе здравоохранения. под ред. Семеновой Т.В. М.: ГЭОТАР-Медиа; 2019: 272. ISBN 978-5-9704-4977-6. [*Zvonnikov V.I., Svistunov A.A., Semenova T.V.* Assessment of the professional readiness of specialists in the healthcare system. ed. Semenova T.V. M.: GEOTAR-Media; 2019: 272. ISBN 978-5-9704-4977-6. (in Russ.)].
2. *Gruppen L.D., ten Cate O., Lingard L.A., Teunissen P.W., Kogan J.R.* Enhanced requirements for assessment in a competency-based, time-variable medical education system. *Acad Med.* 2018; 93 (3S): S 17–S 21. DOI: 10.1097/ACM.0000000000002066.
3. *Osman N.Y., Hirsh D.A.* The organizational growth mindset: animating improvement and innovation in medical education. *Med Educ.* 2020; 55 (4): 416–418. DOI: 10.1111/medu.14446. PMID: 33377544.
4. *Janczukowicz J., Rees C. E.* Preclinical medical students' understandings of academic and medical professionalism: visual analysis of mind maps. *BMJ Open.* 2017; 7 (8): e015897. DOI: 10.1136/bmjopen-2017-015897. PMID: 28821520
5. *Груздев М.В., Тарханова И.Ю., Энзельт Н.В.* Образовательный инжиниринг: концептуализация понятия. *Ярославский педагогический вестник.* 2019; 5 (110): 8–15. [*Gruzdev M.V., Tarkhanova I.Yu., Enzeldt N.V.* Educational engineering: conceptualization of the concept. *Yaroslavl Pedagogical Bulletin/Yaroslavsky Pedagogichesky Vestnik.* 2019; 5 (110): 8–15. (in Russ.)]. DOI: 10.24411/1813-145X-2019-10516.
6. Образовательная инженерия. Понятия. Подходы. Приложения. Под. ред. *И.Д. Рудинского, Е.З. Власовой.* Москва: Горячая линия-Телеком. 2021: 240. [Educational Engineering. Concepts. Approaches. Appendices. Ed. by *Rudinsky I.D., Vlasova E.Z.* Moscow: Hot Line-Telecom. 2021: 240. ISBN 978-9912-0936-6. (in Russ.)].
7. *Dewsbury B., Brame C.J.* Inclusive Teaching. *CBE Life Sci Educ.* 2019; 18 (2): fe2. DOI: 10.1187/cbe.19-01-0021. PMID: 31025917.
8. *Gorbanev I., Agudelo-Londoño S., González R.A., Cortes A., Pomares A., Delgadillo V., Yepes F.J., et al.* A systematic review of serious games in medical education: quality of evidence and pedagogical strategy. *Med Educ Online.* 2018; 23 (1): 1438718. DOI: 10.1080/10872981.2018.1438718. PMID: 29457760.
9. *Киясов А.П., Гумерова А.А., Рашитов Л.Ф., Хасанова Р.Н., Киясова Е.В.* Технологии приобретения компетенций при подготовке врача (опыт Казанского федерального университета). *Мед. обр. и проф. развитие.* 2017; 4: 57–64. DOI: 10.24411/2220-8453-2017-00019. [*Kiyasov A.P., Gumerova A.A., Rashitov L.F., Khasanova R.N., Kiyasova E.V.* Technologies for acquiring competencies in the preparation of a doctor (experience of the Kazan Federal University). *Medical Education and Professional Development/Med Obr Prof Razvitie.* 2017; 4: 57–64. (in Russ.)]. DOI: 10.24411/2220- 8453-2017-00019.
10. *Рудинский И.Д., Давыдова Н.А., Петров С.В.* Компетенция. Компетентность. Компетентностный подход. М.: Горячая линия-Телеком; 2019: 240. [*Rudinsky I.D., Davydova N.A., Petrov S.V.* Competency. Competence. Competence-based approach. M.: Hotline-Telecom; 2018: 240. (in Russ.)]. ISBN 978-5-9912- 0692-1.
11. *Bussotti E.A., Leite M.T., Alves A.C., Cristensen K.* Online training for health professionals in three regions of Brazil. *Rev Bras Enferm.* 2016; 69 (5): 981–985. DOI: 10.1590/0034-7167.2016690506. PMID: 27783743.
12. *Thomas M.P., Kozikott S., Kamateeka M. Abdu-Aguye R., Agogo E., Bello B.G. Brudney K., et al.* Development of a simple and effective online training for health workers: results from a pilot in Nigeria. *BMC Public Health.* 2022; 22 (1): 551. DOI: 10.1186/s12889-022-12943-1. PMID: 35313834.
13. *Gaubert S., Blet A., Dib F., Ceccaldi P.F., Brock T., Calixte M., De Macédo L., et al.* Positive effects of lumbar puncture simulation training for medical students in clinical practice. *BMC Med Educ.* 2021; 21 (1): 18. DOI: 10.1186/s12909-020-02452-3. PMID: 33407416.
14. *Перепелица С.А.* Компетентностный подход в обучении сердечно-легочной реанимации. *Общая реаниматология.* 2022; 18 (6): 59–68. [*Perepelitsa S. A.* Competency-based approach in teaching cardiopulmonary resuscitation. *General Reanimatology/Obshchaya Reanimatologya.* 2022; 18 (6): 59–68. (In Russ. and Engl.)]. DOI: 10.15360/1813-9779-2022-6-59-68.
15. *Боева Е.А., Старостин Д.О., Милованова М.А., Антонова В.В., Каргин Д.Ч., Абдусаламов С.Н.* Оценка качества компрессий грудной клетки, проводимых медицинскими работниками в симулированных условиях. *Общая реаниматология.* 2021; 17 (4): 37–47. [*Boeva E.A., Starostin D.O., Milovanova M.A., Antonova V.V., Kargin D.Ch., Abdusalamov S.N.* Assessment of the quality of chest compressions performed by health-care workers under simulated conditions. *General Reanimatology/Obshchaya Reanimatologya.* 2021;

17 (4): 37–47. (In Russ. and Engl.)]. DOI: 10.15360/ 1813-9779-2021-4-37-47
16. *Espinosa C.C., Melgarejo F.S., Ruiz R. M., García-Collado Á.J., Caballero S.N., Rodríguez L.J., Ríos S.P., et al.* Virtual reality in cardiopulmonary resuscitation training: a randomized trial. *Emergencias*. 2019; 31 (1): 43–46. PMID: 30656873.
17. *Anderson T.M., Secrest K., Krein S.L, Schildhouse R., Guetterman T.C., Harrod M., Trumpower B., et al.* Best practices for education and training of resuscitation teams for in-hospital cardiac arrest. *Circ Cardiovasc Qual Outcomes*. 2021; 14 (12): e008587. DOI: 10.1161/CIRCOUTCOMES. 121.008587. PMID: 34779653.
18. *Krishnan A., Das D.K.* Mortality surveillance in India: past, present, and future. *Indian J Public Health*. 2019; 63 (3): 163–164. DOI: 10.4103/ijph.IJPH_433_19. PMID: 31552842.
19. *Nowbar A.N., Gitto M., Howard J.P., Francis D.P., Al-Lamee R.* Mortality from ischemic heart disease. *Circ Cardiovasc Qual Outcomes*. 2019; 12 (6): e005375. DOI: 10.1161/CIRCOUTCOMES.118.005375. PMID: 31163980.
20. *McCoy C.E., Rahman A., Rendon J.C., Anderson C.L., Langdorf M.I., Lotfipour S. Chakravarthy B.* Randomized controlled trial of simulation vs. standard training for teaching medical students high-quality cardiopulmonary resuscitation. *West J Emerg Med*. 2019; 20 (1): 15–22. DOI: 10.5811/westjem.2018.11.39040. PMID: 30643596.
21. *He X., Ma Y., Li Z., Zhang Ju., Zhang Ji., Liang J.* What is an effective cardiopulmonary resuscitation training mode? *Chin Med J (Engl)*. 2022; 135 (9): 1131–1132. DOI: 10.1097/CM9. 0000000000001946. PMID: 35202037.
22. *Perron J.E., Coffey M.J., Lovell-Simons A., Dominguez L., King M.E., Ooi C.Y.* Resuscitating cardiopulmonary resuscitation training in a virtual reality: prospective interventional study. *J Med Internet Res*. 2021; 23 (7): e22920. DOI: 10.2196/22920. PMID: 34326040.
23. *Greif R., Lockey A., Breckwoldt J., Carmona F., Conaghan P., Kuzovlev A., Pflanzl-Knizacek L., et al.* European Resuscitation Council guidelines 2021: education for resuscitation. *Resuscitation* 2021; 161: 388–407. DOI: 10.1016/j.resuscitation. 2021.02.016. PMID: 33773831.
24. *Перепелица С.А.* Интеллект-карта — один из методов формирования компетенций. *Мед. обр. и проф. развитие*. 2020; 11 (4): 98–107 [*Perepelitsa S. A.* Mind map is one of the methods of forming competencies. *Medical Education and Professional Development/ Med Obr Prof Razvitie*. 2020; 11 (4): 98–107. (in Russ.)]. DOI: 10.2441 1/2220-8453-2020-14007.
25. *Андреенко А.А., Лахин Р.Е., Братищев И.В., Кузовлев А.Н., Мусаева Т.С.* Симуляционное обучение в клинической ординатуре по анестезиологии-реаниматологии в Российской Федерации — результаты многоцентрового исследования Федерации анестезиологов-реаниматологов. *Анестезиология и реаниматология*. 2020; (3): 19–26. [*Andreenko A.A., Lakhin R.E., Bratishchev I.V., Kuzovlev A.N., Musaeva T.S.* Simulation training in clinical residency for anesthesiology and intensive care in the Russian Federation — the results of a multiple-center study of the Federation of anesthesiologists and reanimatologists. *Russian Journal of Anaesthesiology and Reanimatology / Anesteziologiya i Reanimatologiya*. 2020; (3): 19–26. (In Russ.)]. DOI: 10.17116/anaesthesiology 202003119

Received 30.05.2023
Accepted 03.10.2023

Instructions for Authors of the General Reanimatology Journal

Based on the «Brief author guidelines for preparing and formatting scholarly papers in journals indexed in international scientific databases'edited by Olga Kirillova under the ASEP (Association of Scientific Editors and Publishers) and RRIEPL (Russian Research Institute of Economics, Politics and Law in Science and Technology) published in 2019, the CSE's White Paper on Promoting Integrity in Scientific Journal Publications, 2012 Update, **ICMJE Recommendations for the Conduct, Reporting, Editing and Publication of Scholarly Work in Medical Journals (December 2016)**, and the European Association of Scientific Editors (EASE) Guidelines for Authors and Translators (available at **https://ease.org.uk/guidelines-toolkits/**).

Version Dated February 2023

When submitting a manuscript to the General Reanimatology journal, the authors guarantee that:

— the manuscript has not been previously published in another journal;

— the manuscript is not currently reviewed for publication in another journal;

— the manuscript does not contain any confidential information;

— all co-authors agree with publication of the current version of the article.

Instructions for the Authors Before Submitting the Manuscript

Before submitting a manuscript for review, make sure that the file contains all the necessary information in Russian or English, lists all sources of information (references), has a full set of figures and tables, all citations are properly formatted.

The editorial board of the «General Resuscitation» journal recommends that authors use the following checklists and charts developed by international health organizations in preparing manuscripts and other materials (**EQUATOR, Enhancing the Quality and Transparency of Health Research, https://www.equator-network.org/reporting-guidelines/; SWIHM, Scientific Writing in Health & Medicine https://www.swihm.com/course/**):

When preparing papers reporting the results of randomized clinical trials, **«CONSORT 2010 checklist of information to include when reporting a randomized trial»**, **https://www.equator-network.org/reporting-guidelines/consort/**, should be used.

When preparing papers reporting the results of non-experimental research, **«The Strengthening the Reporting of Observational Studies in Epidemiology (STROBE) Statement: guidelines for reporting observational studies»**, **https://www.equator-network.org/reporting-guidelines/strobe/**, should be used.

When preparing a systematic review, **«PRISMA (Preferred Reporting Items for Systematic Reviews and Meta-Analyses)»**, **https://www.equator-network.org/reporting-guidelines/prisma/**, should be used. Additionally, we recommend the following outline for the abstract (summary): scope of the problem (1–3 sentences from the introduction); aim of the review (the same wording in the summary and in the introduction); number of sources, criteria and databases of source selection; specific issues considered according to the highlighted subheadings in the body of the review); limitations of the research on the topic; conclusion (an abridged version of the conclusion from the body of the review).

When preparing a clinical case report/series, **«The CARE Guidelines: Consensus-based Clinical Case Reporting Guideline Development»**, **https://www.care-statement.org/checklist/**, or **SWIHM** 2019 recommendations should be used. Russian language form can be found at **www.reanimatology.com** → Section «Authors Guidelines» → Case Report Writing Template for Authors.

When preparing papers reporting the results of qualitative research, **SRQR (Standards for reporting qualitative research)**, **https://www.equator-network.org/reporting-guidelines/srqr/**, should be used.

Full version at www.reanimatology.com

Main information for the manuscript submission

PARAMETER	INSTRUCTIONS
Limitations	
Initial submission	One file in the Word format in Russian for Russian-speaking authors in English for non-Russian-speaking authors, including: — the title of the paper; — full names of all authors; — affiliations of all authors; — IDs of profiles in the scientific databases for each author; — the text of all sections of the paper; — tables, figures, photos with captions and notes; — references; — conflict of interest; — information of study funding; — acknowledgements (optional); — authors' contribution (preferably)
The length of the manuscript	Original manuscript — about 40,000 characters with spaces; Short communication — should not exceed 2,500 words; Review, meta-analysis — 25,000–40,000 characters with spaces
Front page information	
Title of the paper	Should not exceed 15 words
Information about authors	Full name (Peter A. Johnson), author profile ID in the research database(s) for each author (e-Library/RSCI (Rus), ORCID, Scopus, WoS researcher ID if available)
Affiliations	Full name and postal address of the organizations with zip code
Corresponding author	Full name, e-mail address, phone number
The paper outline and references	
Summary (abstract)	250–300 words. Sections: scope of the problem (introduction/background), aim, material and methods, results, conclusion
Highlights (main messages as text or infographics, an optional section following the summary)	1–3 messages in graphic or text form (no more than 40 words per each text message)
Key words	6–8 words listed with a semicolon (;), without a dot at the end
Body of the paper	Sections: introduction (background), material and methods, results, discussion, conclusion
Supplementary information sections	Conflict of interest, funding of the study should follow the Keywords paragraph. Acknowledgements (optional) and authors' contribution (preferably) should be placed at the end of the paper
Illustrations, including tables	Original paper — up to 8; Short communication — no more than 3; Review — up to 8
References	Dating: 70% should be published within the last 5 years, of them at least 30% within the last 3 years. Number: Original paper – 25–45; Short communication — 10–25; Review — 80–120. Format: please see the «References Formatting» section, www.reanimatology.com
Formatting	
Font	Times New Roman, 12 points. The section titles should be typed in bold
Spacing and Indentation	Line spacing — 1.5; Interval before and after the paragraph — none; Interval between sections — one extra spacing; First line indent — 1.25 cm
Fields	2.5 cm on all sides
Page numbering	In the lower right corner

Full version at www.reanimatology.com

Dear Authors,

Thank you for choosing the «General Reanimatology» journal to publish your papers.

We would like to inform you that in 2024 the Editorial especially welcomes articles containing the results of basic clinical and experimental research on the topic of the journal.

In addition, we recommend that you use graphical summaries and highlights (main points of the article), as well as audio or video formats (mp3, mp4, no more than 2 minutes) to accompany your articles.

In these, you can present a summary of the article, briefly comment on the results obtained and/or present the author's point of view on the main problems in the researched field, pose discussion questions to the professional community on the topic of your research.

Additional audio and video files, after pre-publication preparation, will be published together with your accepted paper on the website of the General Reanimatology journal www.reanimatology.com.

The use of graphic, audio, and video formats to accompany the paper expands the audience, increases interest in the material presented, contributes to a better understanding of the results, and consequently increases their visibility.

We wish you success in your scientific and practical activities and further productive cooperation!

Editorial team,
General Reanimatology Journal

САНАТОРНО-КУРОРТНОЕ ЛЕЧЕНИЕ

Важным этапом на пути к полноценной активной жизни (выздоровлению) являются лечебно-профилактические мероприятия под наблюдением опытных докторов и заботливого персонала.

САНАТОРИЙ «ЛЫТКИНО»

Расположен на территории НИИ Реабилитологии, дер. Лыткино, Московской области

- Возможность прохождения высокотехнологичных медицинских исследований;
- Реабилитационные программы;
- Консультации ведущих специалистов НИИ Реабилитологии
- Бассейны и терренкур

САНАТОРИЙ «УЗКОЕ»

Здравница расположена в юго-западном округе Москвы, в живописном месте площадью 155 га. Ухоженная зеленая территория, окруженная вековыми соснами и елями, пруды.

ИНКЛЮЗИВНЫЙ РЕАБИЛИТАЦИОННЫЙ КОМПЛЕКС «ПОРЕЧЬЕ»

Расположенный на 44 гектарах в экологически чистом хвойном лесу под Звенигородом.

- Комфортабельные жилые корпуса;
- Спортивные сооружения на открытом воздухе для проведения спортивных мероприятий и оздоровительных занятий;
- Тренажерный зал;
- Кафе, столовая, банкетный зал;
- Аудитории для занятий, лекториев и других мероприятий.

ДОМ УЧЕНЫХ В ПОС. МОЗЖИНКА

Расположен в центре «Русской Швейцарии» возле Звенигорода, на берегу реки Москвы. Дом ученых был построен в 1955 г. для обслуживания академиков АН СССР и их семейств, проживающих в академических поселках Мозжинка и Луцино, и является местом их культурного отдыха.
Дом ученых сегодня — это:

- Библиотека
- Развивающие и музыкальные занятия с детьми
- Спектакли для детей
- Концерты классической музыки
- Художественные и фото выставки
- Спортивные секции
- Музей истории Мозжинки
- Благоустроенная детская площадка

ФНКЦ РР

НАУЧНО-ИССЛЕДОВАТЕЛЬСКИЙ ИНСТИТУТ РЕАБИЛИТОЛОГИИ

Московская область, Солнечногорский район,
с/п. Соколовское, деревня Лыткино, д. 777
8 (495) 641-30-06 fnkcrr@fnkcrr.ru

«НАУЧНО-ИССЛЕДОВАТЕЛЬСКИЙ ИНСТИТУТ ОБЩЕЙ РЕАНИМАТОЛОГИИ ИМЕНИ В.А. НЕГОВСКОГО»

г. Москва, ул. Петровка, д. 25, стр. 2
8 (495) 694-27-08 niior@fnkcrr.ru

ИНСТИТУТ ВЫСШЕГО И ДОПОЛНИТЕЛЬНОГО ПРОФЕССИОНАЛЬНОГО ОБРАЗОВАНИЯ

г. Москва, ул. Петровка, д. 25, стр.2
8 (495) 650-96-77 edu@fnkcrr.ru

САНАТОРИЙ «УЗКОЕ»

г. Москва, ул. Профсоюзная, д. 123 А, стр. 14
8 (495) 427-94-33 san-uzkoe@fnkcrr.ru

ДОМ УЧЁНЫХ В ПОС. МОЗЖИНКА

Московская область,
Одинцовский район, п. Мозжинка, Дом учёных
8 (495) 992-53-28 dom_uchenih@fnkcrr.ru

ИНКЛЮЗИВНЫЙ РЕАБИЛИТАЦИОННЫЙ КОМПЛЕКС «ПОРЕЧЬЕ»

Московская область,
Одинцовский городской округ,
деревня Сальково
8 (495) 992-54-64 irk@fnkcrr.ru

www.fnkcrr.ru

МИНИСТЕРСТВО НАУКИ И ВЫСШЕГО ОБРАЗОВАНИЯ РОССИЙСКОЙ ФЕДЕРАЦИИ

ФЕДЕРАЛЬНОЕ ГОСУДАРСТВЕННОЕ БЮДЖЕТНОЕ НАУЧНОЕ УЧРЕЖДЕНИЕ

“Федеральный научно-клинический центр реаниматологии и реабилитологии”

ФНКЦ РР

МИССИЯ ФНКЦ РР – через истину медицинской науки – к здоровью и возвращению к качественной жизни в социуме.

Директор
Член-корреспондент РАН
А.В. Гречко